Tracking hematopoietic development from human pluripotent stem cells

A DISSERTATION SUBMITTED TO THE
FACULTY OF THE GRADUATE SCHOOL
OF THE UNIVERSITY OF MINNESOTA
BY

Patrick Ian Ferrell

IN PARTIAL FULFILLMENT OF THE REQUIREMENTS
FOR THE DEGREE OF
DOCTOR OF PHILOSOPHY

Dan S. Kaufman, M.D., Ph.D., Advisor

November 2013

I. Acknowledgements

I would like to thank all members of the Kaufman lab who I have worked with, past and present, for their help and advice throughout my thesis work. As a new member of the lab, I had very little cell culture experience, no qualifications in molecular biology beyond rudimentary PCR and was just learning how to interpret a FACS plot. However, with several months of their guidance, I became adept at long-term maintenance of human embryonic stem cells, was designing and successfully completing schemes for genetic cloning, and competently analyzing mass amounts of my own flow cytometric data on a weekly basis. As scientists, we have a shared responsibility to be patient educators for those around us who are new to the laboratory or a particular technique, keeping careful to remember that we have all been there before, and will probably be there again.

Additionally, I would like to thank my advisor Dan Kaufman for introducing me to the exciting and magical worlds of blood development and stem cells. Beginning graduate school, I knew that I wanted to enter a field which had direct applications to translational medicine, and that my research had to be associated with terms worthy of a party favor. The opportunity to work under Dan's continued guidance has provided me with both of these benefits, and I look forward to wielding the scientific prowess he has bestowed upon me in all of my future endeavors.

II. Dedication

I would like to dedicate this thesis to my parents, John and Ann Ferrell. Their devotion to the education and emotional development of me and my two brothers throughout our childhood is nothing short of remarkable, and I appreciate it more and more each day as I realize the life-long advantages it has provided me. If not for the unwavering financial investments they made in me, even when I did not give them much reason to do so, it is hard to imagine what type of ditch I might be living in today.

III. Thesis Abstract

Hematopoietic stem cells (HSCs) are a powerful resource for both regenerative medicine and the study of human developmental biology. Though much is known about HSC physiology and development in mice, experimental limitations make their characterization a greater challenge in human. As such, human embryonic stem cells (hESCs) and induced pluripotent stem cells (iPSCs) are currently the best systems with which to model early human hematopoietic development *in vitro*, thus providing insight regarding crucial factors delineating HSC emergence, maintenance and subsequent differentiation. However, generation of HSCs from hESCs and iPSCs relies on an intimate understanding of both the *in vivo* hematopoietic microenvironment as well as HSC phenotype for their prospective isolation. Though current *in vitro* protocols can readily generate hESC and iPSC-derived cells with hematopoietic progenitor function, none of these populations has exhibited what should be the hallmark of an HSC: robust, long-term, multilineage reconstitution of an immunodeficient recipient upon transplantation. These studies address this issue by using transgenic hESC and iPSC lines which report the expression of genes known to be crucial for early hematopoietic events in mice so that they may help us to understand how they translate to human development *in vitro*. Furthermore, this effort is complemented by additional studies using hESC-derived stromal populations to provide assays that help assess putative HSC quality, maintenance and the hematopoietic niche.

IV. Table of Contents

V: List of Figures

CHAPTER 1

Background and significance

Hematopoietic Stem Cell Discovery

Stem cells represent a remarkable avenue for discovery in the field of regenerative medicine due to both of their primary, inherent characteristics: the ability to both self-renew and differentiate into more developmentally restricted lineages. Hematopoietic stem cells (HSCs) are of particular importance since they serve as the starting material for one of the most dynamic organs of the human body, replenishing all mature blood lineages throughout the entire adult life. Researchers have been quantitatively analyzing HSCs from a clonal perspective since the first of several ground-breaking studies by Till and McCulloch in 1961[1-5]. The basis for this work was their ability to transplant bone marrow (BM) from one mouse into an irradiated recipient and subsequently enumerate donor-derived hematopoietic colony forming units (CFU) in the recipient's spleen. To demonstrate CFU clonality, they sub-lethally irradiated the donor marrow, causing cell-specific chromosomal abnormalities which were later observed in all the cells of a given CFU. Till and McCulloch demonstrated clonal progenitors which formed mixed myeloerythroid colonies, lymphocytic colonies, and were able to self-renew, thus providing evidence for the existence of single cells in mouse BM capable of long-term survival and multipotent differentiation.

With the advent of reagents allowing for cell separation on the basis of surface antigens, studies began focusing on a phenotypic definition for HSCs in 1984[6,7]. Over the next decade, Weissman's group and others determined that precursors to mature blood cells lacked the extra-cellular markers present on any of these lineages, thus giving rise to HSC enrichment by negative selection using what is know as the Lin (lineage)

cocktail of antibodies[8,9]. After it was discovered that all Lin^- bone marrow cells belonged to a $Thy1.1^{lo}$ subset, stem cell antigen (Sca-1) and c-kit were found to further contribute to HSC selection[9-11]. This $ckit^+Thy1.1^{lo}Lin^-Sca1^+$ (KTLS) subset is currently used as a standard for isolation of long-term repopulating cells from unfractionated mouse BM. More recently, the signaling lymphocytic activation molecules (SLAM) CD244, CD150 and CD48 were also found to enrich mouse HSCs, giving the added benefit of distinguishing between long-term repopulating HSCs (LT-HSCs), which give life-long reconstitution, and their further differentiated multi-potent progenitors (MPPs), which give only transient reconstitution[12].

Human HSCs are of particular importance from a clinical perspective; enabling hematologists to treat hematological diseases by long-term reconstitution of healthy blood cells. Indeed, the first successful allogenic hematopoietic stem cell transplant (HSCT) was performed at the University of Minnesota in 1968 by engrafting BM between two HLA matched siblings[13]. Since then, peripheral blood (PB) and umbilical cord blood (UCB) have also been recognized as clinically relevant sources of HSCs[14,15]. However, the frequency of HSCs in human whole bone marrow is extremely low at about 1 in 10^6 cells[16], thus prompting the need to identify human-specific markers to aid in their purification. $CD34^+$ BM cells were initially recognized as enriched for HSCs due to their enhanced ability for long-term, multilineage reconstitution (LTMR) of both humans and baboons[17,18]. Subsequently, xenograft models in severe combined immune-deficient (SCID) mice became a valuable tool for identifying purified hematopoietic populations capable of LTMR, which are referred to as SCID-repopulating cells (SRCs)[19,20]. Though

LTMR in human is the only way to truly test for HSCs, the SRC assay is currently thought of as an accessible surrogate for assessment of putative HSC quality.

Characterization of the phenotypic signature and physiology of human HSCs is an intense area of interest. While CD34 alone can be used to positively isolate an enriched population of SRCs from UCB, numerous other markers not only enhance purity, but also distinguish between HSCs with long-term and short-term repopulating capability[21]. Similar to mouse, human HSCs are enriched by negative selection with lineage markers in addition to CD38, which is expressed on MPPs but not HSCs[22,23]. It should be noted that the SLAM markers do not aid in human HSC purification, highlighting one of the major differences in mouse and human HSC biology[24]. More recently, it was demonstrated that single $Thy1^{+}Rho^{lo}CD49f^{+}$ UCB cells undergo efficient LTMR, while CD45ra, an isoform of the pan-hematopoietic marker CD45, labels HSCs with decreased LTMR potential[23,25]. Quiescence vs. cell cycle entry is also a key aspect of HSC function, as G_0 HSCs within the BM exhibit enhanced LTMR over those which are actively proliferating[26,27]. Finally, HSCs have been demonstrated to exhibit increased polarity with respect to particular cell adhesion molecules, likely as result of the need to make cell-cell contacts within particular aspects of the BM microenvironment[28].

Vertebrate *in vivo* hematopoiesis

Early in embryogenesis, innervation of the primitive streak results in creation of the three germ layers: ectoderm, endoderm and mesoderm[29]. Subsequently, at embryonic day (E) 7.25, mesodermal cells derived from the posterior portion of the primitive streak

migrate to form the extra-embryonic yolk sac, where the first hematopoietic tissues are formed in association with the vasculature in what is called primitive hematopoiesis[30-32]. Here, pools of nucleated primitive erythrocytes (Ery^{p}) expressing ε-globin form the peripheral blood islands (PBI) in association with the surrounding endothelial vasculature. Explant studies in mouse have shown secretion of bone morphogenic protein-4 (BMP-4) and vascular endothelial growth factor (VEGF) by the surrounding mesoderm and primitive endoderm to be inductive signals in formation of the PBI[33,34]. Likewise, activation of canonical Wnt signaling is implicated in specification of Ery^{P} from mesoderm in mouse ES cells[35]. It is not until E9.5, just after the heart begins to beat, that Ery^{P} enter the circulation and undergo numerous morphological changes, including extrusion of the nucleus[36,37]. These enucleated Ery^{P} continue to circulate until around the time of birth[37].

Three days after the onset of primitive hematopoiesis, at E10.5, a second wave of blood cell emergence begins in the aorta-gonad-mesonephros (AGM) in what is known as definitive hematopoiesis[38,39]. From the ventral aspect of the dorsal aorta within the AGM, definitive HSCs materialize from cells which are bipotential for endothelial and hematopoietic specification, commonly referred to as the hemogenic endothelium[40]. Lineage tracing studies have demonstrated that definitive HSCs bud specifically from a few endothelial cells in the AGM and not from the underlying mesenchyme, though the mesenchyme does provide instructive signals which initiate the endothelial to hematopoietic transition[41,42]. This event has also been recorded by time-lapse microscopy of mouse aortic explants[43,44]. Transplantation studies demonstrate that only

definitive HSCs from the AGM at E10.5 or after are capable of LTMR in adult mice, thus suggesting that progenitors of the primitive wave, at least in their current developmental state, do not contain SRCs[39]. Though it has been shown that E9 c-kit$^+$CD34$^+$ cells from the yolk sac can repopulate a neonate recipient when injected into the liver[45], this finding has no bearing on current clinical applications of HSCT in patients after birth.

The hematopoietic niche

From the AGM, definitive HSCs enter the vasculature and travel to the fetal liver, where they undergo further maturation, and eventually make their way to the BM by E15[46]. Here, HSCs serve the daunting and enormously complex role of replenishing all mature blood lineages throughout the entire adult life, all while maintaining their own competence for multipotency, self-renewal and quiescence. Indeed, this is a highly active, delicate balance which cannot be sustained autonomously, but requires constant aid from the local BM microenvironment known as the hematopoietic niche.

Initial tracking studies in mouse found that HSCs were largely associated with endosteal surfaces in trabecular regions of the long bone[47,48]. Accordingly, osteoblasts, a mesenchymal stromal cell (MSC) derivative which regulates bone formation and thus plays an imperative role in the dynamic structure of these compartments, are also directly related to HSC maintenance[49]. Not only does increasing osteoblast number in the BM promote expansion of HSCs, but homing studies have found BM HSCs to be in direct contact with ostepontin$^+$, N-cadherin$^+$ osteoblasts within the endosteum[50,51]. More recent work has shown perivascular and endothelial cells to be critical for HSC maintenance, as

deletion of stem cell factor (SCF) from both of these cell types, but not osteoblasts or the HSCs themselves, results in HSC depletion[52]. Additionally, the niche appears to be sub-compartmentalized with specialized areas for hematopoietic progenitors at various stages of differentiation. CXCL12, a chemokine necessary for niche HSC retention[53], was found to have various effects in different tissue / niche compartments[54]. Deletion of CXCL12 in endothelial and perivascular cells results in depletion of HSCs but not myeloerythroid or lymphoid progenitors, while deletion from osteoblasts has no effect on HSCs but does decrease early lymphoid progenitors. In addition, osteoblast expression of thrombopoietin (TPO) angiopoietin-1 (Ang-1) and N-cadherin have been shown to promote HSC quiescence, with homotypic N-cadherin interactions anchoring HSCs within the niche[51,55-57].

Due to obvious limitations regarding the study of *in vivo* human developmental biology, much less is known regarding specifics of the human hematopoietic niche or how closely it relates to mouse. However, a few *in vitro* methods have been developed which attempt to recapitulate the BM microenvironment in order to assess the effect of various factors on human HSC maintenance. The most widely utilized of these methods, the long-term culture initiating cell (LTC-IC) assay, was developed over 2 decades ago [58]. LTC-IC takes advantage of primary stromal cell lines, typically BM derived, for co-culture with purified populations of HSCs, and quantifies how well they can produce myeloid colonies over a 5-week period[59]. The output is then considered proportional to the relative abundance and survival of LTC-ICs (an *in vitro* surrogate for SRCs) within the starting population, which can be influenced both by the supporting environment (eg

stromal layers, soluble factors, etc.) and quality of the input HSCs. Recently, it has been shown that human HSCs cultured with BM-derived MSCs overexpressing the Notch ligand Jagged-1 enhanced LTC-IC[60]. Furthermore, similar to mouse, modulation of N-cadherin expression or function via antibody blocking in LTC-IC MSC co-culture assays demonstrates N-cadherin to play a role in human HSC maintenance[61]. Thus, the ability to culture and manipulate human bone marrow stromal cells provides valuable surrogate assays for the identification of crucial factors in the human hematopoietic niche.

Human embryonic stem cells and hematopoiesis

Though study of embryonic developmental models for a variety of vertebrate species has provided valuable insight regarding the early stages of human development, use of a specifically human system may best furnish the bridge to clinically relevant therapeutics. The isolation of human embryonic stem cells (hESCs) in 1998 by Thomson *et al* at the University of Wisconsin-Madison initiated several avenues for discovery [62]. Unlike adult stem cells, which are developmentally restricted to production of a given tissue class, hESCs are pluripotent, meaning they can differentiate into any adult tissue. As such, they are an ideal *in vitro* model for human development as well as a promising, potentially limitless source of material for regenerative medicine. Indeed, investigators have already experienced success using hESC-derived populations to treat patients with spinal cord injury and macular degeneration[63,64]. Furthermore, ongoing work has produced other advances such as hESC-derived pancreatic beta cells[65],

cardiomyocytes for repair of infarct models[66] and hepatocytes to study potential therapies for liver disease[67].

Perhaps one of the most widely investigated areas of developmental biology using hESCs is hematopoiesis. Just a few years after the first hESC isolation, Kaufman *et al* were able to generate hESC-derived hematopoietic CFUs by co-culture with either mouse BM stroma or yolk sac endothelial cells[68]. Typical methods for blood cell generation from hESCs initially relied on stromal cell co-culture, as was done by Kaufman *et al*, where adherent cells derived from niche environments support hematopoietic differentiation. Other studies demonstrated suspension culture as embryoid bodies (EBs), which can differentiate independent of stromal cells. Using variations of these two basic methods, investigators have managed to create the majority of fully mature blood cells, including those from the erythroid, myeloid and lymphoid lineages[69-71]. Derivation of these cells has large implications for both transfusion medicine and immunotherapy[72].

Several studies have described the functional and phenotypic progression of hESCs to hematopoietic progenitors, thus providing insight regarding the fundamental similarities between mouse and human embryonic development. Just as in mouse, hESCs proceed though a *brachuyry* expressing mesodermal stage dependent on the presence of Activin A and Bone Morphogenic Protein-4 (BMP-4) before entering hematoendothelial commitment[73,74]. Likewise, a number of groups have described an hESC-derived $CD31^{+}Flk1^{+}$VE $Cadherin^{+}$ hemogenic endothelium giving rise to hematopoietic progenitors[75-77]. This endothelial to hematopoietic transition has similarly been captured at the single-cell level by fluorescent microscopy in hESC differentiation cultures[78].

Induced pluripotent stem cells

In 2006 and 2007, Shinya Yamanaka revised the concept of lineage fate by reprograming fully differentiated mouse and human fibroblastic cells, respectively, into germline transmittable, induced pluripotent stem cells (iPSCs)[79,80]. The basis for this procedure relied on genetic modification of the adult cells with a combination of genes - Oct-4, Sox-2, C-Myc, and KLF-4 – which play important roles in pluripotency. Since then, investigators have successfully created iPSCs from numerous adult tissues using various combinations of pluripotency factors and methods of genetic transduction[81-85]. Though the exact pathways and mechanisms elicited in reprograming adult cells are not completely understood, it has been determined that human iPSCs possess the potential to differentiate into all tissue types[80,84,86]. As such, human iPSCs represent two major advantages over hESCs (collectively referred to as human pluripotent stem cells, or hPSCs): the ability to generate patient-specific stem cells for regenerative medicine, and to model congenital disorders from a developmental perspective by reprograming of the afflicted adult tissue[87-91].

The search for hPSC-derived HSCs

Despite these successes, one of the most sought after goals in hematopoietic derivation from hESCs/iPSCs has yet to be realized: *in vitro* generation of hPSC-derived HSCs[72]. Though differentiation of progenitor cells displaying an extra-cellular phenotypic signature similar to UCB-derived SRCs is relatively routine, to date, these

cells have not displayed the ability for robust LTMR as does $CD34^+$ UCB. Thus, there exists a critical difference regarding the repopulation potential of hESC/iPSC-derived hematopoietic progenitors as compared to those obtained from primary sources. The ability to produce HSCs *in vitro* could provide essentially limitless amount of material for HSCT. Indeed, a single unit of UCB rarely contains enough HSCs to fully engraft an adult recipient[92]. Likewise, attempts to grow UCB-derived HSCs *ex-vivo*, while managing to greatly expand the initial population, have failed to increase the absolute number of SRCs[93], though recent studies are making progress on this front[94,95]. This is likely due to proliferation at the expense of quiescence resulting in production of MPPs and HSC exhaustion. Though recent studies have demonstrated the application of Stem Regenin-1 (SR1), an antagonist of the aryl-hydrocarbon receptor, to expand SRCs *ex-vivo* by 17-fold[96], further work is required to examine the biological implications and thus clinical relevance of this technique.

Attempts to manufacture SRCs from hPSCs have typically utilized three basic routes: identification and isolation based on novel patterns of extra-cellular markers, modulation of culture conditions and over-expression of hematopoietic genes. The first of these methods typically relies on expression of the hematoendothlial surface antigen CD34 as well as other surface antigens that signify hematopoietic commitment, such as CD45 or CD43. This has met very limited success and relies on the assumption that current culture conditions are capable of producing HSCs. While this expectation seems straightforward since theoretically there must exist a multipotent HSC intermediate if pluripotent stem cells progress to fully differentiated hematopoietic cells, it is entirely

possible that the *in vitro*-produced intermediate lacks several qualities key to HSC function, such as long-term self-renewal and niche homing/retention. We have demonstrated an inability of these cells to survive over 5 weeks in LTC-IC, thus indicating a deficiency in self-renewal (Chapter 4, submitted). Finally, hPSC-derived populations appear to display limited developmental potential, as current differentiation methods promote a severe myeloid bias with production of mature T or B cells being very difficult[72]. Additionally, hESC and iPSC derived blood cells appear to recapitulate development of primitive hematopoietic cells that may not be capable of fully reconstituting hematopoiesis in an adult recipient[97].

In light of these apparent deficiencies, efforts have been directed to modulate culture conditions to more closely mimic *in vivo* hematopoietic development. Ledran *et al* utilized stromal layers derived from mouse AGM and fetal liver for hESC co-culture to demonstrate not only increased development of hematopoietic progenitors, but also engraftment of up to 16% in primary recipients with intra-bone marrow transplantation (IBMT)[98]. Though this marked a significant improvement upon previous studies, it is still significantly less compared to $CD34^+$ UCB, which can achieve 90% engraftment when injected intravenously. Furthermore, it should be noted that IBMT provides an engraftment advantage over intravenous injection, as it eliminates the bone marrow homing burden on the transplanted cells, which fully functional HSCs should readily overcome[99,100]. More recently, it was demonstrated that hESC-derived $CD34^+$ cells generated by co-culture with BM-MSC and $CD14^+$ macrophages (another lineage postulated to play an important role in the hematopoietic niche[101]) were able to engraft

preimmune fetal sheep, though this only has implications for *in utero* HSCT[102]. In order to address the bias for myeloid/primitive development from hESCs and iPSCs, Kennedy *et al* successfully generated mature T-cells by inhibiting signaling pathways crucial to primitive hematopoiesis in a complex, step-wise culture system, thus indicating the existence of a definitive, multipotent progenitor, though the SRC capability of these cells remains unknown[103]. Finally, in perhaps the most impressive method for directed hematopoietic differentiation, two recent studies managed to isolate fully engraftable, multipotent SRCs from hESC and iPSC-derived teratomas in mice[104,105]. While these studies stray from the emphasis on *in vitro* derivation, it is proof of principle that hPSCs are indeed capable of producing multipotent, definitive HSCs when subjected to the appropriate environment. Thus, it seems plausible that improved culture systems combined with enhanced methods for progenitor isolation will eventually materialize in the *in vitro* production of hPSC-derived HSCs.

Genetic modification of hESCs has also been a focus for the enhancement of hematopoietic differentiation. Initially, it was found that enforced of expression of HoxB4 in mouse embryonic stem cells (mESCs), which have also exhibited a lack of *in vitro* SRC production, was able to promote engraftment between 5 and 40% in the bone marrow[106,107]. Naturally, this finding inspired similar studies using hESCs, though the results have not been nearly as encouraging, suggesting that HoxB4 may play differential roles in mouse versus human hematopoiesis[108,109]. A more recent study which induced RUNX1a overexpression in hPSCs demonstrated that these cells had enhanced ability for hematopoietic differentiation and exhibited substantial reconstitution in immunodeficient

mice at 9 weeks after IBMT, producing 10% chimerism in both myeloid and B-lymphoid lineages[110]. Though this provides valuable insight regarding the influence of RUNX1a expression on human hematopoietic development, gene overexpression can create unintended consequences such as unregulated cell growth which would render this method less useful for clinical applications.

Transcription factors in definitive hematopoiesis

As pluripotent cells progress towards hematopoietic lineages, they undergo numerous fate decisions which are persuaded by both extrinsic and intrinsic factors. This typically involves paracrine signals secreted by tissues of the microenvironment initiating a signaling cascade within the developing tissue. In the AGM, where definitive hematopoiesis is initiated, activation of Notch1 signaling and GATA2 expression in the aortic endothelium appear to be crucial upstream factors instigating HSC production in mouse, while both have been shown to be dispensable for yolk sac primitive hematopoiesis[111,112]. Recent studies have also shown Notch signaling promotes hematopoiesis from hESCs. Ectopic expression of Delta-like 4 (DL4) in co-cultured stromal cells increases hESC-derived hematopoietic progenitors, even allowing for subsequent T-cell production[103]. Meanwhile, disruption of Notch signaling in hESC and iPSC cultures demonstrates Notch1 mediated activation of Hes1 is responsible for hematopoietic commitment from the hemogenic endothelium[113].

Downstream of Notch signaling is Runt-related transcription factor-1 (Runx1), a critical factor in the initiation of definitive hematopoietic development. Overexpression

of Runx1 in mice and zebrafish deficient for Notch signaling is able to rescue hematopoiesis in the AGM[114,115]. Conversely, Runx1$^{-/-}$ mice die *in utero* due to severe hemorrhaging and the complete lack of definitive hematopoiesis, with the hemorrhage sites containing Ery^{P}, suggesting that Runx1 does not play a critical role in primitive hematopoiesis, though it can be detected in the yolk sac prior to circulation[116-119]. Runx1 expression has been found in endothelial cells of the dorsal aorta before the emergence of definitive HSCs, but not other endothelial cells, as well as the underlying mesenchyme and emerging intra-aortic HSC clusters[119-121], suggesting that it plays a role in the endothelial to hematopoietic transition within the hemogenic endothelium. Indeed, studies have shown that Runx1 expression, induced by the underlying mesenchyme, is required in vascular endothelial cells for HSC emergence from the AGM, though it is not necessary for HSC maintenance thereafter[42,122-124].

Runx1 control of the endothelial to hematopoietic transition appears to be mediated by the simultaneous suppression of endothelial genes and activation of hematopoietic factors. Though no direct evidence has shown Runx1 to bind to the promoters of endothelial genes, expression of both Flk1 and VE-cadherin decreases following Runx1 activation[125-127]. Pu.1, a master regulator of the myeloerythroid axis in early hematopoietic development, is bound by Runx1 at three sites within its upstream regulatory element during embryonic hematopoiesis with a subsequent increase in expression[128-130]. Pu.1$^{-/-}$ mouse embryos die at later stages of gestation than Runx1$^{-/-}$ embryos (E18.5) and display a severe reduction in KTLS HSCs within the fetal liver[131], while fetal liver cells from Pu.1$^{-/-}$ mice fail to produce myeloid or lymphoid lineages in

irradiated recipients[132]. Finally, C/EBPα, another regulator of myeloid development, is directly activated by Runx1 through binding to a conserved enhancer region[133]. Studies utilizing this enhancer in transgenic mice show C/EBPα to be expressed in HSCs within the bone marrow and fetal liver[134].

MicroRNAs and hematopoiesis

MicroRNAs (miRNAs) are transcribed, RNA nucleotide sequences which do not code for proteins, but rather inhibit expression of other genes at the translational level through base pairing with the mRNA 3' untranslated region[135]. After their initial transcription, pre-miRNAs are processed to a short, 20-21 nucleotide sequence in the cytoplasm by Drosha/Dicer, and are subsequently incorporated into the RNA-induced silencing complex (RISC) which helps guide them to their target sequences[135]. A fairly recent development in our knowledge of the complex mechanisms involved with gene expression control, miRNAs have been implicated in numerous stages and compartments of hematopoietic specification[136-141]. From the perspective of HSC development and function, inducible deletion of Dicer in HSCs confers an engraftment disadvantage in competitive repopulation assays, broadly affiliating miRNAs with HSC homing and maintenance[136]. Likewise, aberrant regulation of several miRNAs are used as prognostic indicators in a variety of cancers including blood malignancies, indicating that they likely play key roles in HSC and progenitor cell fate decisions[142-146]. Furthermore, their strong association with cancer in general has identified miRNAs as regulators of cell cycle and proliferation, both of which must be tightly managed to keep the proper balance between

HSC quiescence, self-renewal and differentiation[147-149]. Thus, the study of miRNA expression and translational regulation in both HSCs and hPSC-derived hematopoietic progenitors seems likely to yield valuable insight regarding the transcriptional profile of a functional HSC.

Thesis Statement

The experiments conducted herein sought to investigate the gene expression patterns that could identify putative hPSC-derived HSCs as they are produced *in vitro* (Chapter 2). To do so, we engineered genetic constructs utilizing known regulatory elements of transcription factors crucial for early development of definitive HSCs to drive expression of the fluorochrome tdTomato (tdTom), which then acts as a reporter of endogenous gene expression. These constructs were stably inserted into the genomic DNA of both H9 hESCs and UCB-derived iPSCs, which were clonally isolated and differentiated under hematopoietic conditions. Such a system is advantageous in that it allows for the visual identification of individual cells expressing a gene of interest without the need to kill them, thus terminating their hematopoietic progression, as is necessary for other methods of intracellular gene expression detection such as immunohistochemistry and whole RNA RT-PCR analysis. Using this reporter model, we have determined RUNX1c expression, an isoform of RUNX1, to identify particular sub-sets of hESC-derived hematopoietic progenitors as they emerge in culture. This result is consistent with similar *in vivo* and *in vitro* models developed in mice and zebrafish, providing evidence for an evolutionary conservation in RUNX1c expression over

hematopoietic development. Furthermore, genetic and functional analysis of the tdTom expressing cells demonstrated them to have several key differences from $CD34^+$ UCB, contributing to evidence suggesting that current methods for differentiation of hPSCs are not capable of producing HSCs. Preliminary studies using the same system for an alternative reporter model using regulatory elements for the hematopoietic transcription factor PU.1 were also conducted (Chapter 3). Here, we show faithful expression of the PU.1 reporter over hESC hematopoietic development with expression patterns largely mirroring that of the RUNX1c reporter, consistent with PU.1 being a direct down stream target of RUNX1. These results suggest that the PU.1 may be used in future experiments to study hematopoiesis from HPSCs.

In a separate set of experiments, we utilized LTC-IC assays to assess the ability of hESC-derived stromal populations to support LTC-ICs from both hESC-derived hematopoietic progenitors and $CD34^+$ UCB over 5 weeks in culture (Chapter 4). This work demonstrated not only that the hESC-derived stromal layers were capable of supporting LTC-IC from $CD34^+$ UCB, but that the resulting LTC-ICs were capable of long-term (12 weeks post-transplantation) engraft in immunodeficient mice. This was in contrast to hESC-derived hematopoietic progenitors, which did not survive for 5 weeks in culture and thus were determined to not contain LTC-ICs. Furthermore, because the survival of LTC-ICs in culture was predictive of their ability to engraft in mice, we have determined that LTC-IC, which is cost-effective and easy to implement, is a valuable surrogate assay for expensive and time consuming *in vivo* studies to assess SRCs in populations of putative hematopoietic progenitors.

CHAPTER 2

The RUNX1 +24 enhancer and P1 promoter identify a unique subpopulation of hematopoietic progenitor cells derived from human pluripotent stem cells

Derivation of hematopoietic stem cells from human pluripotent stem cells remains a key goal for the fields of developmental biology and regenerative medicine. Here, we use a novel genetic reporter system to prospectively identify and isolate early hematopoietic cells derived from human embryonic stem cells (hESCs) and human induced pluripotent cells (iPSCs). We cloned the human *RUNX1c* promoter and +24 enhancer to drive expression of tdTomato in hESCs and iPSCs. We demonstrate that tdTom expression faithfully enriches for *RUNX1c*-expressing hematopoietic progenitor cells. Inhibition of primitive hematopoiesis by blocking Activin/Nodal signaling promoted the expansion of $tdTom^+$ cells. Notably, RUNX1c/$tdTom^+$ cells represent only a limited subpopuation of $CD34^+CD45^+$ and $CD34^+CD43^+$ cells with a unique genetic signature. Specifically, we find significantly lower expression of Let-7 and mir181a microRNAs in the RUNX1c/$tdTom^+$ cell population. These phenotypic and genetic analyses comparing the RUNX1c/$tdTom^+$ population to $CD34^+CD45^+$ umbilical cord blood and fetal liver demonstrate several key differences that likely impact the development of HSCs capable of long-term multilineage engraftment from hESCs and iPSCs.

Introduction

The ability of human pluripotent stem cells (hPSCs) to differentiate into any cell lineage makes them an important resource for studies of developmental biology and regenerative medicine[62]. Specifically, hematopoietic stem cells (HSCs) derived from pluripotent stem cells via *in vitro* culture systems could provide an unlimited supply of material for reconstitution of defective blood lineages *in vivo*. However, this goal has remained very challenging and elusive for several likely reasons[72]. For example, use of still incompletely defined culture conditions may not adequately support development or isolation of HSCs capable of long-term multilineage engraftment, as demonstrated by transplantation into immunodeficient mice (typically termed SCID repopulating cells, SRC). Additionally, hematopoietic populations derived from human embryonic stem cells (hESCs) and induced pluripotent stem cells (iPSCs) via i*n vitro* culture are likely biased toward development of primitive hematopoietic cells, which are not thought to have the ability to reconstitute adult recipients[39,150,151]. To date, standard cell surface antigens have been used to identify hPSC-derived hematopoietic cells. However, none of these populations have demonstrated SRC potential comparable to cells isolated from human umbilical cord blood (UCB)[72,98,150,152-154]. Interestingly, two recent studies using hESCs and iPSCs for *in vivo* teratoma formation in mice found that human HSCs extracted from the resulting teratomas were able to engraft a secondary recipient[104,105]. These results suggest that given the right environment and instructive signals, hESC/iPSCs are indeed capable of deriving functional HSCs.

Here, we aimed to better identify human definitive hematopoietic populations by isolation of cells derived from both hESCs and iPSCs based on expression of the Runt-related transcription factor 1 (Runx1). Runx1 is a master regulator of hematopoiesis in vertebrates and is necessary for emergence of definitive HSCs from hemogenic endothelium in the developing mouse embryo[116,118,123,155,156]. Runx1$^{-/-}$ mice die *in utero* due to a complete lack of a definitive blood system[118]. The Runx1 locus in mice and zebrafish contains two promoters, the proximal P2 and distal P1, which differentially drive expression of the Runx1b/a and Runx1c isoforms, respectively[157-159]. Transgenic reporter models have demonstrated the P2 promoter to be active throughout both primitive and definitive hematopoiesis, while P1 activity is largely restricted to the emergence of the definitive wave[160-162]. Likewise, isolation of hematopoietic populations in the developing mouse embryo based on expression from either promoter demonstrates that cells with P1 activity are enriched for definitive progenitors over the population with only P2 activity[162]. Both promoters rely on an intronic enhancer lying 24 kb downstream from the P1 promoter for expression specific to hematopoietic tissues[161,163]. The +24 enhancer was also shown to be active in hemogenic endothelial cells directly prior to the emergence of HSCs[164]. Interestingly, overexpression of RUNX1a, a splice variant of Runx1b lacking the c-terminal transcriptional regulatory domain, has recently been shown to enhance stem cell expansion and engraftment from both mouse HSCs and hESC-derived populations[110]. While Runx1b$^{-/-}$ mice have severely impaired hematopoietic development, animals deficient for Runx1c$^{-/-}$ only show a modest decrease in definitive hematopoiesis[158].

Given this difficulty to isolate functional HSCs from hESCs and iPSCs, and what appears to be a direct relationship between the onset of Runx1c expression and definitive hematopoiesis in the developing mouse embryo, this study sought to determine whether there exists a similar developmental relationship in human pluripotent stem cells. To do so, we developed a transgenic reporter for RUNX1c in both hESCs and human iPSCs by cloning portions from the endogenous human *RUNX1* locus which correlate with important Runx1c regulatory elements in mouse. These studies demonstrate that RUNX1c expression in human development is restricted to a subpopulation of emerging hematopoietic cells with a unique genetic signature that offers important insight into differences between hESC/iPSC-derived hematopoietic cells and human cell populations isolated from UCB and fetal liver that have SRC potential.

Materials and Methods

Human ES Cell Culture and Gene Transfer

Human ES cells (H9) (University of Wisconsin, Madison, WI) were maintained as colonies on mitomycin C-treated MEFs or on Matrigel-coated plates in ES cell growth medium consisting of Dulbecco's modified Eagle's medium (DMEM)/Ham's F-12 medium (F12) (Invitrogen, Carlsbad, CA, http://www.invitrogen.com) supplemented with 15% Knockout Serum Replacer (Invitrogen), 1 mM L-glutamine (Cellgro/Mediatech, Herndon, VA, http://www.cellgro. com), 0.1 mM β-mercaptoethanol (Sigma-Aldrich, St. Louis, http:// www.sigmaaldrich.com), 1% minimum essential medium nonessential amino acids (Invitrogen), 4 ng/ml basic fibroblast growth factor (R&D Systems Inc.,

Minneapolis, http://www.rndsystems.com), and 1% penicillin-streptomycin (Invitrogen) incubated at 37°C in a humidified atmosphere containing 5% CO_2. Five days before nucleofection, human ES cells were transferred to Matrigel-coated plates to remove MEFs. For 1 hour prior to nucleofection, cells were treated with 10 μM Y-27632 (Millipore, Billerica, MA, www.emdmillipore.com) to increase viability. At nucleofection, 2 x 10^6 cells per sample were dissociated with 1 ml of 0.05% Trypsin supplemented with 2% chick serum for 4 minutes, quenched with FBS and washed with PBS to remove traces of media. Cells were then pelleted, re-suspended in 100 μl of nucleofector solution (Kit V; Amaxa Inc., Gaithersburg, MD, http://www.amaxa.com) with 6 μg of transposon plasmid and 2 μg of SB100x transposase plasmid (Addgene, Cambridge MA, www.addgene.org) using program setting B-16. Nucleofected cells were immediately resuspended in human ES cell growth medium prewarmed to 37°C supplemented with 10 μM Y-27632 and seeded onto MEFs for continued culture. Successful transfectants were selected days 3-7 post nucleofection using 4 μM zeocin (Invivogen, San Diego, CA, USA), and clonal lines were derived by single cell passage of the selected, bulk population onto MEFs using 0.05% Trypsin + 2% chick serum. After 7 days of clonal growth, individual colonies were transferred to separate wells of MEFs for continued culture.

Cloning and Plasmids

Transposon-encoding plasmids were constructed using standard molecular cloning techniques. Transposons were constructed using T2 inverted terminal repeat sequences as described (Cui 2002), separated by 1,800 base pairs (bp) of bacterial sequence consisting

of the ColE1 bacterial origin of replication and kanamycin (Kan) resistance gene. pKT2/mCAG:GFPzeo (Fig. 1A) encodes a fusion between the green fluorescent protein (GFP) reporter gene and the zeocin (Zeo) drug-selection marker (Invivogen) transcriptionally regulated by a CpG- free enhancer/elongation factor 1-α promoter/intron sequence (CLP) (Invivogen). pKT2/R1c:tdTomato was constructed by cloning the cDNA for tdTomato (provided by Roger Tsien) attached to the Rabbit β-globin poly A flanked upstream by 950 base pairs of the RUNX1c P1 distal promoter and downstream by 250 base pairs of the +24 intronic enhancer between the T2 elements of pKT2/mCAG:GFPzeo (Fig 1a). The RUNX1c P1 distal promoter and +24 enhancer were amplified from H9 genomic DNA using standard PCR. The Sleeping Beauty 100 transposase (Addgene) was designed as previously described[165].

Hematopoietic Differentiation of hPSCs as Spin EBs

H9 hESC and UCB-derived iPSC transgenic Runx1c reporter lines were adapted to passage as single cells using TrypLE (Invitrogen) as previously described[166]. Single-cell adapted lines were subject to hematopoietic differentiation as Spin Embryoid Bodies, also previously described[166]. Briefly, after harvest into single cells, the cells were resuspended in BPEL media supplemented with Bmp4 (20 ng/mL), VEGF (20 ng/mL) and SCF (40 ng/mL) and plated at a density of 3,000 cells / well in a 96-well plate and spun in a centrifuge to create mono-layer cell aggregates. For SB studies, inhibitor was applied days 2-5 at 6 μM. After 6 days of incubation, the EBs were transferred to gelatinized, 24-well adherent plates in BEL media supplemented with VEGF (40 ng/mL), SCF (50 ng/mL), IL-3 (30 ng/mL), IL-6 (30 ng/mL), TPO (30 ng/mL) and EPO (3

U/mL). The EBs remained in these conditions for the rest of the differentiation with one half media changes every 3-4 days. To harvest for analysis, the media containing the non-adherent fraction was removed from each well while the adherent cells were detached with 0.05% trypsin containing 2% chick serum for 4-8 minutes. Both fractions were combined and filtered to create a single-cell suspension and subjected to subsequent analysis. For cell sorting, 10 μM Y-27632 was added 1 hour prior to the described harvest procedure and DNaseI (Stem Cell Technologies, Vancouver, BC, Canada, www.stemcell.com) was added to the FACS sorting buffer at 0.2 mg/mL in order to promote cell survival and prevent cell clumping.

Flow Cytometry

Single cell aggregates of the combined Spin EB adherent and non-adherent fractions were incubated with allophycocyanin (APC) conjugated mouse anti-human CD31, CD41a, CD43, CD45, CD73, CD235a or CD45ra and phycoerythrin (PE) Cy7-conjugated CD34 or the corresponding isotypope control antibody (BD Biosciences) in FACS buffer (DPBS containing 2% FBS and 0.1% sodium azide) for 15–20 minutes at 4–8 °C. Flow cytometric analysis was performed using the LSRII flow cytometer (BD Biosciences, San Jose, CA, http://www.ebioscience.com). Dead cells were stained with Sytox Blue (Invitrogen) immediately prior to running through the flow cytometer. Data from flow cytometry was analyzed using FlowJo software (TreeStar, Ashland, OR, www.treestar.com).

Hematopoietic CFC Assay

Cell populations were obtained either directly from the disaggregation procedure outlined in the hematopoietic differentiation methods or following the cell sort. After enumeration, cells were washed in Iscove's Modified Dulbecco's Medium (IMDM) containing 2% FBS and seeded at a density of $2.5x10^3$ to $0.5x10^5$ / mL in H4436 Methocult media (Stem Cell Technologies), then allowed to incubate at 37°C in a humidified atmosphere containing 5% CO_2. After 7-14 days of incubation, colonies were enumerated and scored.

RNA isolation and quantitative PCR analysis

Cell fractions were harvested as described. Total RNA was isolated using the miRvana RNA isolation kit (Invitrogen), and then analyzed for concentration and purity on a Nanodrop spectrophotometer and reverse transcribed with the NCode VILO miRNA cDNA synthesis kit (Invitrogen). For quantitative PCR assays, cDNA was amplified in triplicate using Sybr Green qPCR mix (Applied Biosystems) and gene specific primers in a BioRad PCR thermocycler. Triplicate C_T values for each sample were then averaged and normalized to the correlate values for GAPDH.

Nanostring gene array analysis

After preparation, all RNA samples were analyzed using Nanostring reagents and technical specifications at the University of Minnesota Genomics Center. Briefly, for mRNA analysis, individual fluorescent bar codes conjugated to sequences which

recognize 100 bp regions for a panel of 230 cancer-related transcripts were hybridized to 100 ng of sample RNA overnight. These complexes were immobilized to a streptavidin-coated cartridge by a capture probe to allow for data acquisition and washed to remove excess probe. Cartridges were then placed in a Digital Analyzer which recognized each barcode as a single transcript and counted absolute values quantities for each. These values were then subjected to a technical normalization using Nanostring nSolver software in reference to hybridization controls, a set of housekeeping genes (CLTC, GAPDH, GUSB, HPRT1, PGK1, TUBB) and codes containing no transcript. In the case of miRNAs, a pre-hybridization step was utilized in which mature miRNA-specifc miR-tags were ligated to individual miRNAs. This miR-tag served as the hybridization target region. Using the normalized values, heat maps were created to show median-centered expression of each gene using Cluster 3.0 and JavaTreeView software algorithms applied to log2 transformed data.

Results

hESCs express hematopoietic transcription factors in a temporally distinct manor

We first wanted to determine if hESCs undergoing hematopoietic differentiation express crucial regulators of hematopoiesis in a stepwise-fashion similar to mice. To do this, we co-cultured H9 hESCs with mouse M2-10B4 bone marrow-derived stroma in serum containing media, a method we have regularly used for supporting hematopoiesis from pluripotent cells[68,76,167]. We then analyzed BRACHYURY, PU.1, RUNX1c,

RUNX1b, GATA1 and GATA2 at various time points by RT-PCR to determine their relative levels and patterns of expression. BRACHYURY was expressed up to day 7 but not thereafter, consistent with mesodermal development (Supplementary Figure 1.1A). At this time, expression of RUNX1b, the predominant RUNX1 isoform detected in both primitive and definitive hematopoiesis, and GATA2, which binds the PU.1 promoter to suppress myeloid development was detected (Supplementary Figure 2.1A)[119,128]. Subsequently, by day 14, GATA1 gradually increased corresponding with a gradual decrease in GATA2, consistent with the "GATA switch" seen in mouse, wherein GATA1 suppresses expression of GATA2 by displacing it from the chromatin as hematopoietic progenitors progress to more mature lineages (Supplementary figure 1.1A)[168]. Between days 18 and 25, RUNX1c expression gradually increased with PU.1 immediately following on Day 25 (Supplementary figure 1.1A). This pattern corresponds to mouse *in vivo* studies which demonstrate that Runx1c expression follows that of Runx1b with subsequent expression of PU.1 in further restricted myeloid progenitors[129,160,161]. Flow cytometric analysis demonstrating a large increase in committed, $CD34^{+}CD45^{+}$ hematopoietic progenitors on day 25 further substantiated the RT-PCR data (Supplementary Figure 2.1B). Together, these results suggest that hESCs express crucial transcription factors in a temporal fashion over hematopoietic commitment similar to mouse

Generation of transgenic Runx1c reporter hESCs and iPSCs

Tracking the emergence of early, definitive hematopoietic progenitor cell populations containing HSCs from hESCs requires a reporter gene which distinguishes not only hematopoietic from non-hematopoietic cells, but also specifically identifies definitive cells within the hematopoietic compartment. The *RUNX1c* P1 distal promoter has been shown to be specifically associated with emerging HSCs in the aorta-gonad-mesonephros (AGM)[160,164]. Likewise, hematopoietic cells from the mouse embryo displaying P1 and Runx1b proximal P2 promoter activity are enriched for definitive hematopoietic potential in the CFU assay as opposed to cells showing P2 activity alone[158,160]. Both promoters require the +24 intronic enhancer for hematopoietic specific expression[161,163]. Therefore, we constructed a reporter cassette using conserved regions of the human *RUNX1* locus showing homology to the mouse P1 promoter and +24 enhancer to track definitive hematopoietic differentiation from hESCs and iPSCs. A 1 kb fragment of the P1 promoter and 250 bp of a conserved intronic region representing the human +24 enhancer were cloned from H9 hESC genomic DNA (Figure 1.1A). Both of these fragments were inserted flanking tdTomato (tdTom) cDNA to best represent the layout of the endogenous locus. Immediately upstream we included a constitutively driven GFPzeo fusion gene to easily identify and select for cells with a successfully integrated transgene (Figure 1.1A). Initial testing of this construct in K562, a leukemic cell line known to express RUNX1c, demonstrated activity of the regulatory elements through tdTom expression, while an alternative construct without the P1 promoter or +24 enhancer added did not show tdTom expression, giving us confidence that the MCAG

promoter would not inappropriately drive tdTom (Supplementary Figure 1.2A,B). Using the pKT2 transposon as a backbone, this entire construct was stably inserted into H9 hESCs as well as an umbilical cord blood (UCB) derived iPSC line by co-nucleofection with a plasmid containing the *Sleeping Beauty (SB)* transposase. We have previously demonstrated SB to be highly efficient at stable gene modification in hESCs[169]. After selection for hESCs and iPSCs containing the stably inserted transgene, single cell clones were obtained. For both the hESC and iPSC reporters, two clones were carefully analyzed for the ability to undergo hematopoietic differentiation. There was no discernable difference in the pattern and overall timing of hematopoietic marker expression among all four clones and an hESC line which did not contain the transgene (Supplemental figure 1.3). This consistency among individually derived clones and non-transgenic hESCs indicated that hematopoietic differentiation was not effected by the presence or position of the transgene. Karyotypic analysis showed no sign of obvious genetic abnormalities in either reporter line used for these studies (Supplementary figure 1.4).

The human P1 promoter and +24 enhancer elements drive tdTomato expression mimicking that of endogenous RUNX1c.

To test whether the human *RUNX1c* cis-regulatory elements in our transgene would drive expression of the tdTomato (tdTom) reporter to faithfully represent expression of endogenous RUNX1c, we used the spin embryoid body (EB) method for hematopoietic differentiation of the hESC reporter. With the spin EB method, single-cell

adapted hPSCs are evenly distributed in a 96 well plate where they aggregate into EBs while undergoing mesoderm development and early hematopoietic commitment. After 5-6 days, they are then transferred to a 24-well plate and subjected to additional hematopoietic cytokines (Supplementary Figure 1.5). Under these conditions, we saw the first $CD34^+$ and $CD31^+$ hematoendothelial cells arise by day 3 (Figure 1.1B). By day 7 an initial wave of early hematopoietic cells expressing CD41a or CD43 could be seen, while more mature populations expressing CD45 typically did not emerge until around day 12 (Figure 1.1B). It was at this point that we also saw the first $tdTom^+$ cells (Figure 1.1C). The emergence and proliferation of the $tdTom^+$ population directly correlated with an increase in endogenous RUNX1c expression by qPCR (Figure 1.1D). Specificity of tdTom expression in $RUNX1c^+$ cells is further demonstrated by enrichment for endogenous RUNX1c transcript in the sorted $tdTom^+$ population as compared to unsorted and $tdTom^-$ cells, which had near undetectable levels of RUNX1c (Figure 1.1E). Because $CD73^+$ mesenchymal/stromal cells are also produced in these EB conditions, we analyzed our $tdTom^+$ cells for CD73. Notably, all $CD73^+$ cells are $tdTom^-$, indicating that tdTom expression was specific for the developing hematopoietic populations (Figure 1.1F). Finally, we observed by fluorescent microscopy that tdTom expression was first visible in the non-adherent, cobblestone-like hematopoietic cells which began proliferating days 11-13 (Figure 1.1G). Together, these results suggest that our reporter system faithfully reports the expression of RUNX1c in human cells and that RUNX1c expression is limited to hematopoietic populations.

tdTomato expression enriches for hematopoietic progenitors and is restricted to sub-sets of hematoendothelial progenitors

We next wanted to determine which early endothelial and hematopoietic cell surface antigens were expressed on the tdTom$^+$ cells. All of the emerging populations expressing CD34, CD31, CD41a, CD43 and CD45 initially lacked tdTom expression, though each turned tdTom$^+$ at later time points (Figure 1.2A). By day 12, the first cells positive for tdTom were CD31$^+$, CD43$^+$, CD34$^+$, CD45$^-$ and showed mixed expression for CD41a (58 +/- 15%) (Figure 1.2A and B). As the tdTom$^+$ cells expanded past 20% of the total population at day 17, the CD34 expression decreased to 14.7 +/- 5.6% of total tdTom+ cells, while CD45 increased to 64.4 +/- 21.8%, indicating that the initial wave had differentiated into more mature lineages (Figure 1.2A,C). CD31 and CD43 continued to be expressed on the vast majority of tdTom$^+$ cells, with tdTom being restricted to the CD31^{low}, CD43^{hi} subsets (Figure 1.2A,C). CD41a showed no discernable change in expression on the tdTom$^+$ population at 50.7 +/- 23.5% after expansion of the initial wave (Figure 1.2C). CD235a, a marker for erythrocytes[170] and CD45RA, which is absent on multi-potent HSCs with T-cell potential[25,171,172] showed limited to no expression on the emerging tdTom$^+$ population (Supplementary figure 1.5D).

We also wanted to analyze the CD34$^+$CD45$^+$ and CD34$^+$CD43$^+$ populations for expression of tdTom since these markers enrich for hematopoietic progenitors[68,74,173,174]. At both the points of tdTom emergence and expansion, neither of these populations showed significant enrichment for tdTom over the bulk population (Figure 1.2D-F),

indicating that these cells are heterogeneous for expression of RUNX1c, with a majority of them lacking it. As a more functional assay, we found that the isolated tdTom^{+} cells were enriched for hematopoietic progenitors, demonstrated by increased ability to form typical hematopoietic colonies (430 +/- 143 per 10^5 cells) as compared to both tdTom negative (131 +/- 15 per 10^5 cells) and unsorted cells (163 +/- 28 per 10^5 cells) (Fig 1.2G).

Fluorescent microscopy of the differentiating EBs showed tdTom expression to vary in intensity within the non-adherent, hematopoietic population. On day 12, when the first emerging tdTom^{+} cells could be detected by flow cytometry, we noticed single tdTom^{bright} cells that were often associated with the adherent, tdTom^{-} endothelial outgrowths (Figure 1.3A,B). We were also able to see rare instances of tdTom expression in what appeared to be cells of endothelial origin (Figure 1.3C-F). It is hard to speculate on the frequency of these cells or the exact time they appeared due to their rarity, meaning they may not have been detected by flow cytometric analysis. In some instances, we noticed an endothelial cell which appeared to be giving rise to a tdTom^{+} hematopoietic cell through asymetrical division (Figure 1.3D-F). These results suggest that the emerging tdTom^{+} cells are produced by rare cells of the adherent layer, which is consistent with early stages of *in vivo* hematopoiesis wherein the hemogenic endothelium of the AGM begins to express Runx1 before giving rise to a RUNX1^{+} definitive HSC[44,124,160,175].

Inhibition of primitive hematopoiesis through the Activin/Nodal pathway increases the proliferation of tdTom$^+$ cells.

In order to test whether expression of our RUNX1c reporter could distinguish between primitive and definitive hematopoietic populations, we applied a known inhibitor of Activin/Nodal signaling, SB-431542. Activin is known to be required for the development of primitive erythrocytes in mouse embryonic stem cells (mESCs)[35,176]. It has recently been shown that use of SB in hESC differentiation cultures restricts the development of primitive erythroid progenitors, which originated from the CD34$^+$CD43$^+$ subset, while promoting definitive progenitors with T-cell potential from a select CD34^{hi}CD43$^-$ population[103]. Our initial studies showed that application of SB within the first day of differentiation completely ablated hematopoietic development, while applying it days 3 and beyond showed little to no effect on the differentiation (Supplemental figure 1.6). Applying the inhibitor from days 2-5 during mesoderm specification gave an optimal effect with substantial inhibition of CD34$^+$CD43$^+$ and CD34$^+$CD41a$^+$ cells (Figure 1.4A). At earlier stages, between days 7 and 12, we saw the largest decrease in CD34$^+$CD43$^+$ and CD34$^+$CD41a$^+$ populations, as well as a near complete loss of primitive erythroid progenitors in the CFU assay, consistent with previous studies[103] (Fig 1.4A,B). Similar to our previous findings with this reporter, tdTom$^+$ cells first emerged between days 12-14 in both SB and untreated samples. Notably, the tdTom$^+$ fraction increased 2-fold in SB treated samples, accompanied by a 2-fold increase in proliferation (Figure 1.4C,D). Furthermore, sub-gating on the CD34$^+$CD43$^+$ and CD34$^+$CD45$^+$ populations demonstrated each to be enriched 2 fold for percentage of tdTom expressing

cells over the untreated group (Fig 1.4E,F). These results suggest that inhibition of primitive hematopoiesis in our differentiation cultures, while not affecting the timing of tdTom emergence or pattern of expression within progenitor subsets, did promote the expansion of $tdTom^+$ ($RUNX1c^+$) cells.

iPSC RUNX1c reporter displays similar characteristics

To test whether the RUNX1c reporter construct used in our H9 hESCs would yield similar results in alternative human pluripotent cells, we inserted our RUNX1c reporter into an iPSC line that had been derived in our lab from $CD34^+$ UCB cells, which we termed Dub7 (Supplemental Figure 1.7). Our group has previously demonstrated effective hematopoietic development from the Dub7 line as well as other human iPSCs [177]. We again derived individual clones which had successfully integrated the transgene. As with the hESC reporter, the emergence and expansion of $tdTom^+$ cells closely correlated with expression of endogenous RUNX1c (Supplemental Figure 1.8A). Fluorescent microscopy demonstrated tdTom expression to be specific for non-adherent hematopoietic cells, as opposed to the expanding stromal layers (Supplemental Figure 1.8B). Additionally, sorted $tdTom^+$ cells were found to be enriched for endogenous RUNX1c transcripts compared to both $tdTom^-$ and unsorted populations (Figure 1.5A). As such, we demonstrated that the reporter transgene accurately reflected expression of endogenous RUNX1c in the Dub7 iPSC line.

Flow cytometric analysis demonstrated tdTom coexpression patterns with hematopoietic cell surface antigens very similar to the H9 hESC reporter line, with

tdTom$^+$ cells being restricted to the CD31$^+$ and CD43$^+$ compartments, while CD73, CD45RA and CD235A were expressed almost exclusively on tdTom$^-$ cells (Fig 1.5 B-G). iPSC-derived tdTom$^+$ cells were enriched for hematopoietic progenitors compared to tdTom$^-$ and unsorted cells as demonstrated by the CFU assay (Figure 1.5H). Additionally, we subjected the differentiating cells to the activin/nodal SB inhibitor as with the hESC reporter. Similar to the hESCs, we found optimal inhibition for increased hematopoietic development between days 2-5 of differentiation. Though the increase in tdTom$^+$ cells was not as robust in the SB treated iPSC samples, we did consistently demonstrate greater tdTom expression in CD31$^+$, CD41a$^+$, CD43$^+$ and CD45$^+$ cells (Fig 1.5I). Taken together, these data demonstrate that RUNX1c has a similar expression pattern during hematopoietic development in iPSCs and hESCs.

Genetic Analysis of hematopoietic populations

We next evaluated gene expression patterns between our hESC and iPSC-derived hematopoietic populations and CD34$^+$ UCB / CD34$^+$ fetal liver (FL). Both UCB and FL contain HSCs and have robust SRC capability[178-180]. We conducted gene array analysis using a panel of 230 hematopoietic/cancer-related genes as well as 800 miRNAs. Undifferentiated, tdTom$^+$, tdTom$^-$, CD34$^+$CD45$^+$ and CD34$^+$CD43$^+$ populations were collected on day 13 of Spin EB differentiation from both the hESC and iPSC RUNX1c reporter cell lines. We also analyzed CD34$^+$CD45$^+$ cells isolated from UCB and FL. Clustering within the mRNA samples showed similarity between all hESC and iPSC-derived CD34$^+$CD45$^+$, CD34$^+$CD43$^+$ and tdTom$^+$, with the tdTom$^-$ and undifferentiated

sources grouping separately (Figure 1.6A). The $CD34^+$ UCB/FL clustered within the same tree as the hESC and iPSC-derived hematopoietic cells, but established an entirely separate branch. Thus, we were able to define clear differences in expression patters between these samples and the hESC/iPSC-derived cells. Interestingly, we noticed an upregulation of genes commonly associated with cell proliferation in hPSC-derived samples as compared to UCB and FL, including CCND1, CCND3 and BRCA1 (Figure 1.6B).

miRNA analysis was conducted using the same RNAs. To more closely examine only relevant transcripts, total normalized expression for each miRNA was averaged across all hematopoietic samples (excluding $tdTom^-$ and undifferentiated cells) and the top 105 were used for cluster analysis (Figure 1.6C). As with the mRNAs, the hPSC-derived hematopoietic samples and 34^+ UCB/FL clustered separately from the $tdTom^-$ and undifferentiated cells. Furthermore, 34^+ UCB and FL were again clustered together, revealing groups of miRNAs with distinct expression patterns when compared to the hPSC-derived samples. The most clear example of this was the Let-7 miRNA family, including Let-7a, Let-7b and Let-7g, which all showed increased expression in UCB and FL (Figure 1.6D). Interestingly, Let-7a has been shown to target CCND1 both directly and indirectly to suppress cell proliferation[181-185]. Our gene array data also demonstrates mir181a to be upregulated 10-fold in $CD34^+$ UCB as compared to any of the hESC or hPSC-derived samples (Figure 1.6D). miR181a has previously been found to be upregulated in $CD34^+CD38^-$ UCB as compared to the slightly more committed

$CD34^+CD38^+$ progenitors[138]. Furthermore, ectopic expression of mir181 in hematopoietic stem/progenitor cells has been shown to enhance B-cell development[186].

Finally, we conducted qPCR analysis for individual genes within the HoxA cluster, as these have been reported to have reduced expression in hPSC-derived samples as compared to SRCs[187]. Notably, we found that the sorted $tdTom^+$ population from both the hESC and iPSC reporter lines have reduced expression for all genes tested within the HoxA locus (Figure 1.6E). Taken together, this genetic analysis demonstrates that there are numerous key hematopoietic mRNAs and miRNAs which are deficient for expression in both hESC and iPSC-derived hematopoietic progenitors as compared to populations known to contain SRCs.

The hESC and iPSC-derived $tdTom^+$ fractions do not contain LTC-IC

We have recently shown that hESC-derived $CD34^+CD45^+$ and $CD34^+CD43^+$ cells developed through the Spin EB system, though able to proliferate and produce CFU for 2 weeks, were not able to maintain in culture for 5 weeks, thus suggesting that they do not contain LTC-IC, providing further evidence regarding their inability to engraft in immunodeficient mice (unpublished). This is in contrast to $CD34^+$ UCB, which do contain LTC-IC and display robust engraftment. Given that both the hESC and iPSC-derived $tdTom^+$ populations were enriched in hematopoietic progenitors and showed gene expression patterns similar to hPSC-derived hematopoietic progenitor populations and $CD34^+$ UCB, we subjected them to the LTC-IC assay to determine if they would be able to maintain in long-term culture. Interestingly, after 2 weeks of co-culture with M2-10B4

stromal cells, we noticed that while a majority of the sorted $tdTom^+$ population maintained a non-adherent, hematopoietic morphology (Figure 1.7A), some of them had lost tdTom expression and attached to the plate surface, gaining an endothelial morphology (Figure 1.7B), while others became adherent and maintained tdTom expression (Figure 1.7C). Flow cytometric analysis confirmed that 5% of the GFP^+ fraction, presumably derived from the sorted $tdTom^+$ cells, had lost expression of tdTom and were $CD45^-CD31^+$ (Figure 1.7D). The remaining 95% of the GFP^+ cells maintained tdTom expression and were $CD34^-CD31^+CD43^+CD45^+$ (Figure 1.7D). Moreover, a portion of the $tdTom^+$ displaying a hematopoietic morphology could be seen lodged under and around the GFP^+ endothelial cells (Figure 1.7E,F). Just as in the Spin EB differentiation culture, we could see instances of $tdTom^+$ endothelial cells giving rise to $tdTom^+$ hematopoietic cells, again mimicking the endothelial to hematopoietic transition (Figure 1.7G). However, despite an enhanced ability for $tdTom^+$ fraction to produce CFU immediately post-sort, they failed to proliferate or produce CFU at both 3 and 5 weeks after entering the assay, suggesting that these cells do not contain LTC-ICs and thus would more than likely fail to engraft in immunodeficient mice (data not shown).

Discussion:

In the present study, we have shown that the distal P1 promoter and +24 intronic enhancer that regulate *RUNX1c* expression have increased activity in a specific subpopulation of hematopoietic cells derived from both hESCs and iPSCs. Isolation of the $RUNX1c^+$ ($tdTom^+$) cells derived from hESCs and iPSCs demonstrates this

population has a distinct genetic signature based on both mRNA and miRNA expression compared to hematopoietic cells isolated by typical phenotypic surface antigens such as CD34, CD41, CD43, and CD45. While other studies have previously examined the phenotypic qualities of Runx1c-expressing cells using reporter models in both zebrafish and mice, to our knowledge this is the first such report developed in human pluripotent stem cells. Previous *in vitro* and *in vivo* studies evaluating expression of the three Runx1 isoforms during mouse development have found the onset of Runx1c expression to be specific for emerging, definitive mESC-derived HSCs, as opposed to Runx1b and Runx1a, which were expressed throughout hematopoiesis[160]. Furthermore, the same report found increased Runx1c expression in the AGM region of E10.5-E11.5 mouse embryos, where the first definitive HSCs arise[160].

It can be noted that the design of our minimal promoter/enhancer reporter system differs from the knock-in reporter systems that have been used for other studies of hematopoiesis from hESCs[188,189]. However, the construct used for these studies does contain ample portions of the P1 promoter and +24 enhancer from hESC genomic DNA as dictated by homology to regions utilized for similar reporter systems which have been successful in mice[161,164]. Our results demonstrate excellent specificity of RUNX1c expression in the $tdTom^+$ cells. Specifically, we show a complete lack of tdTom in non-hematopoietic tissues such as the $CD73^+$ cells, and the timing of tdTom expression closely correlates with that of endogenous RUNX1c. Furthermore, there is an advantage to use of our reporter construct based on the efficiency to engineer multiple cell lines using the *Sleeping Beauty* system over a short period of time. Indeed, we are able to use

both hESCs and iPSCs for these studies. From both hESCs and iPSCs, we were able to generate several transgenic clones and validate consistency in both overall hematopoietic differentiation and expression of the tdTom/RUNX1c reporter construct. This comparison between different starting cell populations provides greater confidence the expression patterns seen were not a consequence of transgene integration effects. Additionally, use of this transgene system can avoid problems associated with haploinsufficieny that may be seen with direct knock-in approaches[155,190]

One possible point of contention may be over the relative contributions between the promoter and enhancer, and whether they are working cumulatively, as would be expected, or if just one of them is active in our system. One study by Markova *et al* examining differential activity of both the P1 and P2 promoters as well as two enhancer elements, including the +24 enhancer, in several human cell lines provides some insight[191]. Here, the P1 was silent in HEK293 endothelial cells, which showed low P2 activity, and that both promoters were active in K562 erythroid cells and Jurkat lymphoid cells, with P2 showing 10-fold more activity in K562 than P1. Inclusion of the +24 enhancer increased activity of both promoters in Jurkat cells but not HEK293, which would appear to support mouse *in vivo* data showing enhancer activity to be specific for hematopoietic tissues[161,163,164]. This information, combined with the evidence that our reporter was specific for hematopoietic tissues and could even be seen in some putative differentiating hematoendothalial cells, leads us to believe that, at a minimum, the enhancer must be active in our system. It is difficult to speculate on the activity of the P1 promoter. Consequently, we cannot rule out the possibility that tdTom expression was

representative of enhancer activity alone rather than RUNX1c specifically, though this information would indeed still be valuable.

These studies demonstrate that emerging tdTom$^+$ populations of hematopoietic cells appears to recapitulate mouse and zebrafish systems[164,175]. Lam *et al* used a Runx1-eGFP zebrafish reporter to demonstrate Runx1 expression in aortic endothelial cells (ECs) subsequent to emergence of definitive HSCs, while Ng *et al* found pronounced +24 enhancer activity specific to ECs lining the ventral wall of the dorsal aorta along with the associated HSC clusters. Though such *in vivo* models are not feasible in humans, Park *et al* used hESCs and hiPSCs to show large quantities of CD34$^+$CD45$^+$ hematopoietic progenitors arising directly from the adherent EC population, suggesting that a similar bipotential hematoendothelial subset exists in human hematopoietic ontogeny[78]. Our finding through fluorescent microscopy that the RUNX1c reporter is expressed in rare but visible adherent endothelial cells which in some cases appeared to be undergoing asymmetrical cell division giving rise to a tdTom$^+$ hematopoietic cell correlates with each of these studies and provides further evidence for the role of *RUNX1c* in the human endothelial to hematopoietic transition. This conclusion is also supported by our finding that all tdTom expressing cells were positive for the hematoendothelial marker CD31.

Our mRNA and miRNA genetic analysis provides some potentially valuable insight regarding the engraftment deficiencies of hESC/iPSC-derived hematopoietic progenitors as compared to UCB and FL. While it seems probable that culture conditions are a cause of this discrepancy, determining variations in specific gene expression networks will help to explain exactly what these deficiencies are. We have identified

several miRNAs, including the Let-7 family and mir181a, which are underexpressed in hESC/hPSC derived cells as compared to $CD34^+$ UCB/FL. This was then supported by an increase in cell cycle/proliferation-promoting genes *CCND1*, *CCND3* and *BRCA1*, highlighting potential miRNA-mRNA interactions involved with these networks. These pathways have implications regarding crucial HSC qualities such as quiescence and multilineage differentiation. Furthermore, similar to studies showing a positive role for HoxB4 in mESC-derived progenitor engraftment[106,107], we have demonstrated that expression from the HoxA locus appears to be deficient in our hESC/iPSC-derived progenitors.

Though RUNX1c delineates putative definitive HSCs in mice, additional characterization of $RUNX1c^+$ human cells as well as selection on the basis of other key transcription factors is necessary. Regulatory elements for several other hematopoietic transcription factors such as Pu.1 and C/EBPα, both direct targets of RUNX1 and critical regulators of myeloid development, may also be utilized to create reporters[128,130,133,192]. Indeed, using the system described here to quickly and efficiently create minimal promoter/enhancer reporter cell lines from hESCs and iPSCs will allow us to readily accumulate profiles on other specific subpopulations of cells that express critical transcription factors (or multiple transcription factors) to potentially better isolate and define a truly functional, definitive HSC derived from hESCs and iPSCs. Finally, our genetic analysis of hESC/hiPSC-derived $tdTom^+$, $CD34^+CD45^+$ and $CD34^+CD43^+$ cells in comparison to $CD34^+$ UCB/FL provides numerous potential targets for gene modification which could make production of HSCs from hESCs and iPSCs a possibility.

Figure 1.1. RUNX1c reporter construct design and differentiation of transgenic cells. Stable integration of a reporter driven by *RUNX1c* regulatory elements into H9 hESCs allows for fluorescent labeling of emerging RUNX1c^{+} hematopoietic populations over a directed differentiation time course. **A.** The RUNX1c reporter was constructed using 1 kb of the human endogenous RUNX1c promoter (P1), placed directly upstream of tdTom, and 250 bp of the +24 intronic enhancer, placed directly downstream of tdTom to mimick the layout of the endogenous locus. Both the promoter and enhancer have been shown in murine studies to be essential for faithful, hematopoietic-specific expression of a Runx1c reporter. A constitutive GFPzeo fusion gene follows the reporter to allow for positive selection of cells obtaining the transgene. The entire cassette lies between the T2 IR/DR transposon elements for stable genomic insertion by the *Sleeping Beauty* transposase. **B.** Hematopoietic differentiation of the H9 hESC RUNX1c reporter as Spin EBs. EBs were disaggregated and analyzed for co-expression of hematopoietic extra-cellular markers on days 3, 7 and 12. **C.** Similar hematopoietic differentiation of the H9 hESC RUNX1c reporter as in 1.1B but with flow cytometric analysis for expression of the tdTom reporter. **D.** Time-course differentiation with analysis of disaggregated EBs on days 11-14 for the %tdTom^{+} proportion by flow cytometry as well as expression of endogenous RUNX1c by qPCR. Graphic bars represent the average from 4 independent experiments. **E.** Day 13 post-sort qPCR analysis. tdTomato^{+} cells show enrichment for endogenous RUNX1c transcript over both the tdTomato^{-} and pre-sort populations. Graphic bars represent the average and standard error from three

independent experiments. **F.** Differentiated reporter cells expressing the mesenchymal marker CD73 do not express tdTom. **G**. Fluorescent microscopy of day 21 Spin EBs showing a large expansion of hematopoietic cells which are tdTom^{+}.

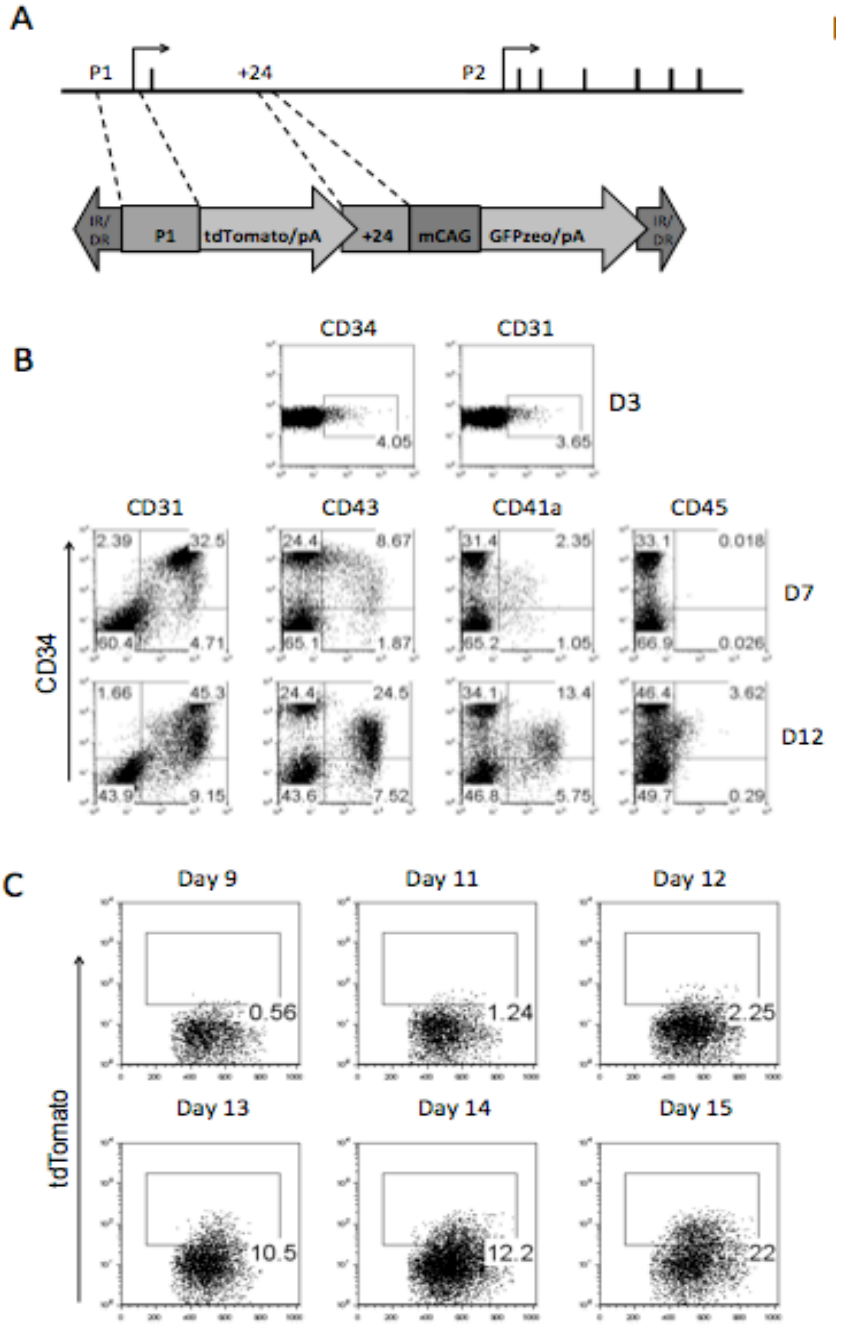

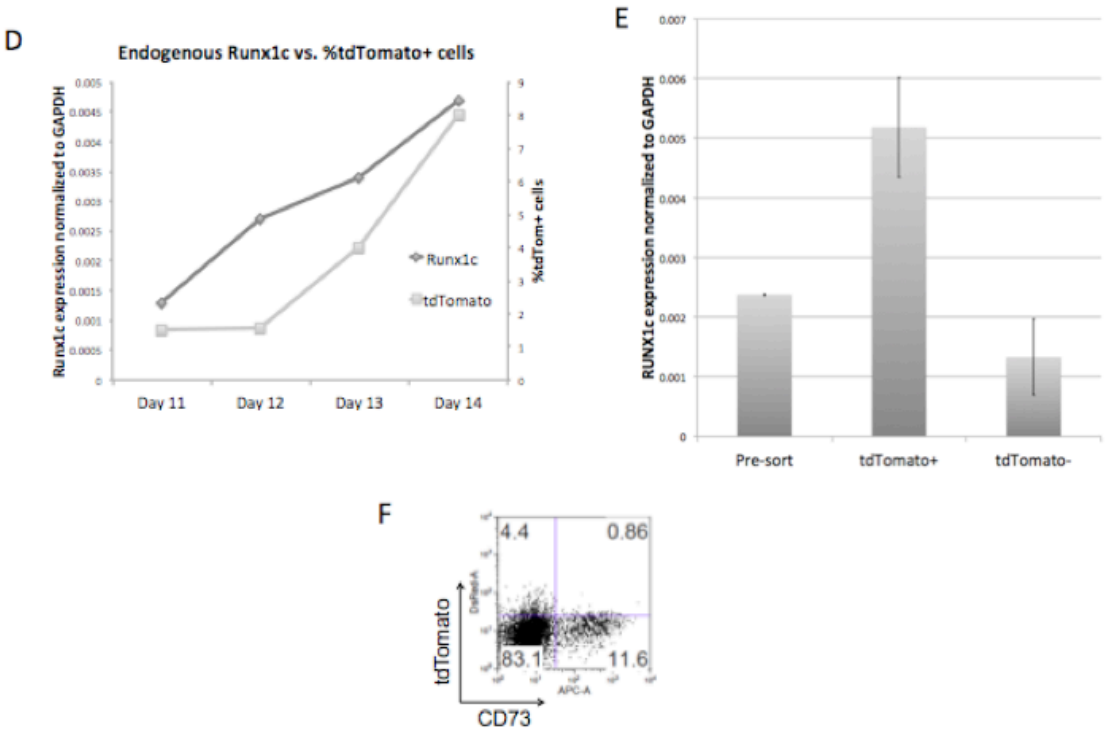
D
Endogenous Runx1c vs. %tdTomato+ cells
Runx1c expression normalized to GAPDH
%tdTom+ cells
Runx1c
tdTomato
Day 11
Day 12
Day 13
Day 14
E
RUNX1c expression normalized to GAPDH
Pre-sort
tdTomato+
tdTomato-
F
4.4
0.86
83.1
11.6
tdTomato
CD73
G

Figure 1.2: Hematopoietic progenitor potential and phenotypic analysis of tdTom$^+$ cells. **A.** Flow cytometric analysis of RUNX1c reporter over hematopoietic differentiation time course for tdTom and various hematoendothelial markers. **B**. Flow cytometric analysis of emerging tdTom$^+$ cells when they were less than 10% of the total population. Shown is the percent of the tdTom population expressing either CD34, CD31, CD43, CD41a or CD45. **C**. Similar analysis to Figure 1.2B but after tdTom$^+$ cells expanded to over 20% of the population. Graphic bars for B,C represent averages and standard error from 5 independent experiments. **D**. CD34$^+$CD45$^+$ and CD34$^+$CD43$^+$ cells were subgated and assessed for tdTom expression on days 13 and 15 of differentiation. **E,F**. Percent of CD34$^+$CD45$^+$ and CD34$^+$CD43+ cells expressing tdTom compared to the bulk population shows little to no tdTom enrichment in these hematopoietic progenitors at both the emerging (E) and expanded (F) tdTom time points. Graphic bars represent the average and standard error from four independent experiments. **G**. Hematopoietic progenitor potential of the tdTom$^+$ population as assessed by ability to form hematopoietic colonies in methylcellulose. H9 reporter cells were differentiated for 13 days as spin EBs then FACS sorted for tdTom expression and placed in CFU. Samples contained 1x10^5 cells at plating and colonies were enumerated after 6-7 days of incubation. Graphic bars represent the average and standard error from three independent experiments.

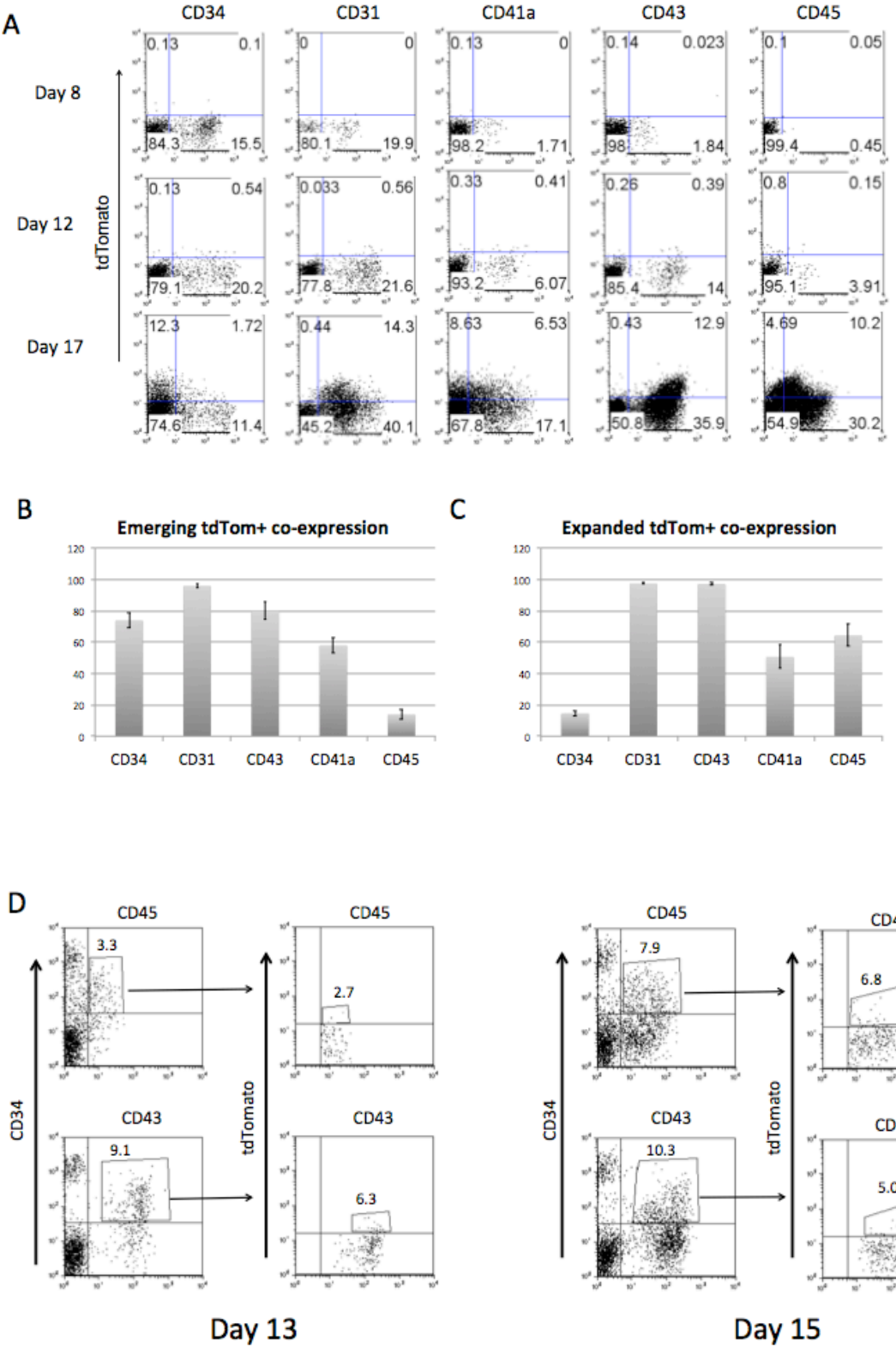
A
CD34
CD31
CD41a
CD43
CD45
Day 8
Day 12
Day 17
tdTomato
0.13
0.1
84.3
15.5
0
0
80.1
19.9
0.13
0
98.2
1.71
0.14
0.023
98
1.84
0.1
0.05
99.4
0.45
0.13
0.54
79.1
20.2
0.033
0.56
77.8
21.6
0.33
0.41
93.2
6.07
0.26
0.39
85.4
14
0.8
0.15
95.1
3.91
12.3
1.72
74.6
11.4
0.44
14.3
45.2
40.1
8.63
6.53
67.8
17.1
0.43
12.9
50.8
35.9
4.69
10.2
54.9
30.2
B
Emerging tdTom+ co-expression
120
100
80
60
40
20
0
CD34
CD31
CD43
CD41a
CD45
C
Expanded tdTom+ co-expression
120
100
80
60
40
20
0
CD34
CD31
CD43
CD41a
CD45
D
CD45
3.3
CD45
2.7
CD43
9.1
CD43
6.3
CD34
tdTomato
Day 13
CD45
7.9
CD45
6.8
CD43
10.3
CD43
5.0
CD34
tdTomato
Day 15

E

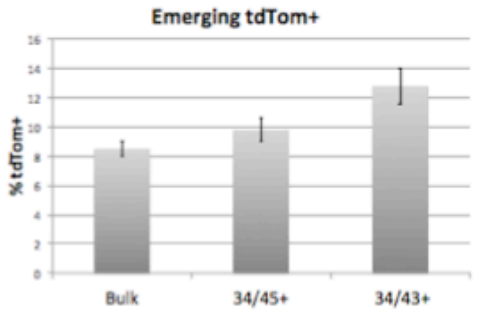
Emerging tdTom+
% tdTom+
16
14
12
10
8
6
4
2
0
Bulk
34/45+
34/43+

F

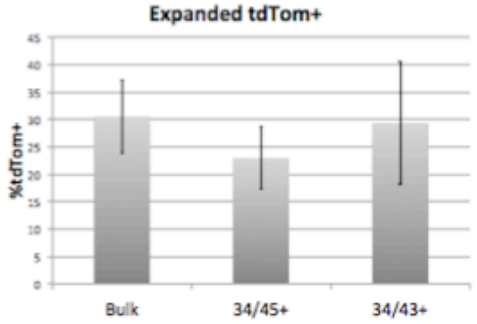
Expanded tdTom+
%tdTom+
45
40
35
30
25
20
15
10
5
0
Bulk
34/45+
34/43+

G

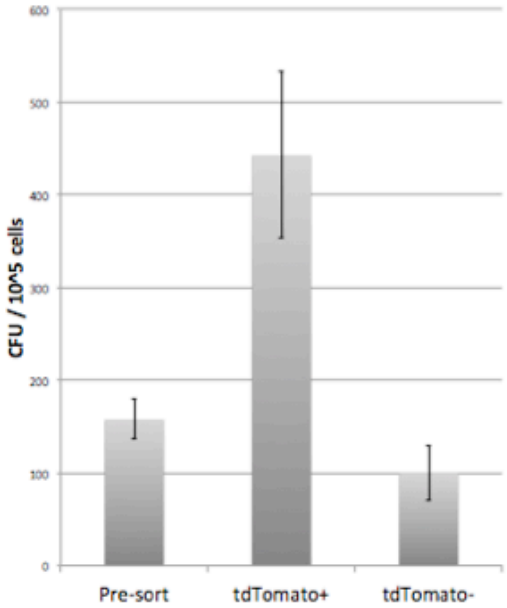
CFU / 10^5 cells
600
500
400
300
200
100
0
Pre-sort
tdTomato+
tdTomato-

Figure 1.3: Fluorescent microscopy of H9 hESC RUNX1c reporter line differentiating under hematopoietic conditions. A,B. Day 13 cells viewed under 20x magnification. A single $GFP^{+}tdTom^{bright}$, non-adherent hematopoietic cell can be seen among several $GFP^{+}tdTom^{-}$ hematopoietic cells. **C-F**. Day 13 unsorted cells imaged under 40x magnification. tdTomato expression can be seen in cells with both endothelial and hematopoietic morphology. In some cases, a $GFP^{+}tdTom^{-}$ endothelial cell can be seen giving rise to a $GFP^{+}tdTom^{Bright}$ cell through asymmetrical division (D-F). There were also instances of the endothelial cells being $tdTom^{Bright}$ themselves.

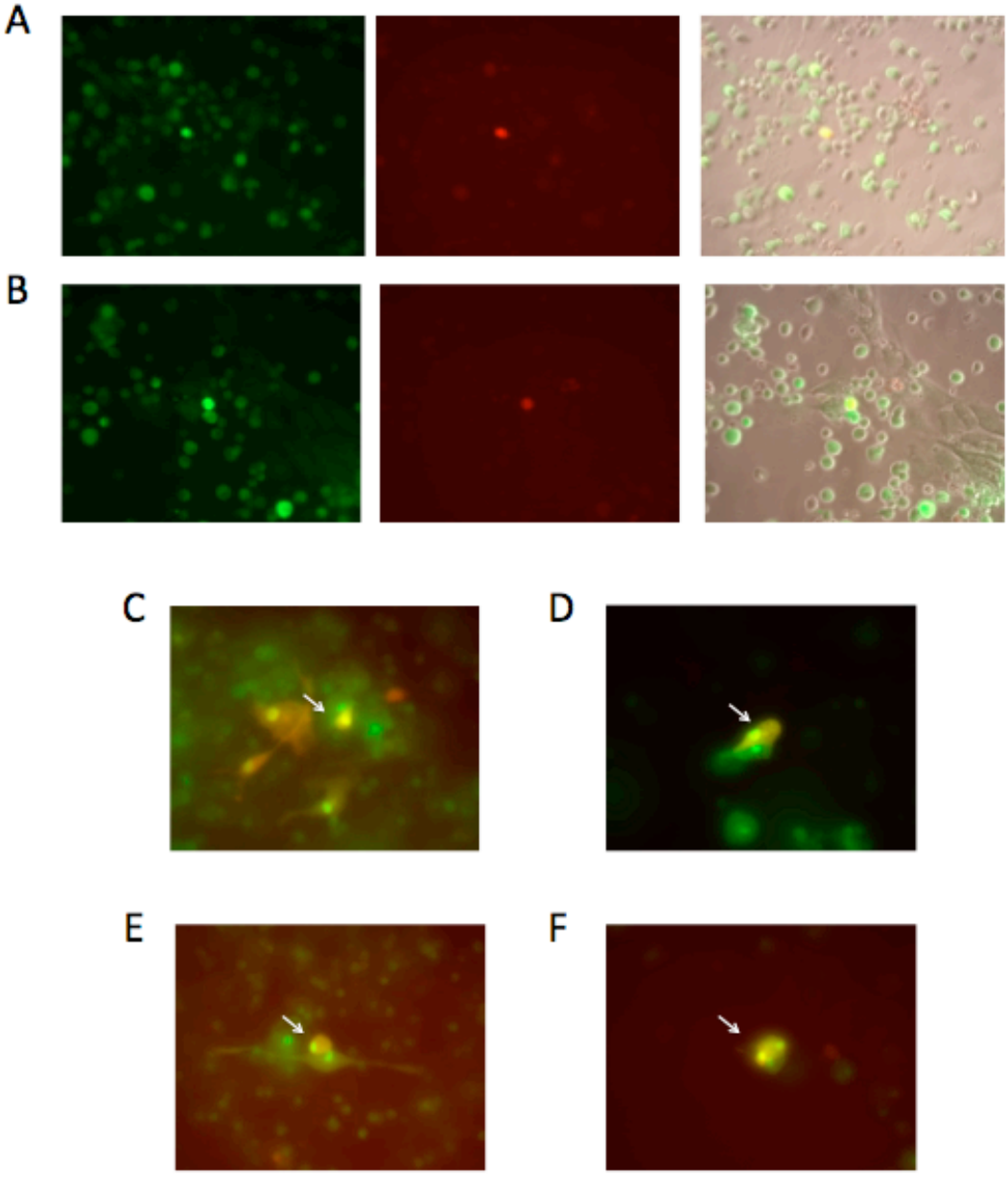
A
B
C
D
E
F

Figure 1.4: Inhibition of primitive hematopoiesis through activin/nodal signaling promotes proliferation of tdTom$^+$ cells. **A.** Day 14 flow cytometric analysis of the RUNX1c reporter for early hematopoietic markers with (SB) or without (NA) application of the SB inhibitor. **B**. Colony forming unit assay for cells harvested on day 12 of differentiation showing proportions of CFU-M, CFU-GM and CFU-E. **C.** Day 14 flow cytometric analysis of the RUNX1c reporter for early hematopoietic markers and tdTom with (SB) or without (NA) application of the SB inhibitor. **D**. Cell proliferation in differentiating EBs analyzed days 0-14. Numbers shown are cells per EB harvested. **E,F.** Assessment of tdTomato expression from the CD34$^+$CD45$^+$ and CD34$^+$CD43$^+$ populations for both untreated and SB treated samples. Graphic bars for B, D and F represent averages and standard error from three independent experiments.

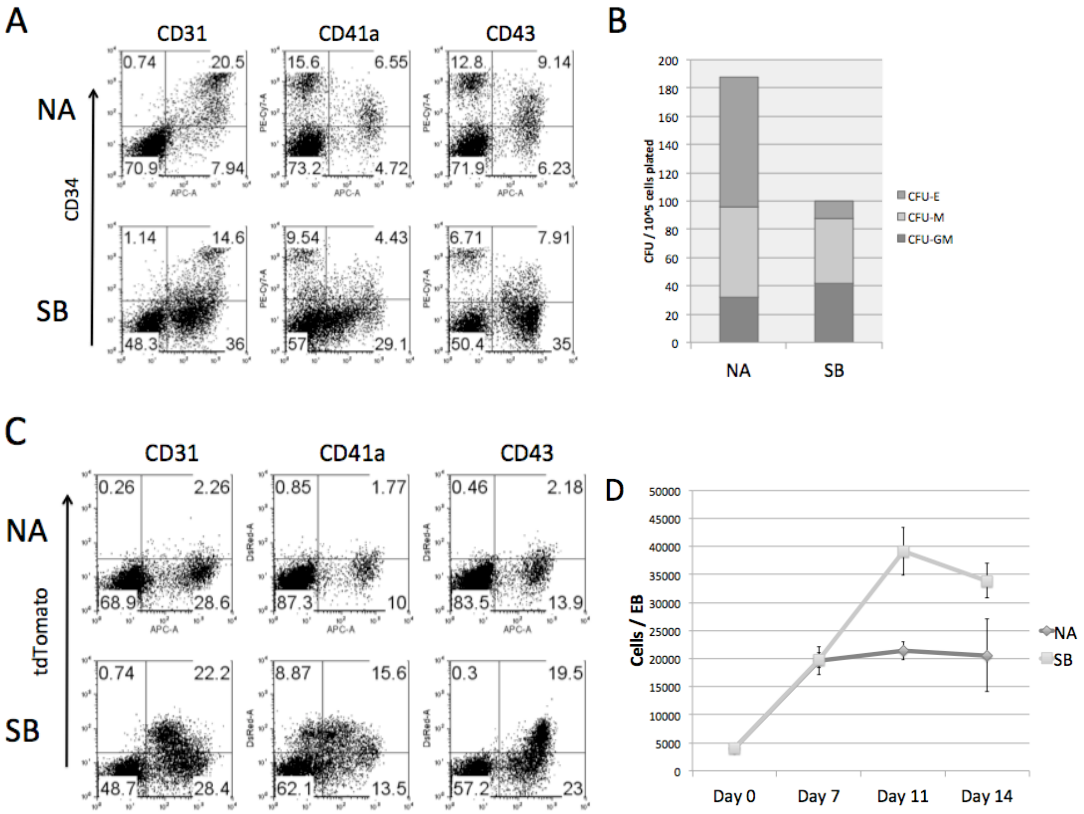

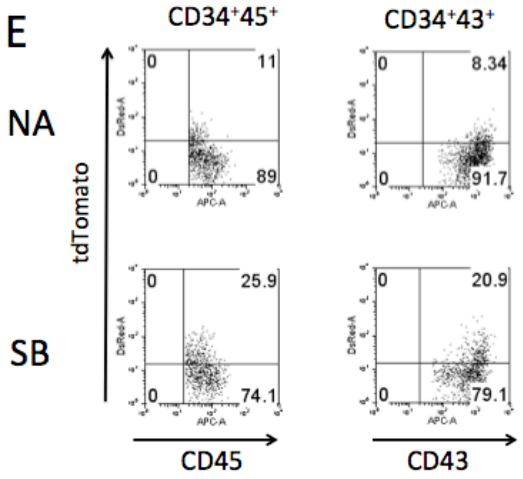
E
CD34+45+
CD34+43+
NA
SB
tdTomato
0
11
89
8.34
91.7
25.9
74.1
20.9
79.1
DsRed-A
APC-A
CD45
CD43

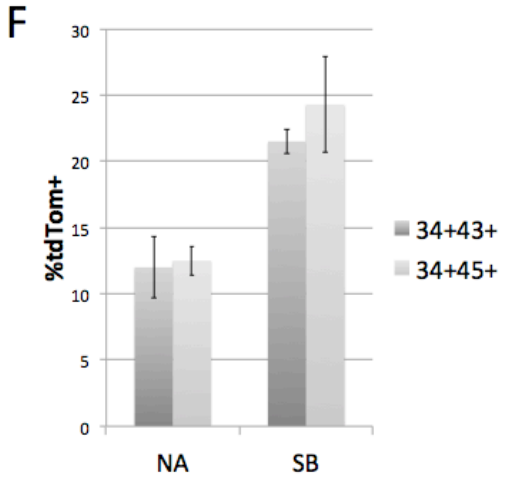
F
%tdTom+
30
25
20
15
10
5
0
NA
SB
34+43+
34+45+

Figure 1.5: Hematopoietic differentiation of human cord blood-derived iPSC RUNX1c reporter. **A.** qPCR analysis for expression of endogenous RUNX1c mRNA in Spin-EB differentiated tdTom^{+} cells vs. the unsorted and tdTom^{-} population. **B-G.** Flow cytometry for co-expression of tdTom with various hematoendothelial and hematopoietic extra-cellular markers in differentiating reporter cells. **H.** Colony forming unit assay enumerating hematopoietic progenitors from Spin-EB derived tdTom^{+} cells vs. the unsorted and tdTom^{-} population. **I.** Flow cytometric analysis showing the effect of SB Activin/Nodal inhibitor on expression of tdTom with various hematopoietic extra-cellular markers over hematopoietic differentiation. Cells were analyzed between days 12 and 14 depending on the timing of the expression of tdTom and the extra-cellular marker. Graphic bars for A and H represent averages and standard error from two independent experiments.

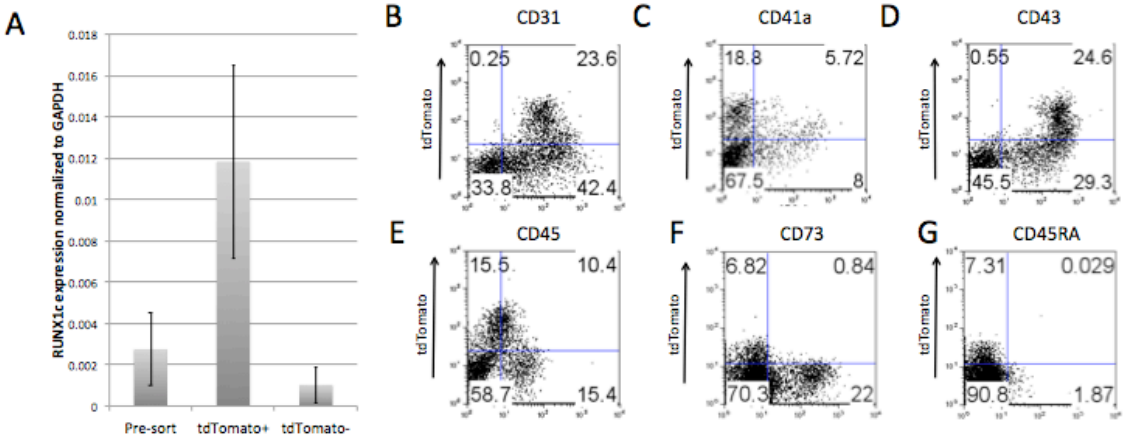

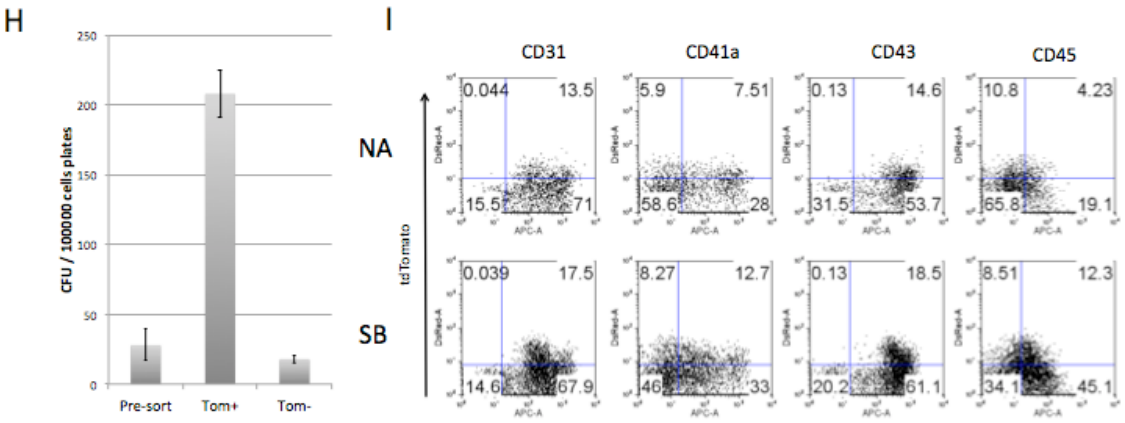
H
I
CFU / 100000 cells plates
250
200
150
100
50
0
Pre-sort
Tom+
Tom-
CD31
CD41a
CD43
CD45
NA
SB
tdTomato
0.044
13.5
15.5
71
5.9
7.51
58.6
28
0.13
14.6
31.5
53.7
10.8
4.23
65.8
19.1
0.039
17.5
14.6
67.9
8.27
12.7
46
33
0.13
18.5
20.2
61.1
8.51
12.3
34.1
45.1

Figure 1.6: Gene expression analysis comparing hPSC-derived hematopoietic populations to CD34$^+$ UCB and CD34$^+$ fetal liver. A. Dendogram representation of mRNA array analysis for 230 cancer related genes from sorted hESC and iPSC populations as well as CD34$^+$ UCB. Similarity between samples is represented by positioning within the cluster tree. 2 biological replicates were averaged for each sample with the exception of UCB, which used 4 **B.** Graphs representing the numerical data used to make dendograms in 2.6A showing expression of CCND1, CCND3 and BRCA1. **C.** Same samples from 1.6A but analysis for miRNAs. The 105 highest expressed of 800 total analyzed are represented in the dendogram. **D.** Graphs representing numerical data used to make dendograms in 2.6B. Graphic bars represent average and standard error for fold change from UCB for 2 independent experiments for B,D. **E.** qPCR analysis for HOXA cluster genes in tdTom$^+$ cells from hESC/iPSC Runx1c reporter lines as well as CD34$^+$ human UCB. Graphic bars represent averages and standard error for three independent experiments.

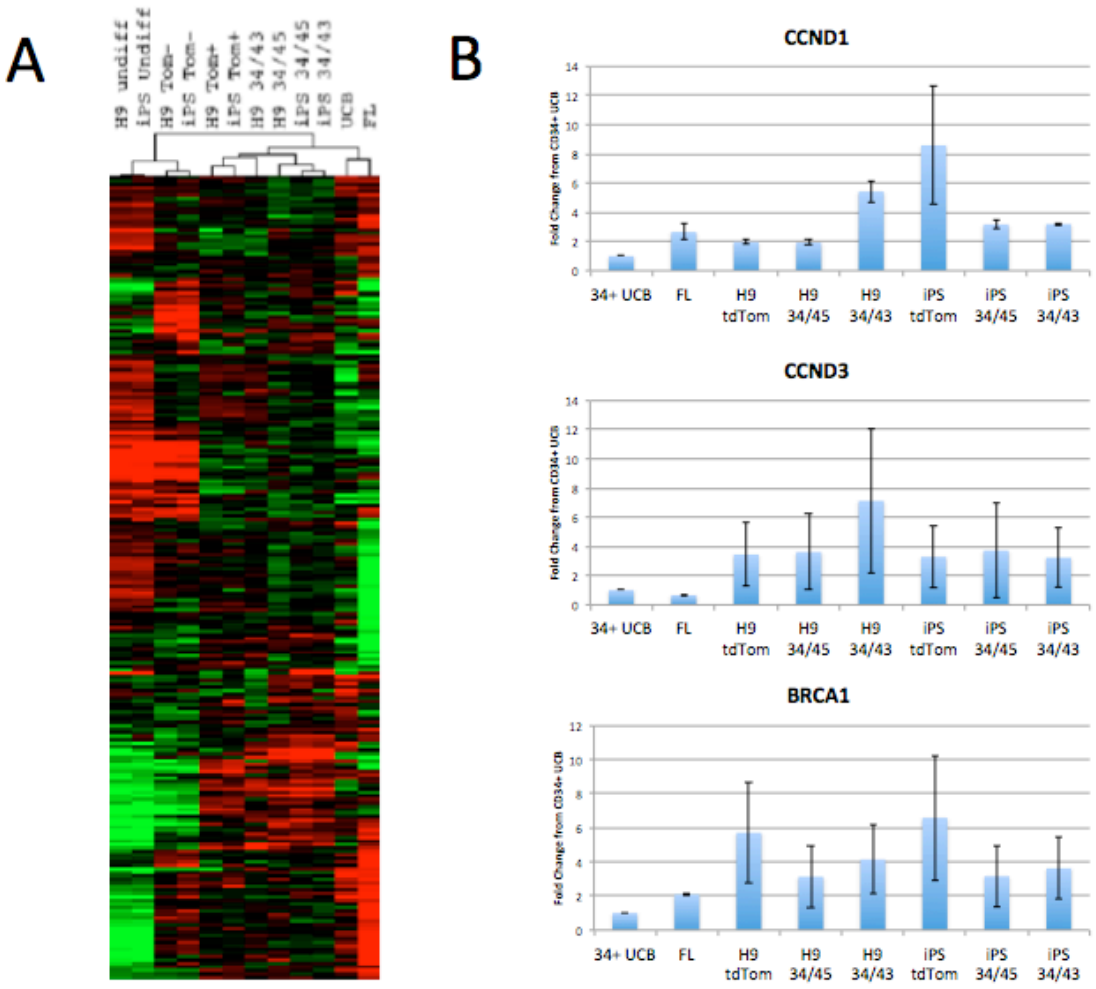
A
H9 undiff
iPS Undiff
H9 Tom-
iPS Tom-
H9 Tom+
iPS Tom+
H9 34/43
H9 34/45
iPS 34/45
iPS 34/43
UCB
FL
B
CCND1
Fold Change from CD34+ UCB
34+ UCB
FL
H9 tdTom
H9 34/45
H9 34/43
iPS tdTom
iPS 34/45
iPS 34/43
CCND3
BRCA1

C

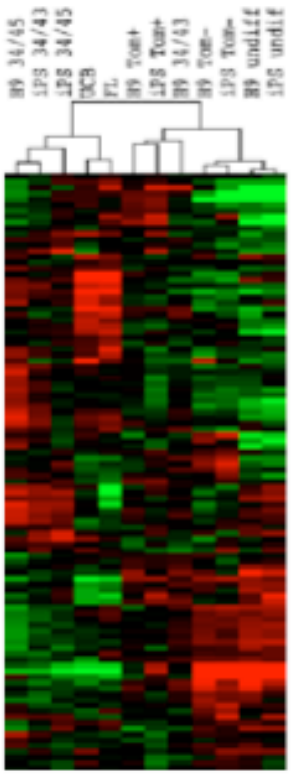
H9 34/45
IPS 34/43
IPS 34/45
UCB
FL
H9 Tom+
IPS Tom+
H9 34/43
H9 Tom-
IPS Tom-
H9 undiff
IPS undiff

E

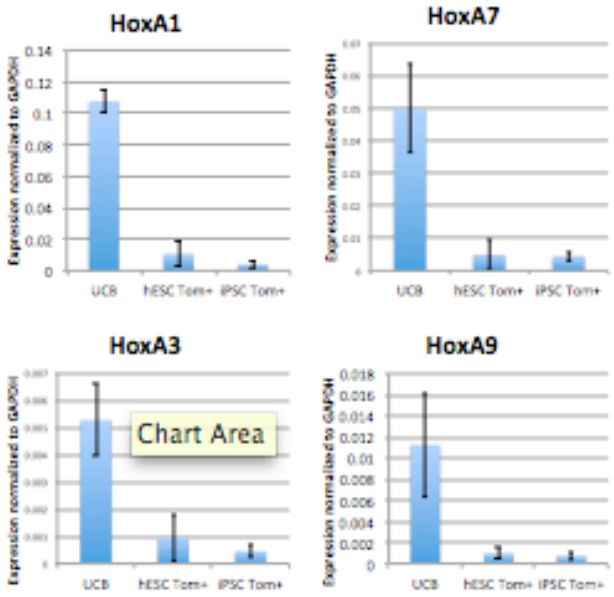
HoxA1
HoxA7
HoxA3
HoxA9
Expression normalized to GAPDH
UCB
hESC Tom+
iPSC Tom+
Chart Area

D

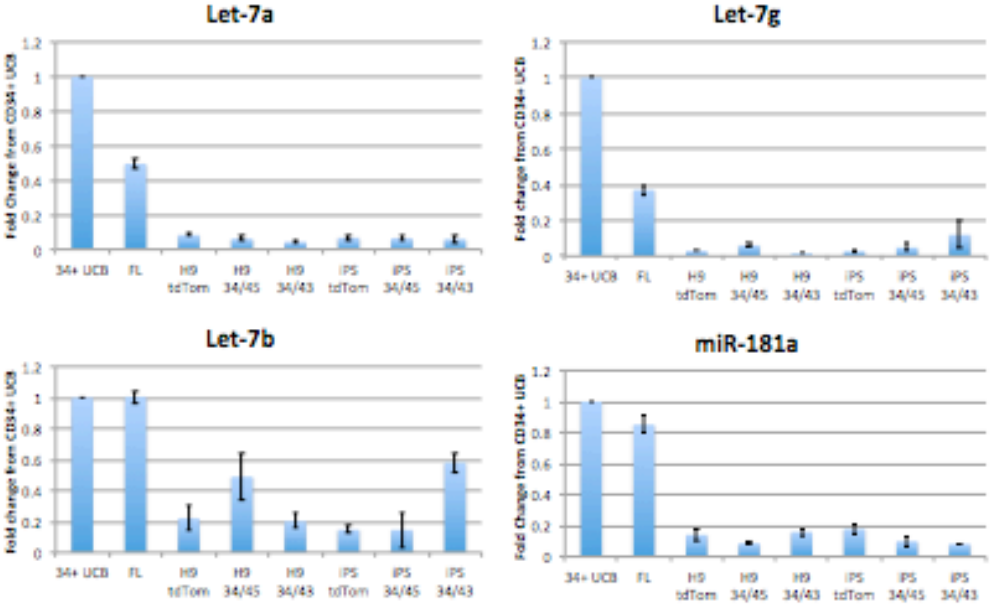
Let-7a
Let-7g
Let-7b
miR-181a
Fold Change from CD34+ UCB
34+ UCB
FL
H9 tdTom
H9 34/45
H9 34/43
iPS tdTom
iPS 34/45
iPS 34/43

Figure 1.7: The sorted tdTom fraction assumes both hematopoietic and endothelial morphologies in the long term endothelial assay but does not contain LTC-ICs. A-C. Fluorescent microscopy of the $tdTom^+$ fraction one week after being seeded onto M2-10B4 stromal cells in the LTC-IC assay showing $tdTom^+$ hematopoietic cells (A), $tdTom^-$ (but $tdTom^+$)-derived GFP^+ endothelial cells (B) and $tdTom^+$ endothelial cells (C). **D.** Flow cytometric analysis at 2 weeks in LTC-IC showing expression of tdTom, GFP and hematoendothelial extracellular markers. **E,F.** $tdTom^+$ hematopoietic populations associate with adherent endothelial cells. **G.** Adherent cells appear to express tdTom during asymmetrical division giving rise to a $tdTom^+$ hematopoietic cell.

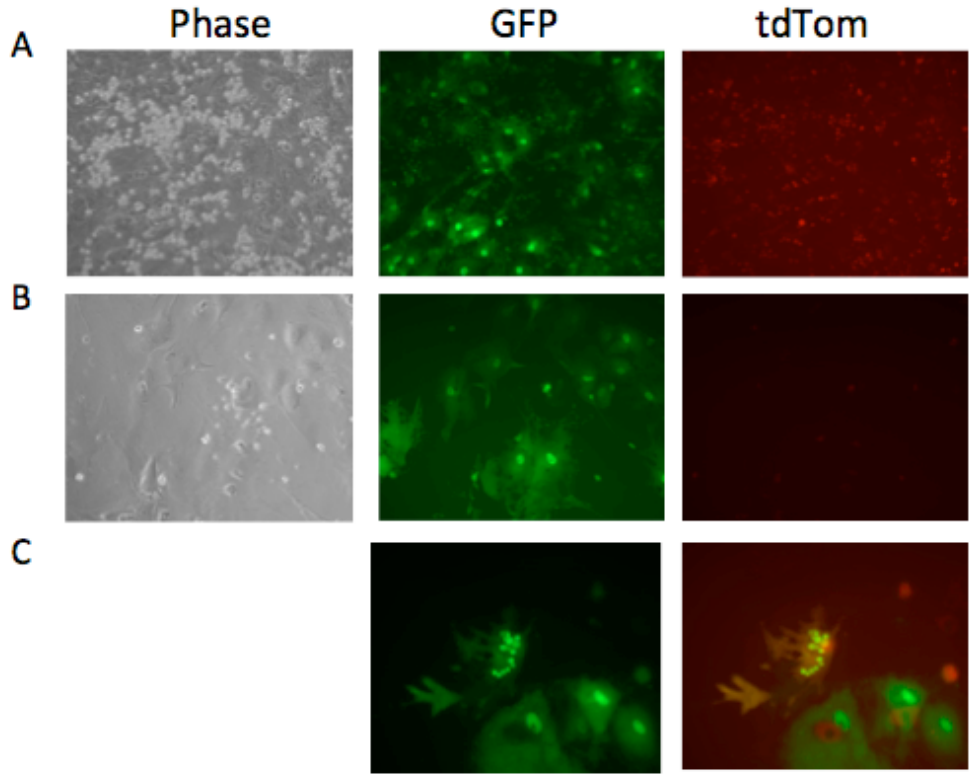

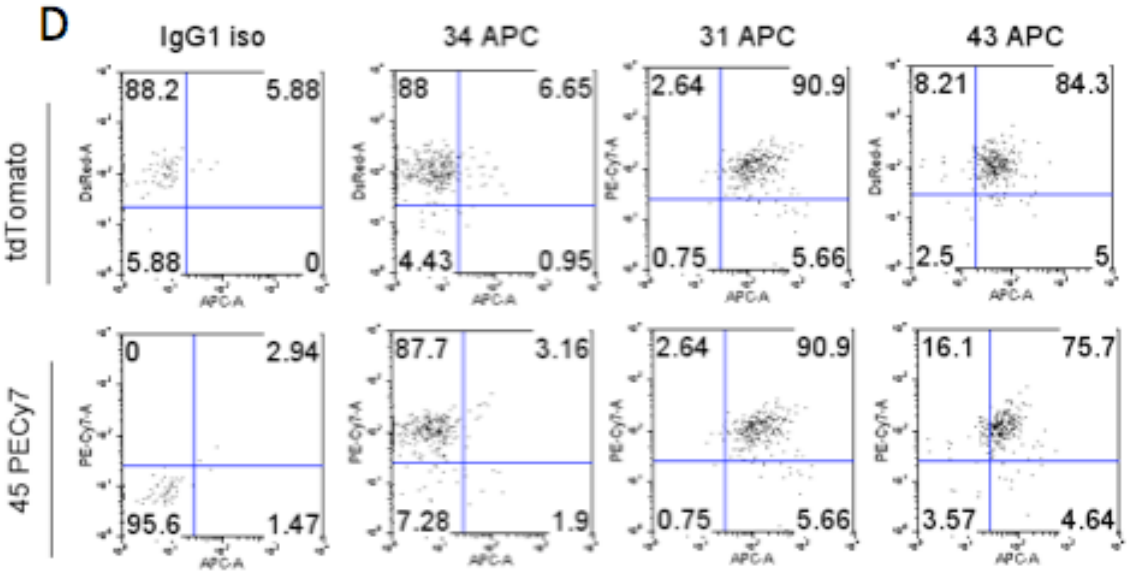
D
IgG1 iso
34 APC
31 APC
43 APC
tdTomato
45 PECy7
88.2
5.88
5.88
0
88
6.65
4.43
0.95
2.64
90.9
0.75
5.66
8.21
84.3
2.5
5
0
2.94
95.6
1.47
87.7
3.16
7.28
1.9
2.64
90.9
0.75
5.66
16.1
75.7
3.57
4.64
DsRed-A
PE-Cy7-A
APC-A

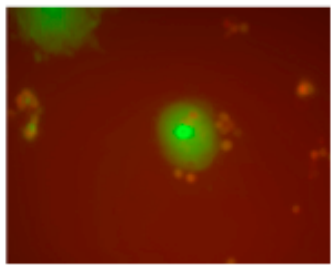
E

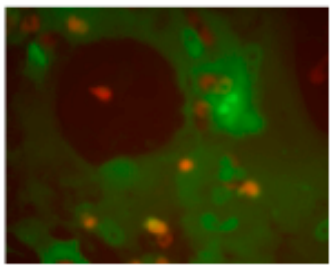
F

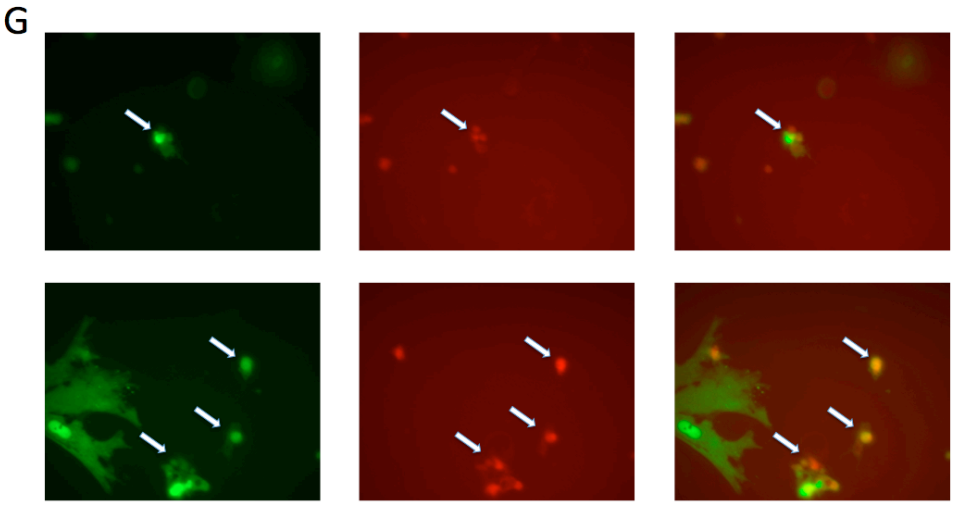
G

Supplementary figure 1.1: Phenotypic analysis of differentiating H9 hESCs.

Expression of intracellular hematopoietic transcription factors and extracellular markers in H9 hESCs over a differentiation time course. Non-transgenic hESCs were differentiated on M210 mouse bone marrow cells in R-10 media. **A.** RT-PCR analysis of early hematopoietic genes BRACHYURY (Bry), RUNX1b, RUNX1c, PU.1, GATA1 and GATA2. **B.** Flow cytometric analysis of these same cells for coexpression of hematopoietic markers CD34 and CD45.

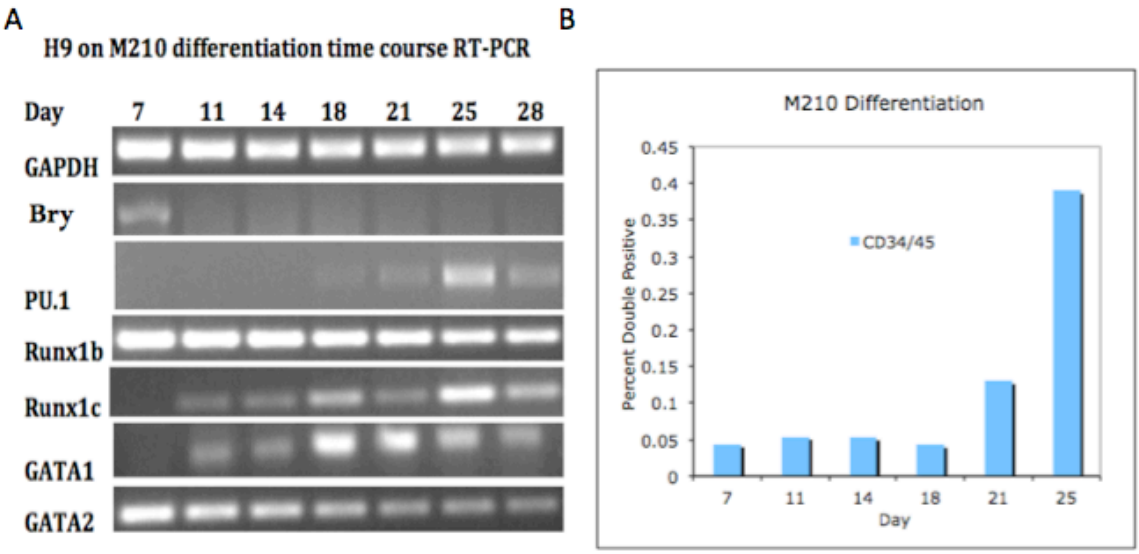

Supplementary figure 1.2: The RUNX1c reporter construct shows activity in K562 cells. **A.** RUNX1c-expressing K562 leaukemic cells were transiently nucleofected with the RUNX1c reporter construct containing the P1 promoter and +24 enhancer flanking tdTom along with a control plasmid only lacking the promoter and enhancer. **B.** RT-PCR analysis of K562 along with undifferentiated H9 hESCs, 293s and human umbilical vein endothelial cells HUVEC showing that RUNX1c expression is specific for hematopoietic cells.

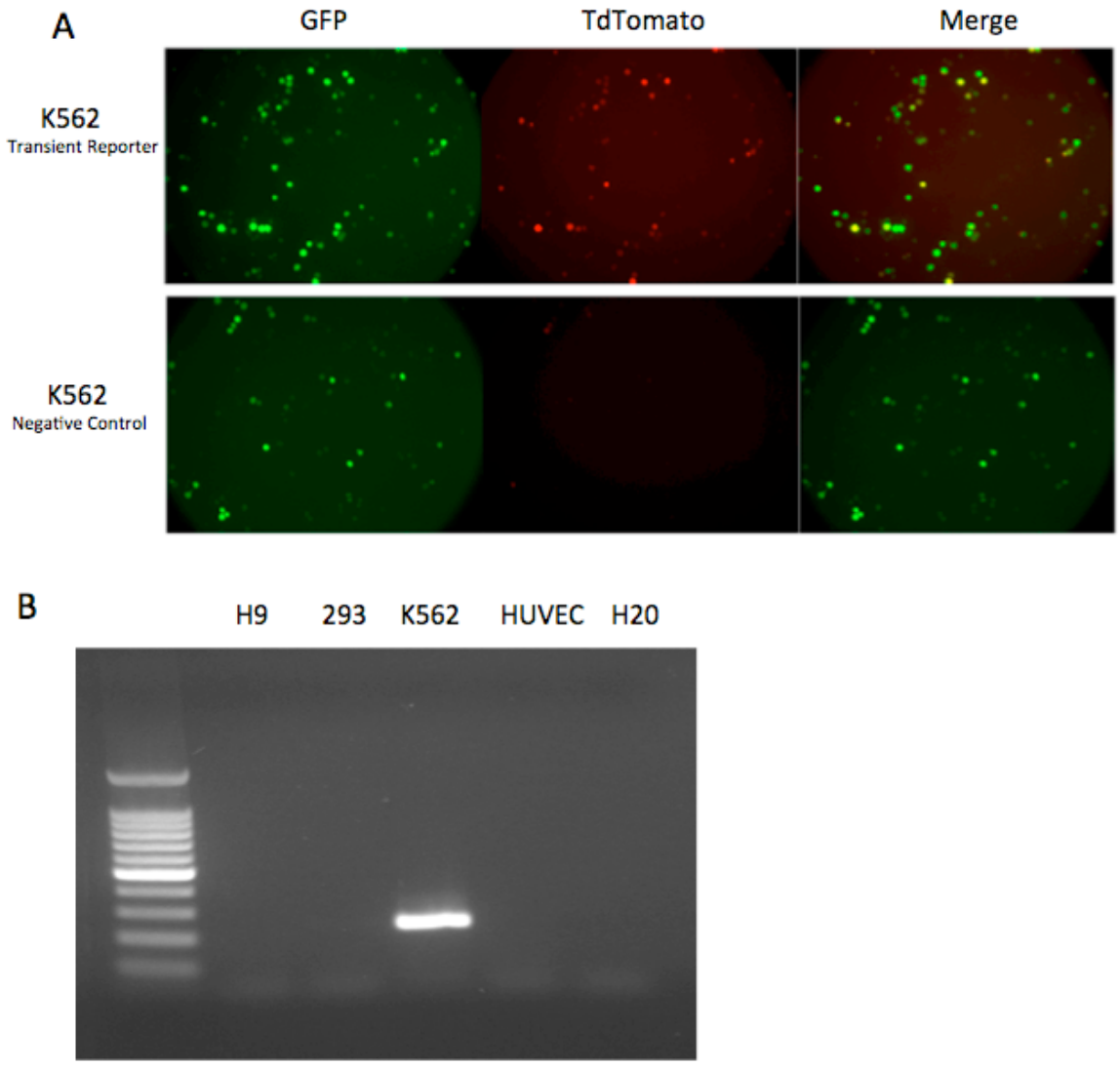

Supplementary figure 1.3: Runx1c reporter clones from both the hESC and iPSC lines are capable of hematopoietic differentiation and show similar patterns of tdTom expression. Reporter lines were differentiated as Spin EBs as described and analyzed by flow cytometry on day 17 for expression of hematoendothelial extracellular markers as well as tdTom. In addition, a non transgenic hESC line was analyzed in parallel to show that transgene integration did not effect the ability to undergo hematopoietic differentiation.

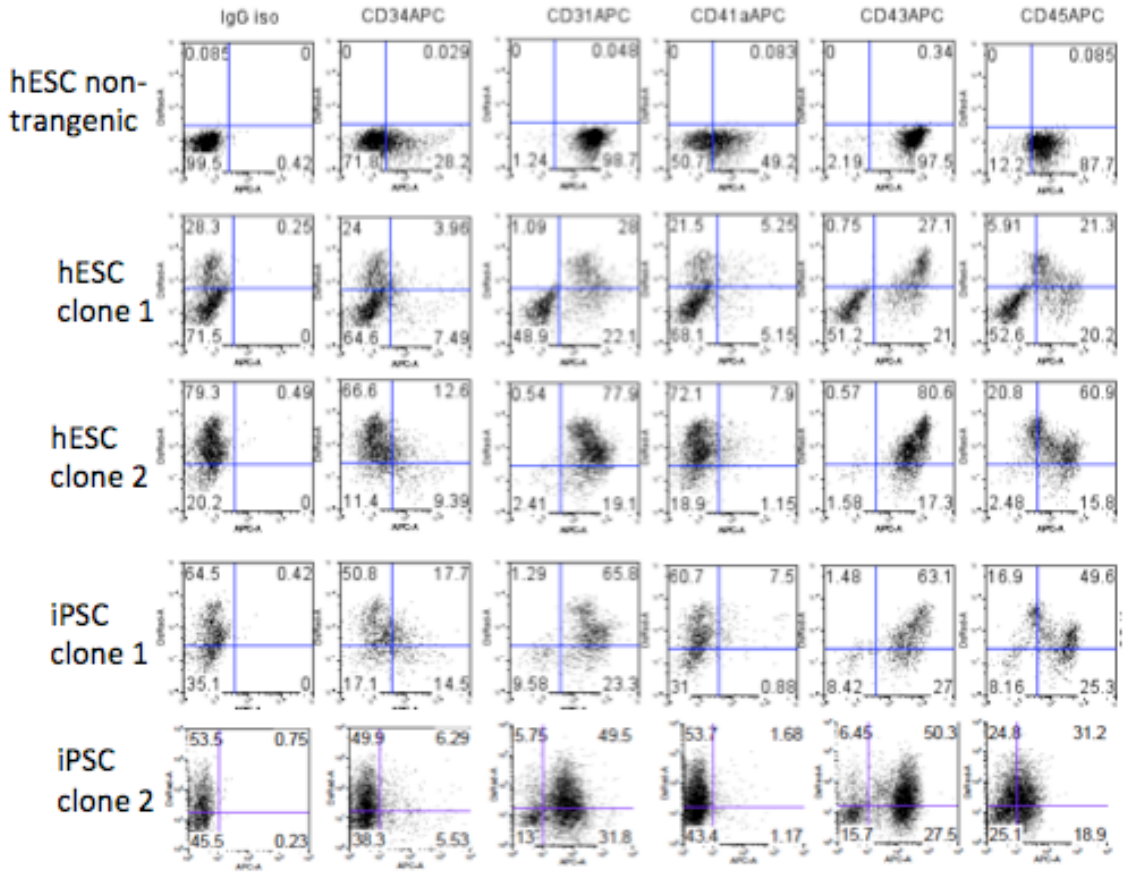

Supplementary figure 1.4: Karyotyping analysis shows no gross genetic abnormalities in either the hESC or Dub7 iPSC RUNX1c reporter lines

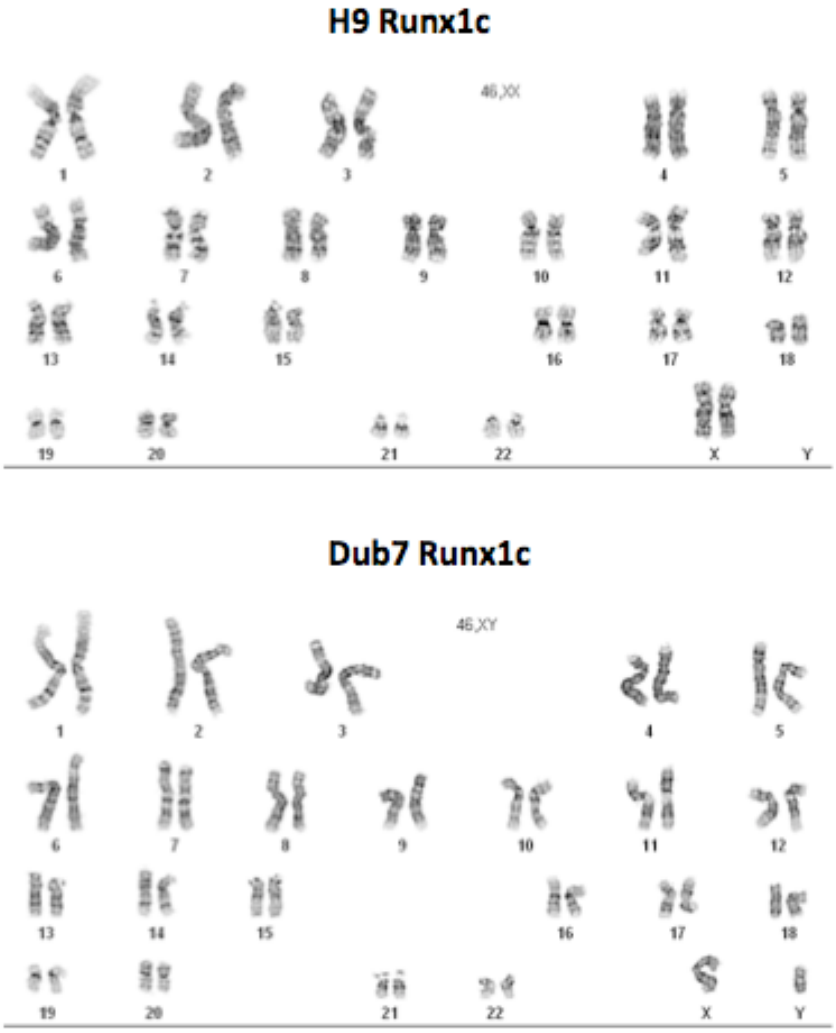

Supplementary figure 1.5: Spin Embroid Body hematopoietic differentiation of hPSCs **A.** hESCs adapted to single cell culture are evenly distributed in a 96-well plate and given cytokines to promote mesoderm/early hematopoietic development. **B.** Image of EB after transfer to an adherent 24-well plate for development of more mature hematopoietic lineages using SCF, VEGF, TPO, EPO, IL-3 and IL-6. **C.** Schematic for Spin EB hematopoietic differentiation showing the two separate stages. **D.** Flow cytometric analysis or co-expression of tdTom with glycophorin A and CD45ra.

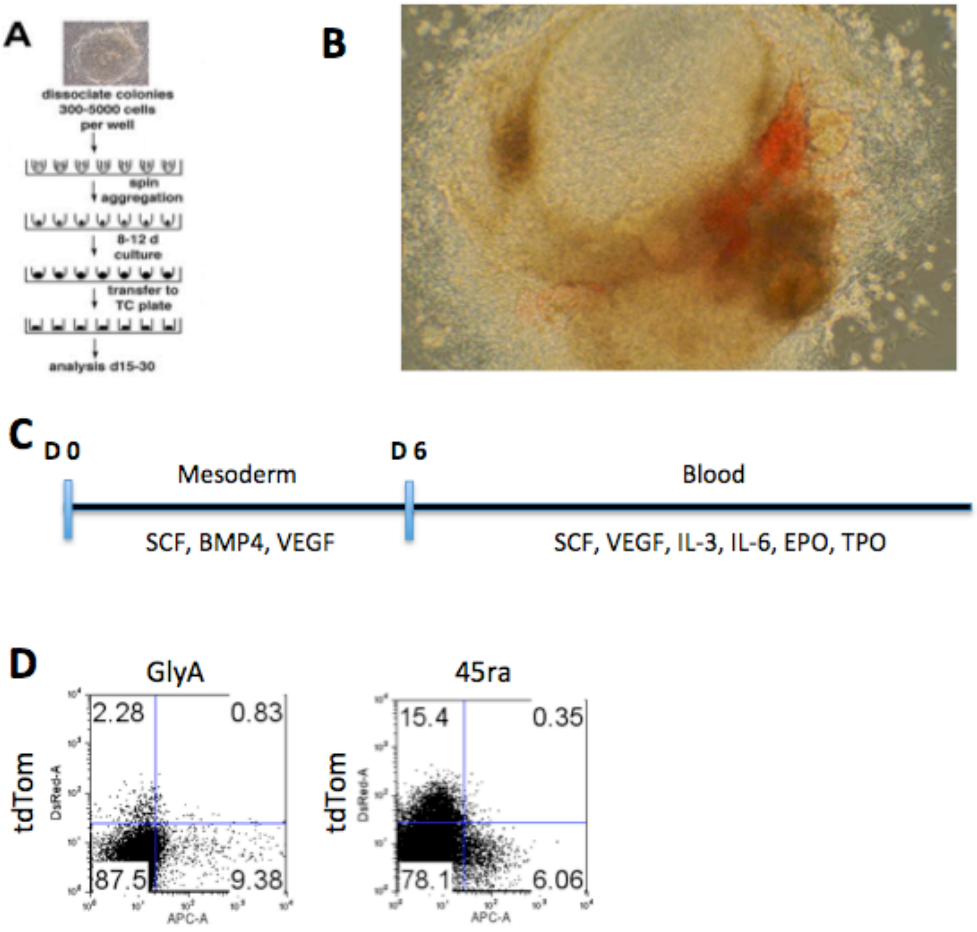

Supplementary figure 1.6: Application of the Activin/Nodal inhibitor to stage 1 Spin EBs at varying times to monitor alterations in hematopoietic differentiation.

Exposing the EBs to SB from the outset of their development completely abolishes hematopoiesis while applying day 3 and after has no effect. Application between days 2 and 5 showed the desired partial reduction in $CD34^{+}CD41a^{+}$ and $CD34^{+}CD43a^{+}$ populations.

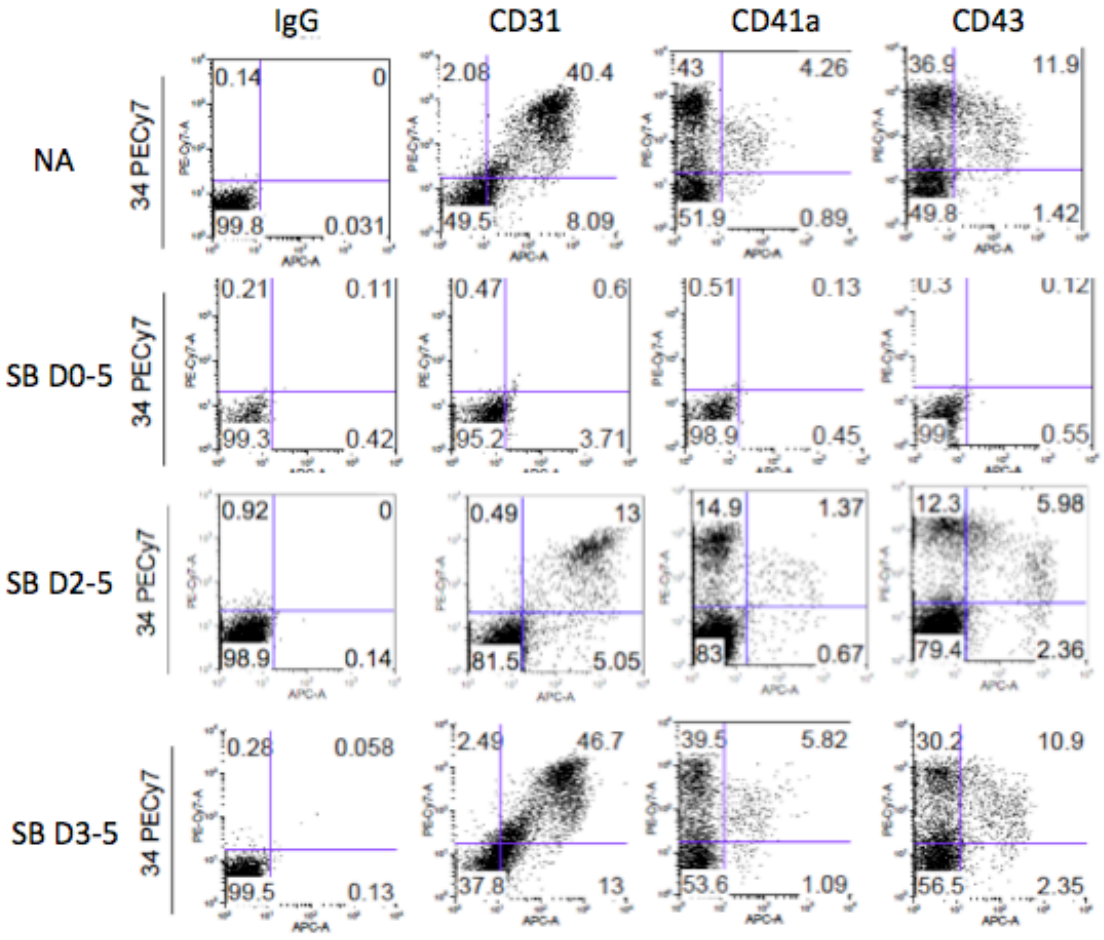

Supplementary figure 1.7: Reprogramming and characterization of the Dub7 CD34^{+} umbilical cord blood iPSCs. A. Method for viral transduction of CD34^{+} umbilical cord blood and subsequent culture/maintenance. **B.** Immunohistological staining of a Dub7 colony shows ubiquitous expression of pluripotency markers Oct4, Sox2, Nanon and Tra-1-81. Pluripotency markers are FITC-conjugated while blue images show staining of cell nuclei for DAPI. **C.** Teratoma formation in mouse demonstrated that the Dub7 cells were capable of differentiating into all 3 germ layers. **D.** Karyotyping analysis shows no gross genetic abnormalities.

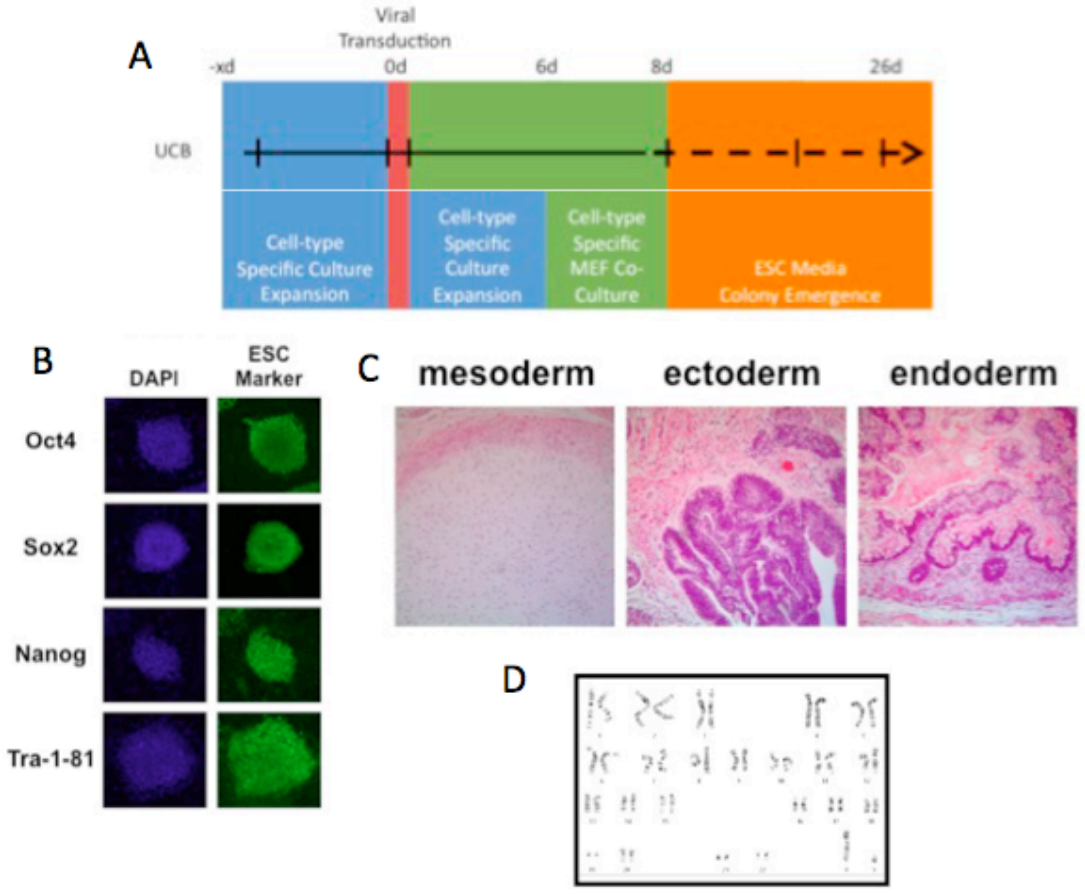

Supplementary figure 1.8: **The Dub7 CD34^{+} UCB-derived iPSC line shows accurate reporting of endogenous RUNX1c expression.** Dub7 iPSC RUNX1c reporter cells were differentiated as spin EBs. Expression of endogenous RUNX1c by qPCR from the bulk population and the proportion of tdTom^{+} cells by flow cytometry were measured on days 11, 13 and 15. Values representative of one experiment.

A

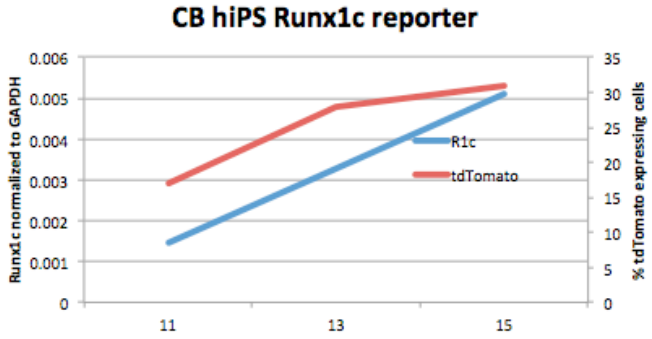

B

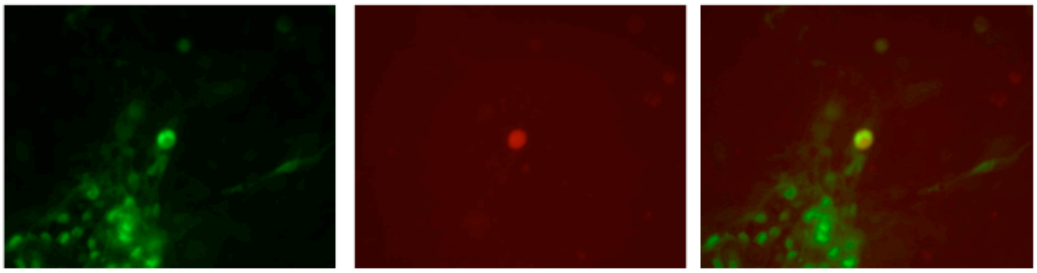

CHAPTER 3

The human Pu.1 promoter and upstream regulatory element are activated upon hESC hematopoietic differentiation

Successful identification of putative HSCs derived from hESCs will likely require the ability to determine the differential expression patterns of several intra-cellular transcription factors on an individual cell basis. To this end, we have created transgenic hESCs which drive expression of tdTom from PU.1 cis-regulatory elements that have been shown to exhibit both inhibitory and activating effects as HSCs transition into multipotent progenitors. We demonstrate that the PU.1 promoter and upstream regulatory element (URE) are activated in sub sets of cells as they undergo hematopoietic commitment, and that reporter expression is conciminent with expression of endogenous PU.1. Furthermore, tdTom expression patterns closely mimic those of a similarly constructed RUNX1c reporter cell line, consistent with direct activation of Pu.1 by Runx1 at its URE in mouse studies. Use of a combination of these reporter hESCs may help us to gain further insight regarding the expression profile for emerging hESC-derived hematopoietic progenitors.

Introduction

Pu.1, a member of the ETS-family of transcriptional regulators named after its affinity for purine-rich sequences, is a master regulator of myelopoiesis and indispensable for fetal hematopoietic development[193,194]. Mice deficient for Pu.1 expression die at 18.5 days of gestation and are found to lack production of mature B-cells, T-cells and macrophages[131]. This is at least in part due to an initial failure to support KTLS HSCs in the fetal liver[131]. Unsurprisingly, selective ablation of Pu.1 in fetal liver HSCs confers an inability to engraft immunodeficiant mice, which was directly related to an 11-fold decrease in homing to the BM within 48 hours[132,195]. Mice hypomorphic for Pu.1 show decreased long-term multilineage reconstitution which can be rescued by restoring Pu.1 expression[196]. In addition to its proximal promoter, genetic analysis of the entire Pu.1 locus has found numerous distal and intronic elements which regulate its lineage specific expression throughout hematopoiesis[128,197]. This includes an initial suppression in HSCs via binding of GATA2 to promoter and later upregulation in myeloid progenitors mediated by binding of Runx1 to three sites within the -14 kb upstream regulatory element (URE)[128,130,198,199]. Pu.1 then acts through direct, antagonist interactions with GATA1 to dictate the myeloerythroid axis[192,200]. Progenitors primed for myeloid development show increased expression of Pu.1 at the expense of GATA1, with the opposite being true for erythroid progenitors.

In the present study, we sought to investigate the role of PU.1 expression in human hematopoietic development by creating transgenic PU.1 reporter hESCs. By cloning regulatory elements from hESC genomic DNA which were synonomous with the

conserved proximal promoter and -14 kb URE in mouse to drive expression of tdTom, we are able to show that these elements are activated upon initiation of hematopoiesis in a human system, and that they are specific for a subset of developing hematopoietic lineages. Furthermore, consistent with the finding that Pu.1 is directly targeted by Runx1 for transcriptional activation in mice, we demonstrate that the tdTom expression patterns for the PU.1 reporter are similar to those of a previously developed reporter for RUNX1. Thus, this PU.1 reporter may be useful in a more detailed characterization of hESC-derived hemtopoietic progenitors.

Materials and Methods

All materials and methods used in these studies are described in chapter 2.

Results

Bioinformatical analysis shows conserved, active PU.1 regulatory elements in human hematopoietic cells

Initial studies searching for Pu.1 regulatory elements in mouse discovered approximately 35 kb of upstream sequence which was able to regulate Pu.1 expression, including a DNase hypersensitive 3.5 kb HindIII fragment 14 kb upstream of the transcriptional start site which regulates myeloid specific expression[198]. We decided to determine whether a bioinformatical approach could predict a similar upstream regulatory element in the human *PU.1* locus. Using the University of California Santa Cruz genome browser and the 3.5 kb mouse HindIII fragment as a reference, we found an upstream

segment of the of the human locus at -17 kb to show high levels of conservation (Figure 2.1A). In addition, data compiled from ENCODE showed this region as well as the proximal promoter to have increased levels of H3K27 acetylation in K562 leukemic cells, indicating an open chromatin structure for access to transcription factors (Figure 2.1 B,C). This was in contrast to non-hematopoietic human umbilical vascular endothelial cells (HUVEC), which lacked H3K27Ac at the promoter, and H1 hESC, which had no acetylation at all (Figure 2.1 B,C). Our bioinformatical analysis indicated that both the promoter and an upstream regulatory element were activated specifically in human hematopoietic cells and that they would likely be accurate reporters of PU.1 expression in hESCs.

The human PU.1 promoter and URE drive tdTom expression in K562

We next wanted to determine if either the promoter alone or a combination of the promoter and URE could drive expression of tdTom in K562 cells. To do this, we constructed two versions of a PU.1 reporter plasmid: one with an 800 bp portion of the promoter/5' UTR cloned directly upstream of the tdTomato coding region (PU.1-P) (Figure 3.2A), and another with an additional 1.2 kb section of the URE which included the highest levels of H3K27 acetylation and Runx1 binding sites (PU.1-P+URE) (Figure 3.2B). In each case, tdTom was followed by a constitutively active GFPzeocin fusion protein which was used to determine nucleofection efficiency. After nucleofecting either plasmid into K562, we demonstrated that both PU.1-P and PU.1-P+URE were able to drive expression of tdTom (2.2C). Furthermore, the addition of the URE appeared to

increase the proportion of $tdTom^+$ cells. Accounting for nucleofection efficiency, we found that 60% of cells containing PU.1-P+URE (GFP^+) were $tdTom^+$, compared to 50% for PU.1-P (Figure 2.2D). Moreover, PU.1-P+URE was able to drive tdTom expression in 48% of $CD45^+$ K562 while only 29% of PU.1-P CD45 expressing cells were $tdTom^+$ (Figure 3.2C). Finally, after stable integration of both transgenes in undifferentiated H9 hESCs, we did not see any expression of tdTom (Figure 2.2E). Together, these data demonstrate that the PU.1 promoter alone substantially drives expression of the tdTom reporter, but is enhanced by the URE, and that both regulatory elements are inactive in undifferentiated hESCs.

The Pu.1 promoter and URE faithfully drive reporter expression in hESCs

In order to determine if a combination of the Pu.1 promoter and URE drive expression of the transgene in hESC-derived hematopoietic progenitors, we clonally isolated hESCs with stable insertion of the PU.1-P+URE. We then single-cell culture adapted and subjected them to hematopoietic differentiation by the Spin EB method. Comparison of 2 independently derived clones showed that hematopoietic development was not significantly effected by insertion of the transgene (Supplementary Figure 2.1) Fluorscence microscopy demonstrates that tdTom expression appears to be restricted to the non-adherent, cobblestone-like hematopoietic populations, with the expanding stromal layers showing only GFP expression (Figure 2.3A). This finding was corroborated by flow cytometric analysis showing expression of CD73, a mesynchymal marker, to be confined to the $tdTom^-$ population (Figure 2.3B). Furthermore, RT-PCR

analysis of the bulk population shows that the onset and increase in endogenous Pu.1 transcript correlates with the proportion of tdTom$^+$ cells (Figure 2.3C). Finally, CFU analysis of the sorted tdTom$^+$ cells shows them to be highly enriched for hematopoietic progenitors as compared to the tdTom$^-$ cells (Figure 2.3D). These data establish that activation of the PU.1 regulatory elements in our system accurately reflects the expression of endogenous PU.1.

tdTom expression in the PU.1 reporter mimics that of a reporter for RUNX1c

In order to determine if there is a relationship between expression of PU.1 and and RUNX1c, a direct upstream regulator of Pu.1 in mice, we compared the timing and expression patterns of tdTom with other extracellular hematopoietic markers in parallel with reporters for both genes. We have previously engineered a tdTom reporter using minimal regulatory elements for RUNX1c which we showed to exhibit faithful tdTom expression (unpublished). In each of our differentiations, expression of tdTom in the PU.1 cells appeared to mirror that of the RUNX1c reporter in both timing and patterning, with tdTom first detected around day 12 and being restricted to the CD31$^+$ and CD43$^+$ subsets (Figure 2.4A). In some cases we saw a marginal difference in the percent of cells expressing tdTom on a given day, but this was likely due to dissimilar differentiation speeds between the two different cell lines and not inherent qualities of the reporters (Figure 2.4A). Sub-gating on the CD34$^+$CD45$^+$ and CD34$^+$CD43$^+$ hematopoietic progenitor populations revealed that they only possessed a minority of tdTom$^+$ cells (Figure 2.4B). In both cases, the proportion of the gated population expressing tdTom

was even less than the tdTom$^+$ percent in the bulk, ungated cells, indicating that there was a slight negative enrichment for tdTom in these progenitor sub gates. These findings suggest that the PU.1 promoter and URE are activated in a similar subpopulation as the RUNX1c regulatory elements during human hematopoietic development, consistent with PU.1 being a direct downstream target of RUNX1c.

Discussion

Here, we show that a combination of the PU.1 proximal promoter and URE can drive expression of tdTom in hESCs, and that they do so in a manor which is faithful to expression of endogenous PU.1 over hematopoietic development. Furthermore, we demonstrate that the activation of these regulatory elements appears to mirror activation of human RUNX1c regulatory elements, as shown by similar expression patterns between the two reporters. This result is appropriate given the direct role RUNX1 has been shown to have in activating PU.1 expression in early mouse hematopoietic development.

Though the ability to track PU.1 expression over hematopoietic development from hPSCs could be very useful in describing, though *in vitro* assays, early myelopoiesis and how it is differentially regulated from erythropoiesis, it remains to be seen if this reporter has the ability to distinguish emerging SRCs. While a lack of Pu.1 expression in HSCs in the fetal liver leads to a decrease in progenitor numbers and deficient engraftment in the bone marrow, this does not mean that PU.1 expression can be used to track HSCs. In fact, due to its positive influence in myeloid development, it would be easy to conclude that cells expressing PU.1 have recently transitioned from a multipotent

HSC to a further restricted progenitor. McIvor *et al* demonstrated that enforced, transient Pu.1 expression in multipotent progenitors eliminated their ability to self-renew[201]. This again indicates that Pu.1 is expressed at higher levels in restricted progenitors not capable of engraftment. As such, it might be possible to use Pu.1 expression as a means for negative selection when attempting to identify HSCs. Indeed, as with the use of extra-cellular markers, hPSC-derived HSC isolation will likely rely on the tracking of multiple transcription factors.

Figure 2.1: Bioinformatical analysis of the human PU.1 promoter and URE using the UCSC genome browser showing Chr. 11 bases 47,398,806 – 47,425,159. The coding region for PU.1 (SPI1) is on the minus strand and is read right to left in this image. **A**. Diagram showing the PU.1 translational start site along with 20 kb of the upstream region. Underlying graphs represent the mammalian conservation using the PHAST package and H3K27 acetylation patterns from experimental data derived through ENCODE. **B**. Close up of the promoter region comparing H3K27 acetylation levels between K562, HUVEC and H1 hESC. **C**. Close up of the PU.1 URE comparing H3K27 acetylation.

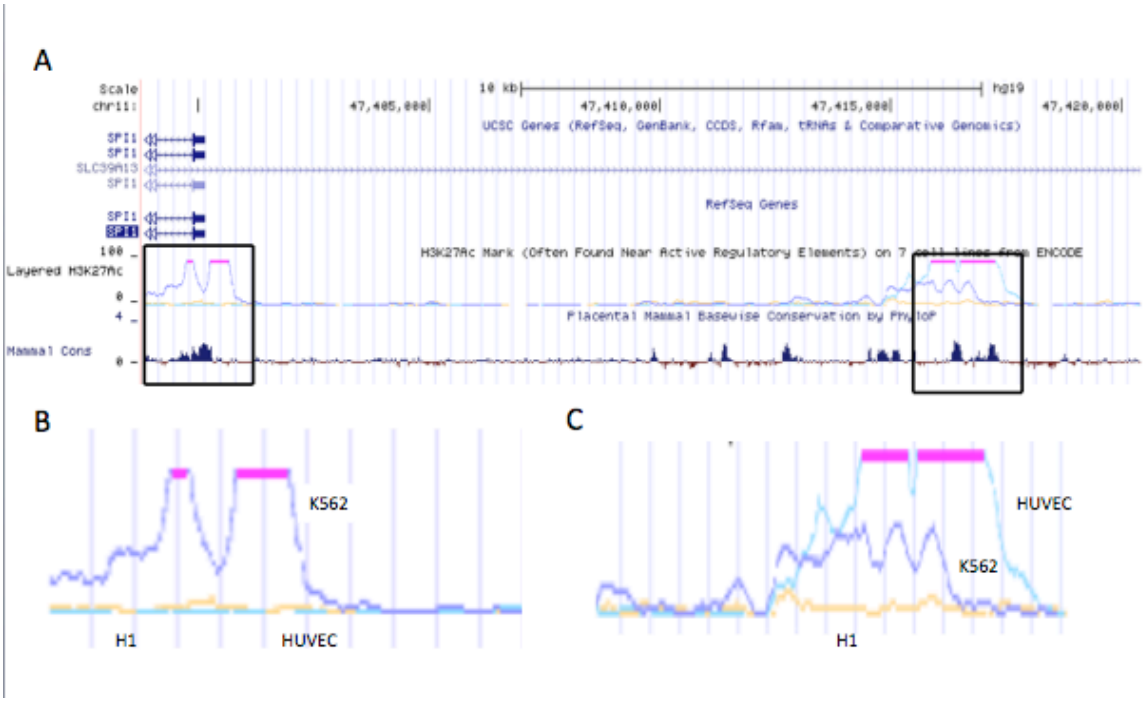

Figure 2.2: Activity of the Pu.1 promoter/5' UTR and URE in K562 and undifferentiated H9 hESCs. **A.** Diagram of the construct utilizing the promoter/5' URE to drive expression of tdTom followed by a constitutively driven GFPzeocin fusion protein. **B.** Same as in A but with the addition of 1.2 kb of the URE upstream of the promoter/5' URE. **C.** K562 leukemic cells were nucleofected with either Pu.1 reporter plasmid and assessed for expression of tdTom, GFP and CD45 by flow cytometry after 2 days. Images are shown at 20x magnification. Top row: PU.1-P. Bottom row: PU.1-P+URE. **D.** Flow cytometric analysis of K562 nucleofected in 2.2C. **E.** H9 hESCs were nucleofected with either plasmid then selected for zeocin resistance. Colonies stably expressing the Pu.1 reporter transgene are shown at 20x magnification.

A


IR/
DR
Promter/UTR
tdTomato/pA
mCAG
GFPzeo/pA
IR/
DR

B


IR/
DR
URE
Promter/UTR
tdTomato/pA
mCAG
GFPzeo/pA
IR/
DR

C

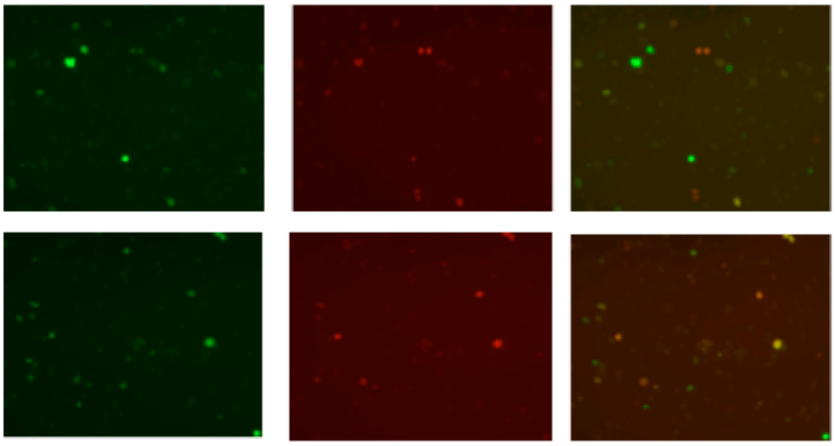

D

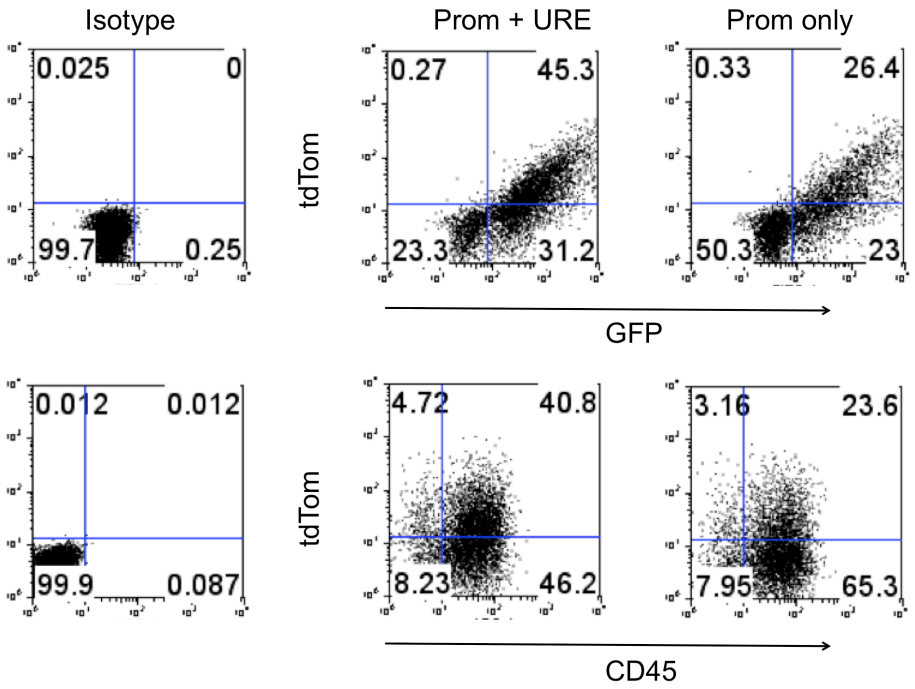
Isotype
Prom + URE
Prom only
0.025
0
99.7
0.25
0.27
45.3
23.3
31.2
0.33
26.4
50.3
23
tdTom
GFP
0.012
0.012
99.9
0.087
4.72
40.8
8.23
46.2
3.16
23.6
7.95
65.3
tdTom
CD45

E

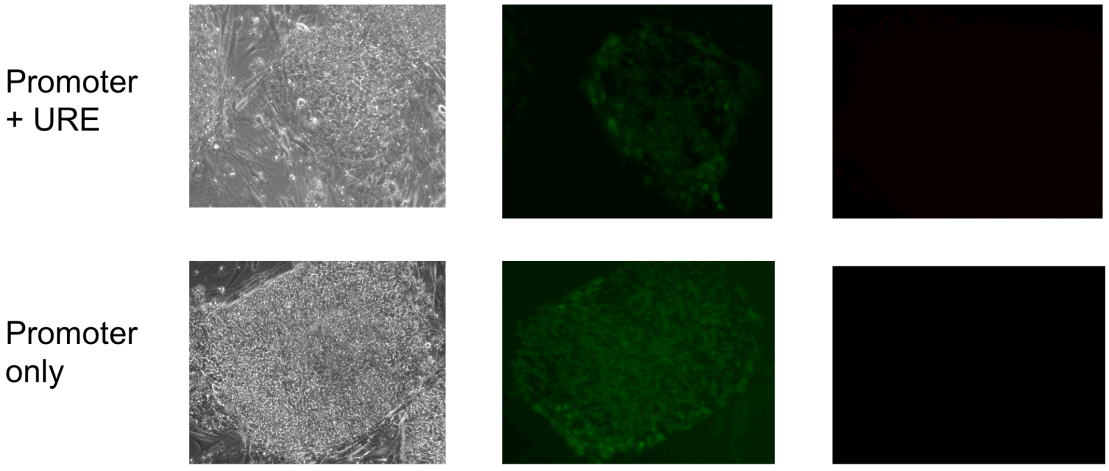
Promoter
+ URE
Promoter
only

Figure 2.3: tdTom expression correlates with endogenous PU.1 and is specific to hematopoietic populations. **A**. Fluorescent microscopy of the Pu.1 reporter differentiating as Spin EBs on Day 15. GFP expression is constitutively driven by the MCAG promoter while tdTom is driven by the Pu.1 promoter and UTR. **B**. Flow cytometric analysis for expression of the mesenchymal marker CD73 and tdTom shows that tdTom expression is specific for hematopoietic cells. **C**. Proportion of tdTom expressing cells by flow cytometry versus expression of endogenous PU.1 transcript in the bulk population by qPCR over a hematopoietic differentiation time course. qPCR values are displayed as relative expression to GAPDH. **D.** Colony forming unit assay for sorted $tdTom^+$ vs $tdTom^-$ populations. Reporter H9s were differentiated for 15 days, sorted, and then enumerated after 7 days in methylcellulose. Values represent the averages from one experiment.

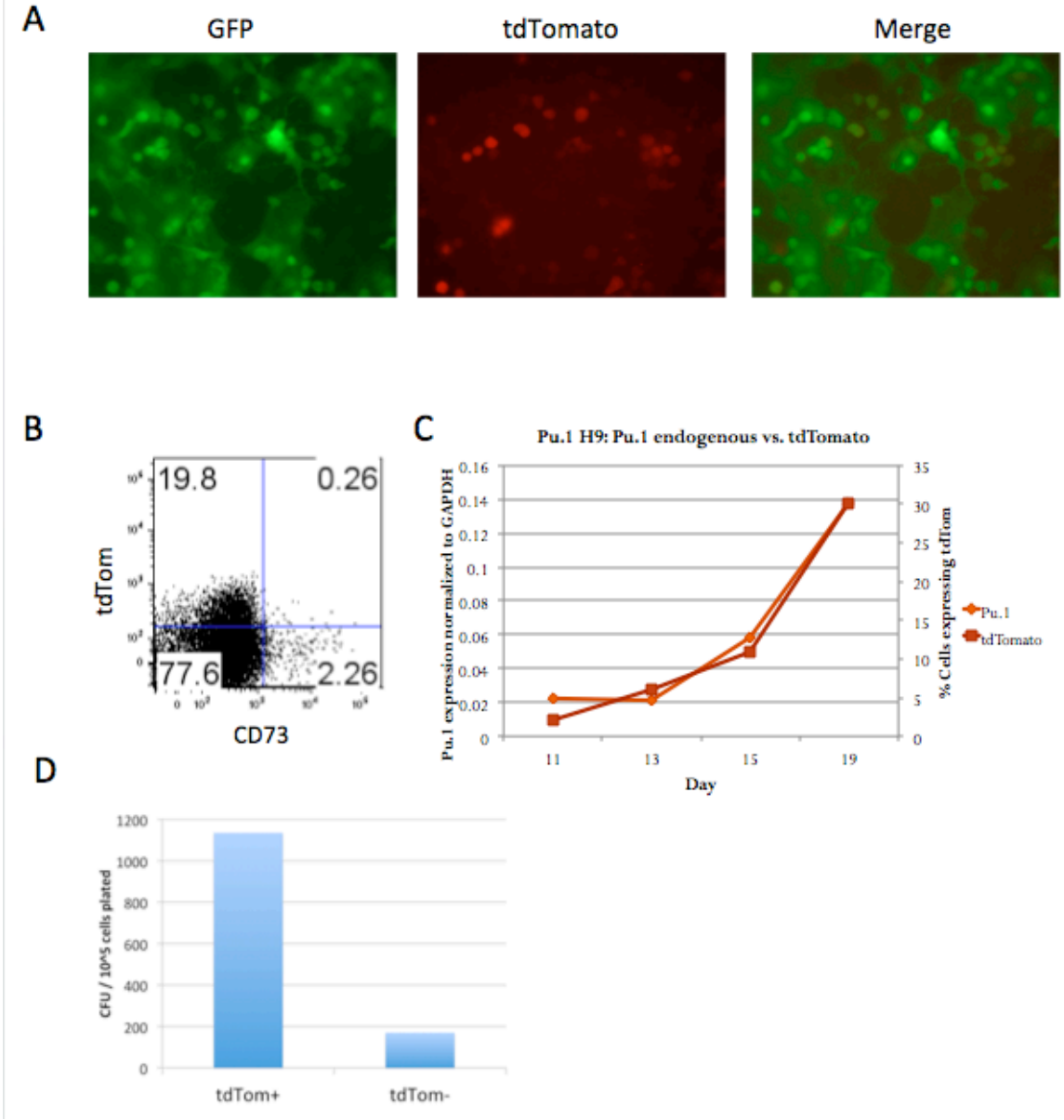
A
GFP
tdTomato
Merge
B
19.8
0.26
77.6
2.26
tdTom
CD73
C
Pu.1 H9: Pu.1 endogenous vs. tdTomato
Pu.1 expression normalized to GAPDH
% Cells expressing tdTom
Day
Pu.1
tdTomato
D
CFU / 10^5 cells plated
tdTom+
tdTom-

Figure 2.4: Comparison of the PU.1 hESC reporter to an hESC reporter for RUNX1c. A. Both the PU.1 and RUNX1c reporter were differentiated in parallel as spin EBs and analyzed for tdTom expression as well as various hematoendothelial extracellular markers. Shown is the flow cytometric analysis from day 14 of differentiation. **B.** Subgating on the $CD34^{+}CD45^{+}$ and $CD34^{+}CD43^{+}$ progenitor populations to assess for frequency of tdTom expression on day 12 of differentiation. Also shown is tdTom expression in the bulk, ungated population.

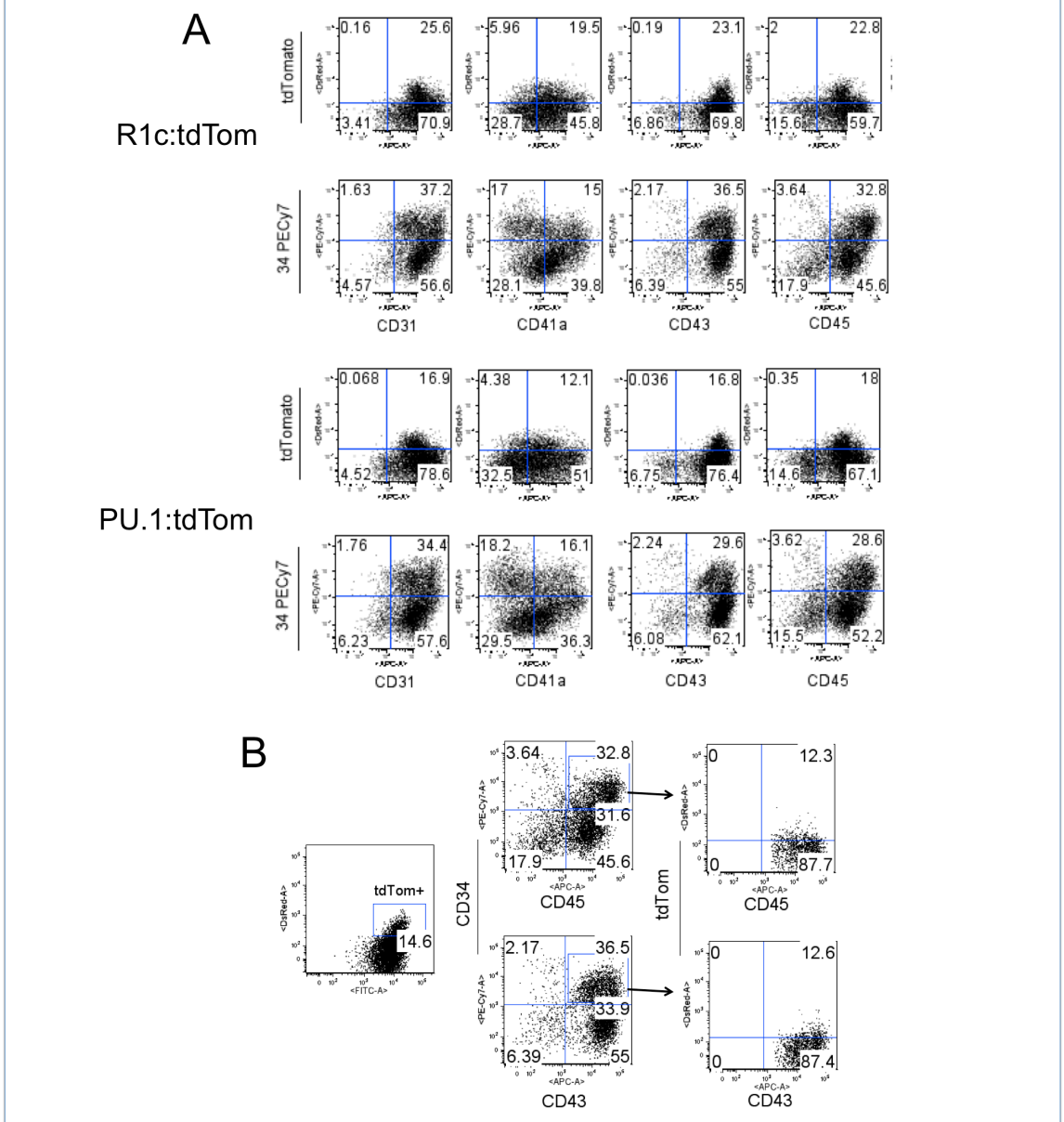
A
R1c:tdTom
PU.1:tdTom
tdTomato
34 PECy7
CD31
CD41a
CD43
CD45
B
tdTom+
CD34
tdTom
CD45
CD43

Supplementary figure 2.1: Two independently derived PU.1 reporter transgenic clones are able to undergo hematopoietic differentiation. Clones were derived by single cell passing and picking of individual colony outgrowths. After expansion, clones were assessed for their ability to undergo hematopoietic differentiation as spin EBs.

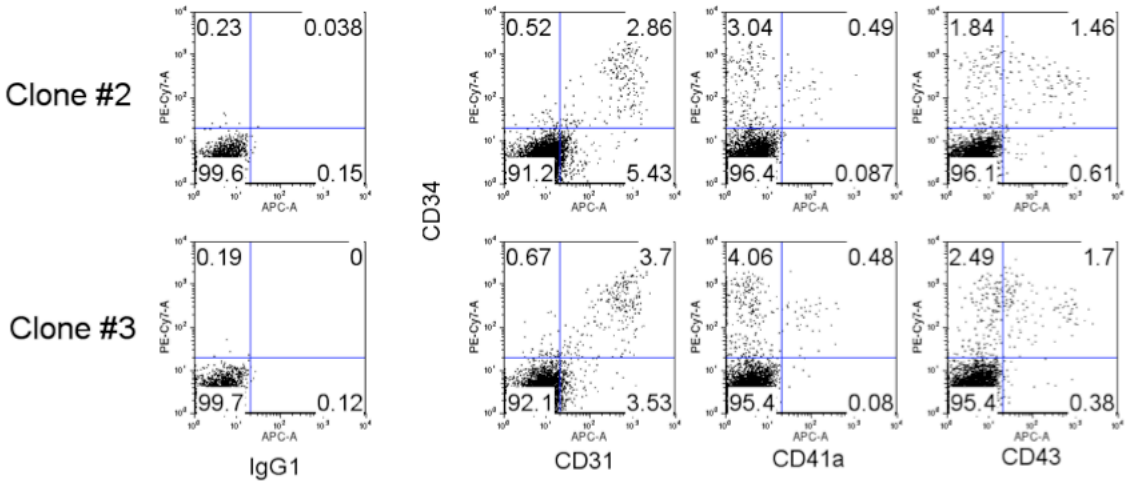

CHAPTER 4:

Functional assessment of hematopoietic niche cells derived from human embryonic stem cells

To evaluate hematopoietic niche cell populations isolated from human embryonic stem cells (hESC)s, we tested the ability of hESC-derived stromal lines to support $CD34^+$ umbilical cord blood (UCB) and hESC-derived $CD34^+45^+$ cells in long-term culture initiating cell (LTC-IC) assays. Specifically, these hematopoietic populations were cocultured with hESC-derived mesenchymal stromal cells (hESC-MSCs) and hESC-derived endothelial cells (hESC-ECs) and assessed for their LTC-IC potential in comparison to coculture with bone marrow-derived MSCs and mouse stromal line M2-10B4. We found that the hESC-derived stromal lines supported LTC-ICs from UCB similar to M2-10B4 cells and better than BM-MSCs. However, none of the stromal populations supported LTC-IC from $CD34^+45^+$ cells. Engraftment data using the output from LTC-IC assays showed long-term repopulation (12 weeks) of NSG mice to directly correlate with LTC-IC support on a given stromal layer. Therefore, hESC-derived stromal lines can be used to efficiently evaluate putative hematopoietic stem/progenitor cells derived from hESCs or other cell sources. Likewise, results showing lack of LTC-IC from hESC derived $CD34^+45^+$ cells are consistent with *in vivo* data showing these cells to be deficient for long-term, multilineage engraftment.

Introduction:

Quantification of putative hematopoietic stem cells (HSCs) in human bone marrow or cord blood is typically assessed by its potential to mediate long-term, multilineage engraftment when transplanted into immunodeficient murine recipients[25,202]. However, *in vitro* surrogate assays are extremely attractive due to their relative ease of implementation, lower cost and improved throughput of results. The long-term culture initiating cell (LTC-IC) assay serves this purpose by quantifying the ability of putative HSCs in a given population to be cultured for an extended period, typically 5 weeks. LTC-IC readout is then quantitatively assessed both by proliferation and the ability to produce hematopoietic colony forming units (CFU), with the CFU output at the end of the assay being proportional to the number of LTC-ICs in the starting population[59]. Distinct supporting stromal layers and the addition of hematopoietic cytokines can have varying effects on maintenance of LTC-ICs[58,203-206].

Along with the ability to assess putative HSCs in hematopoietic populations, LTC-IC is also a valuable tool for investigating cell types and factors which play a role in HSC maintenance. Numerous *in vivo* studies have examined aspects of the mouse hematopoietic niche, typically in the bone marrow or fetal liver[50,52,207,208]. The generation of knock-out and transgenic mice has been extremely useful in these experiments, as it allows researchers to selectively and systematically evaluate the functional importance of individual niche factors[52,54]. Study of the human hematopoietic niche, however, is largely limited to analysis of BM biopsy specimens or culture methods

which attempt to recapitulate the human hematopoietic microenvironment, such as LTC-IC[209-211]. As such, genetic modification of primary human BM cell populations for use in LTC-IC has been a valuable tool in dissecting niche-related gene expression which modulates HSC function, though manipulation and continued culture of these cells is often difficult[60,212]. Human embryonic stem cells (hESCs) are capable of differentiating into any adult tissue, can be cultured long-term, and are easy to genetically modify[62,169]. Therefore, the prospect of using hESC-derived niche populations represents an effective, versatile way to study human HSC maintenance *in vitro*.

Previously, our group and others have derived both mesenchymal stromal cells (MSCs) and endothelial cells (ECs) from hESCs [213-218]. MSCs and ECs are important components of the osteogenic and vascular hematopoietic niches and hESC-derived stromal cells can provide autologous supporting cell populations for putative hESC-derived HSCs. Here, we test the capacity of these hESC-derived stromal layers to support LTC-IC from $CD34^+$ UCB and hESC-derived $CD34^+CD45^+$ cells. Cell proliferation and LTC-IC quantification of input populations were measured over a 5-week period and compared to use of bone marrow-derived mesenchymal stem cells (BM-MSCs) and the murine stromal line M2-10B4. Finally, we subjected the surviving LTC-IC populations to repopulation assays in order to determine a relationship between LTC-IC support and the ability for long-term engraftment.

Materials and Methods

Cell Culture

H9 human embryonic stem cells were adapted to single cell passage with TrypLE Select (Invitrogen Corp., Carlsbad, CA, USA) as previously described and were maintained as undifferentiated cells via coculture with irradiated mouse embryonic fibroblasts as previously described[76,166,219]. Karyotype of TrypLE-adapted H9 was found to be normal. M2-10B4 murine bone marrow stromal cells, mesenchymal stem cells derived from H9 hESCs (hESC-MSCs), bone marrow (BM-MSCs), and endothelial cells derived from H9 hESCs (hESC-ECs) were cultured as previously described[213,214]. For LTC-IC assays, M2-10B4, hESC-MSCs, hESC-ECs, and BM-MSCs were incubated with the appropriate cell culture media containing 10 μg/mL mitomycin C (Accord Healthcare, Durham, NC) before attachment to gelatin coated 24-well plates or flat-bottom 96-well plates. The use of all human tissue was approved by the Committee on the Use of Human Subjects in Research at the University of Minnesota.

Hematopoietic Differentiation of hESCs as spin EBs

H9 were differentiated using the previously described spin EB method[166]. Briefly, TrypLE-adapted H9 were dissociated to a single cell suspension via 5 minute incubation with TrypLE Select. The undifferentiated H9 were plated at 3000 cells per well into untreated, round-bottom, 96-well plates in BPEL media[166] containing 40 ng/mL human Stem Cell Factor (Peprotech, Rockey Hill, NJ), 20 ng/mL human vascular endothelial growth factor (R&D Systems, Minneapolis, MN), and 20 ng/mL human bone

morphogenic protein 4 (R&D Systems). After 12 days in spin EB culture, the differentiated hESC spin EBs were harvested and made into a single cell suspension using 0.05% trypsin/EDTA (Invitrogen) supplemented with 2% chicken serum (Sigma, St. Louis, MO). The differentiated cells were analyzed via flow cytometry and hematopoietic colony-forming cell (CFC) assay for the presence of hematopoietic progenitor cells[68].

Positive Selection of $CD34^+$ and $CD34^+CD45^+$ cells via magnetic sorting

Single cell suspensions of 11-12 day H9 spin EB cultures were obtained as described above. Cells were resuspended in DPBS (ThermoFisher Hyclone, Logan, UT) containing 2% FBS and 1 mM EDTA (Invitrogen) before magnetic sorting. EasySep Human CD34 Positive Selection kit (StemCell Technologies, Vancouver, BC) was used to isolate $CD34^+$ cells from differentiated hESCs. For enrichment of the $CD34^+CD45^+$ cell population, the EasySep PE Selection kit (StemCell Technologies) was used on $CD34^+$ cells labeled with anti-human CD45-PE. $CD34^+$ cells were positively selected via magnetic sorting from UCB mononuclear cells using the Miltenyi CD34 microbead kit (Miltenyi Biotec, Boston, MA) and AutoMACS Pro Separator (Miltenyi). $CD34^+$ UCB were frozen down in 90% FBS + 10% DMSO and stored in liquid nitrogen until use. Enrichment for $CD34^+$/$CD34^+CD45^+$ cells was assessed via staining with mouse anti-human CD34-APC, CD45-PE, CD43-PE, CD41a-PE, CD31-PE and corresponding isotype controls (all from BD Biosciences, Sparks, MD).

Bulk Culture LTC-IC

M2-10B4, hESC-MSCs, hESC-ECs, and BM-MSCs were treated with mitomycin C before plating on fibronectin-coated or gelatin-coated 24-well plates at 10^5 to 2 x 10^5 cells/well. For a combined hESC-MSC + hESC-EC condition, 5 x 10^4 hESC-MSCs and 5 x 10^4 hESC-ECs were to each well. Cells were allowed to adhere overnight before addition of UCB- or hESC-derived hematopoietic progenitor cells.

5 x 10^3 $CD34^+$ UCB or 2.5 x 10^4 to 10^5 $CD34^+CD45^+$ hESC-derived cells were plated per well of mitotically inactivated cells in 1 mL/well Myelocult H5100 media (StemCell Technologies) containing 10^{-6} M hydrocortisone (Sigma). Cultures were incubated at 37°C, 5% CO_2. Cells were fed with fresh medium by half medium changes every 7 days. At the indicated time points, cells were harvested via collection of nonadherent cells and dissociation of the adherent cell layer with 0.05% trypsin containing 2% chicken serum for 5 minutes. The nonadherent and adherent cells were combined and clumps removed by 70μm filter (BD Biosciences, Sparks, MD) for counting and transfer to hematopoietic CFC assay. Photos were taken on an Olympus CKX41 microscope attached to a Nikon D90 camera in Myelocult H5100 media.

Hematopoietic CFC assays

$CD34^+$ UCB or $CD34^+CD45^+$ hESC-derived cells were cultured for the indicated number of days on M2-10B4 or the human-derived cell layers before harvest to a single cell suspension. Colony forming assays were performed by culturing these cells in semi-solid Methocult H4435 Enriched (StemCell Technologies). 2.5 x 10^4 to 5 x 10^4 UCB-

derived cells or 5 x 10^4 to 10^5 hESC-derived cells were cultured per 35 mm culture dish (Greiner, Monroe, NC). After 14 days, the plates were scored for colony-forming units according to standard criteria[68]. For each adherent cell population, CFC yield per 10^3 $CD34^+$ UCB or 10^5 $CD34^+CD45^+$ hESCs initially placed into LTC-IC culture was determined by dividing the total number of cells harvested per well by the number of cells put into CFC assay, and using this factor to multiply the total number of colonies yielded by CFC assay.

Limiting Dilution CFC assay

For comparison of LTC-IC frequency from $CD34^+$ UCB cultured on various feeder layers, $CD34^+$ UCB were plated in limiting dilutions (semi-log dilution from 300 to 3 cells/well) in flat-bottom 96-well plates with a confluent monolayer of M2-10B4, hESC-MSC, hESC-EC, or BM-MSC. Cells were cultured in the same media/incubation conditions as described above for bulk LTC-IC culture and were similarly provided with fresh media every 7 days. After 5 weeks of culture, cells were placed in hematopoietic CFC assay conditions by removing all but 20 μL of media from each well and replacing with 100 μL of Methocult H4435 Enriched per well. After 14 days in Methocult, wells were scored for the presence of hematopoietic colonies. Frequency of LTC-ICs from each feeder condition was calculated by Poisson distribution (L-Calc software, StemCell Technologies) based on the number of wells at each cell dose with one or more hematopoietic colonies after 5 weeks of culture.

In vivo engraftment

All animals were housed, treated, and handled in accordance with the guidelines set forth by the University of Minnesota Institutional Animal Care and Use Committee and by the National Institutes of Health's Guide for the Care and Use of Laboratory Animals. The day before engraftment, 6-8 week old NOD-*scid IL2rγnull* (NSG) mice were irradiated. On the day of engraftment, LTC-ICs were harvested as described in bulk culture LTC-IC. Cells were then enumerated, resuspended in IMDM and injected through the tail vein at a dose equivalent of 7.5 – 10 x 10^3 initially seeded $CD34^+$ UCB cells per mouse. At both 4 and 8 weeks, mice were bled through the facial vein for analysis of peripheral blood. At 12 weeks, each mouse was bled then sacrificed for the collection of spleen and bone marrow. All tissue samples were treated with ammonium chloride for the lysis or red blood cells and blocked with human serum then stained with conjugated antibodies and analyzed in a flow cytometer as described.

Results

hESC-derived stromal cells support LTC-IC from $CD34^+$ UCB

We evaluated the ability of hESC-MSCs and hESC-ECs to support LTC-ICs using UCB- and hESC-derived hematopoietic cells compared to BM-MSCs and M2-10B4. All human cell populations (hESC-ECs, hESC-MSCs, and BM-MSCs) as well as a combined layer of hESC-MSCs and hESC-ECs, supported short-term expansion of CFCs from $CD34^+$ cells isolated from UCB ($CD34^+$ UCB). After three weeks, UCB cultured with hESC-MSCs, hESC-ECs, and hES-MSCs+hESC-ECs resulted in at least as

many CFCs per initial input $CD34^+$ UCB as use of M2-10B4 cells, and more than BM-MSCs (Figure 3.1A). Over this time, the UCB $CD34^+$ cell population expanded most rapidly on hESC-MSCs, hESC-ECs, and the combined hESC-MSC/EC condition (Figure 3.1B; also see Fig. 3.1E for photographs of representative cultures).

After five weeks of LTC-IC conditions, both hESC-MSC and hESC-ECs supported LTC-ICs from UCB similar to M2-10B4, yielding on average 85 +/- 29 and 74 +/- 12 LTC-IC-derived CFCs per 10^3 input UCB, respectively. This result compares to 104 +/- 56 CFCs per 10^3 input UCB co-cultured with M2-10B4 cells (Figure 3.1C). Likewise, UCB $CD34^+$ cells co-cultured with hESC-MSC or hESC-EC cells continued to maintain a population of non-adherent cells (Figure 3.1E, bottom row) with total cell numbers of 158 +/- 78 x 10^3 and 172 +/- 60 x 10^3, respectively, which was similar to use of M2-10B4 cells (Figure 3.1D). These LTC-IC assays demonstrated highest frequency when UCB $CD34^+$ cells were cultured on M2-10B4 cells (1:33), though hESC-MSCs and hESC-ECs supported a far higher frequency of LTC-IC than BM-MSC (1:204, 1:229, and. 1:7846, respectively; Figure 3.1F). These data demonstrate that our hESC-derived ECs and MSCs are able to support LTC-ICs from UCB over a 5 week period similar to M2-10B4 and better than BM-MSCs

hESC-derived hematopoietic progenitors do not contain LTC-ICs

We next evaluated the ability for hESC-derived stromal cells and M2-10B4 to support LTC-ICs from hESC-derived $CD34^+CD45^+$ hematopoietic progenitors (Figure 3.2A). With H9 hESCs, we routinely obtain over 20% total $CD34^+$ and $CD34^+CD31^+$

cells after 8 days of differentiation using a "spin-EB" method[166,220,221] with subsequent emergence of $CD34^+CD43^+$ and $CD34^+CD41a^+$ populations previously shown to indicate early hematopoietic development[173] (Figure 3.2A, top row). Between 11-13 days of differentiation, total $CD34^+$ cells can reach over 50% of total live cells with populations of $CD34^+CD31^+$, $CD34^+CD43^+$, and $CD34^+CD45^+$ ranging from 20-50% of total live cells (Figure 3.2A, bottom row).

After 12 days, differentiating hESCs were sorted for $CD34^+CD45^+$ cells (Figure 3.2B). As expected, the hESC-derived $CD34^+CD45^+$ population was enriched for hematopoietic progenitor cells (CFCs) (Figure 3.2C). However, after 2 weeks of co-culture with either the hESC-MSCs or M2-10B4 cells, they were markedly reduced for CFCs. While coculture of $CD34^+$ UCB yielded 5125 +/- 725 CFC on M2-10B4 for 2 weeks, progenitors from hESCs cultured on M2-10B4 yielded relatively few CFCs (averaging 48 +/- 45 CFC per 10^5 initial $CD34^+CD45^+$ hESCs; Figure 3.2D). After more than 2 weeks of M2-10B4 coculture, hematopoietic progenitor cells, as quantified in the CFU assays, were absent from the hESC-derived cell population. Using hESC-MSCs as supportive stromal cells, 34^+ UCB yielded 12767 +/- 5525 CFC, with hESC-derived progenitors yielding no hematopoietic colonies (Figure 3.2D). $CD34^+CD45^+$ hESC-derived cells did not maintain a nonadherent population in prolonged (5 week) culture on M210 or hESC-MSCs, with total cell number declining markedly after 1 week of culture, unlike $CD34^+$ UCB cells (Figure 3.2F, G & H).

Other hESC-derived populations also failed to demonstrate LTC-IC potential. $CD34^+CD43^+$ cells derived from hESCs differentiated for 8 days and $CD34^+CD45^+$ cells

isolated from hESCs differentiated for a longer period of time (12-15 days) both proliferated for the first 1-2 weeks of culture in LTC-IC assay and then started to decline (data not shown). Both cell populations failed to produce colonies in hematopoietic CFC assay after more than 2 weeks of culture (data not shown). These data demonstrate that, similar to their inability to engraft in immunodeficient mice, hESC-derived $CD34^+CD45^+$ and $CD34^+CD43^+$ hematopoietic progenitors do not contain LTC-ICs.

Stromal support of LTC-IC from $CD34^+$ UCB predicts engraftment potential

We next wanted to determine whether the ability of our hESC-derived stromal layers to support LTC-IC from $CD34^+$ UCB correlated with engraftment potential of the hematopoietic cells after 5 weeks in culture. To do so, we performed LTC-IC assays with $CD34^+$ UCB using M210-B4, BM-MSCs, hESC-MSCs and hESC-ECs as supporting stromal layers for 5 weeks, then injected the bulk harvested cells into NOD/SCID/IL-2Rgc^{null} (NSG) mice at doses equivalent of 7,500 – 10,000 starting $CD34^+$ cells per mouse. We were careful to include both male and female mice in each group, as female NSG mice show more robust HSC engraftment than males[222]. Flow cytometric analysis of peripheral blood at 4 and 8 weeks showed little to no engraftment in each group, with exception to a single female from the hESC-EC group showing 0.4% engraftment (data not shown). For week 12 analysis, all mice were sacrificed and analyzed for engraftment in peripheral blood, spleen and bone marrow. By this point, all groups exhibited limited but noticeable engraftment in at least one of the mice. Relative engraftment between groups was consistent in each tissue, with M210-B4 cultured cells

showing the highest levels, followed by hESC-EC and hESC-MSC (Figure 3.3A,B). BM-MSC cultured cells, while showing some engraftment in peripheral blood, were not detected in the spleen or bone marrow. These results demonstrate that the LTC-ICs maintained on our hESC-derived ECs and MSCs are capable of long-term engraftment in NSG mice. Likewise, we show that the level of LTC-IC support between these different stromal layers is predictive of engraftment potential.

Discussion

We have shown that hESC-derived ECs and MSCs are able to support the survival and proliferation of $CD34^+$ UCB in the LTC-IC assay similar to M2-10B4 and better than BM-MSCs, but that hESC-derived hematopoietic progenitors could not be maintained in LTC-IC regardless of the stromal layer used for support. Based on these data, hESC-derived MSCs and ECs are a viable alternative to M2-10B4 for long-term culture of multipotent hematopoietic cells. Notably, other studies have used coculture with human umbilical vein endothelial cells (HUVEC) as well as MSCs from human bone marrow to expand LTC-ICs from $CD34^+$ UCB[205,223]. However, use of hESC- and iPSC-derived MSCs and ECs has advantages over MSCs and ECs from other human sources. hESCs and iPSCs have the ability to derive multiple cell populations that make up the hematopoietic niche (including MSCs, ECs, and osteoblasts, and osteoclasts) from a single cell line -- providing a shared genetic background between these interacting cells. Moreover, the ability to genetically modify hESCs with relative ease allows a renewable source of cells that express transgenes of interest to hematopoietic

development[169,224]. These benefits provide the means to better mimic the human *in vivo* niche environment using several lineage types derived from a single cell line with either normal or modulated gene expression, thus allowing for a detailed assessment of factors crucial to the maintenance of human HSCs.

hESC-derived cells may differ from their post-natal-derived counterparts in terms of their ability to support hematopoietic cultures, as we observed by comparing hESC-MSCs and BM-MSCs. The differential ability of hESC-MSCs and BM-MSCs to support LTC-ICs from $CD34^+$ UCB reflects our previous findings that demonstrate distinct gene expression patterns for these two MSC populations. For example, hESC-MSCs express higher levels of the hemato-endothelial genes, *vWF and FLK-1*, and the pluripotency - associated genes *REX-1*, *hTERT*, and *CD133* [213]. This apparent enrichment in hemato-endothlial gene expression in hESC-derived MSCs could be the result of their derivation from a single $CD34^+CD73^-$ subset, which itself also gives rise to hematopoietic and endothelial populations, whereas BM-MSCs may be more heterogeneous in their origin and developmental state.

The inability of hESC-derived hematopoietic progenitors to demonstrate LTC-IC potential, in contrast to progenitors from UCB, is consistent with *in vivo* studies of hematopoietic engraftment from hESCs. Although SCID-repopulating cells (SRCs), an *in vivo* surrogate for HSCs, can be isolated from umbilical cord blood, adult bone marrow and peripheral blood, hESC-derived cells have thus far demonstrated relatively limited potential for long-term, multilineage hematopoietic engraftment *in vivo* [98,219,225]. The reasons for this are not completely understood, but our results suggest that these cells

may be more similar to short-term repopulating cells or multipotent progenitors (MPPs) than HSCs, as demonstrated by an initial expansion but quick proliferative exhaustion. Indeed we have shown through gene array studies that, while $CD34^+CD45^+$ and $CD34^+CD43^+$ share expression patterns typical of hematopoietic progenitors, they are distinct from populations capable of long-term engraftment such as $CD34^+$ UCB and $CD34^+$ fetal liver (unpublished). The challenges posed by generation of hematopoietic progenitors with LTC-IC/engraftment potential from hESCs also highlight the need for a better understanding of the in vivo marrow microenvironment – including the role of MSCs, ECs, and related cell types. Finally, this *in vitro* data combined with the results of our *in vivo* engraftment studies using LTC-IC cultured $CD34^+$ UCB suggest that LTC-IC is an accurate indicator for SRC potential, thus providing researchers with an accessible way to screen numerous putative hematopoietic progenitor populations before subjecting them to time-consuming and costly *in vivo* experiments.

Figure 3.1: hESC-derived MSCs and ECs support CFCs and LTC-ICs from $CD34^+$ UCB hematopoietic progenitors. For LTC-IC assays, 3-5 x 10^3 $CD34^+$ UCB/well were cocultured with mitotically-inactivated M2-10B4, hESC-MSCs, hESC-ECs, a 1:1 mix of hESC-MSCs and hESC-ECs, or human BM-MSCs, as indicated. Wells were harvested from each cell condition after 3 weeks to quantify hematopoietic CFU assay, CFC yield and total cell number. **A.** CFC yield/well quantified based on input of 10^3 $CD34^+$ UCB cells in LTC-IC culture and (**B**) total cell number per well (output) after 3 weeks, as this also accounts for cell proliferation over this time course. (**C-D**) Studies to quantify LTC-ICs at 5 weeks were assessed based on LTC-IC yield and total cell number, similar to (**A**) and (**B**). All values shown for (**A**)-(**D**) are the mean +/- SEM of 3 trials, except for the combined hESC-MSC/hESC-EC condition (mean +/- SEM of 2 trials). **E.** Photos of representative wells at 100X final magnification after 3 weeks (top row) and 5 weeks (bottom row) of coculture in Myelocult H5100 media. **F.** Additional studies using limiting dilution LTC-IC analysis with $CD34^+$ UCB were conducted to compare LTC-IC frequency between M210, hESC-MSC, hESC-EC, and BM-MSC cells.

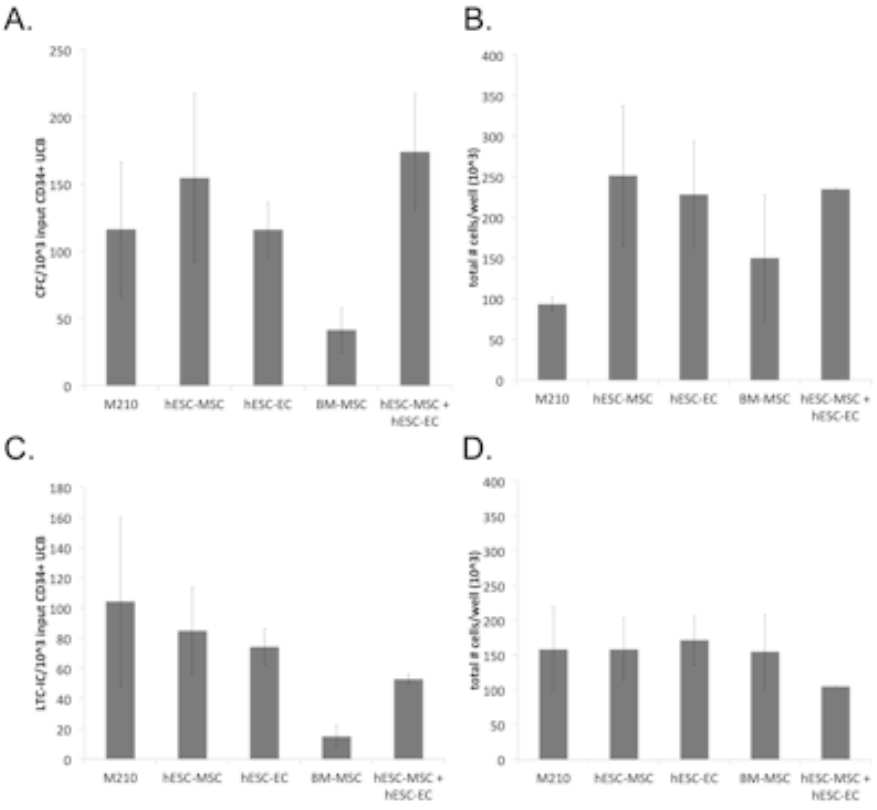

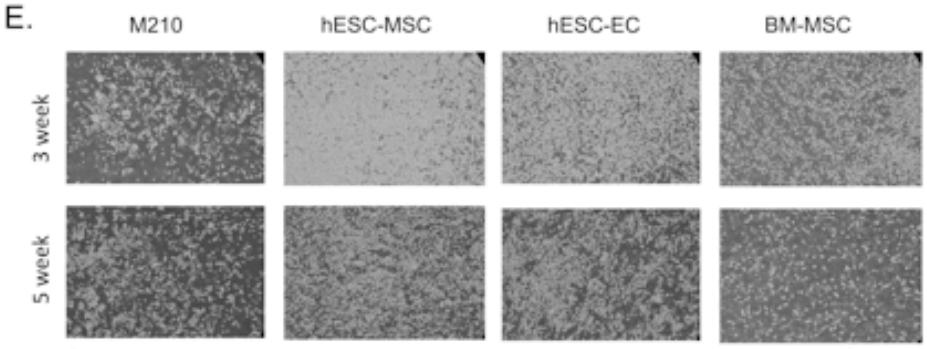

F

	M210	ES-EC	ES-MSC	BM-MSC
Frequency	1:33	1:229	1:204	1:7846
95% confidence interval	(28;40)	(189;276)	(170:245)	(2874;21416)

Figure 3.2: $CD34^+CD45^+$ cells derived from hESCs demonstrate only short-term hematopoietic progenitor potential. Hematopoietic differentiation of hESCs was done via spin-EB culture to derive $CD34^+CD45^+$ hematopoietic progenitor cells. **A.** Phenotypic analyses of hESC-derived cells at day 8 (top row) and day 13 (bottom row) of differentiation. **B.** hESCs differentiated in the spin EB culture system for 12 days were magnetically sorted to enrich for $CD34^+CD45^+$ hematopoietic progenitors. Representative flow cytometry data comparing the pre-sort and post-sort ($CD34^+CD45^+$) populations is shown. **C.** hESCs differentiated for 12 days produced colonies in hematopoietic CFU assay, with enrichment for $CD34^+CD45^+$ cells showing corresponding increase in the frequency of CFCs. **D.** Short-term analysis using 5-10 x 10^4 $CD34^+CD45^+$ hESCs/well and 5 x 10^3 $CD34^+$ UCB/well cocultured in parallel on M2-10B4 and hESC-MSC cells. After 2 weeks of culture, CFC yield per 10^5 UCB- or hESC-derived cells initially plated in M2-10B4 or hESC-MSC coculture was quantified, with values shown as the average of 3 trials +/- SEM. **E.** $CD34^+CD45^+$ hESCs were harvested at regular intervals beginning at day 7 of coculture to assess total cell numbers. **F.** $CD34^+$ UCB cultured in parallel with hESC-derived cells were harvested at regular intervals beginning at day 14 of coculture for assessment of total cell number. Values shown are the mean +/- SEM of three trials. **G-H**. Photographs of representative wells of (**G**) M2-10B4 coculture and (**H**) hESC-MSC coculture were taken after 1 week (top row) and 3 weeks (bottom row) at 100X magnification.

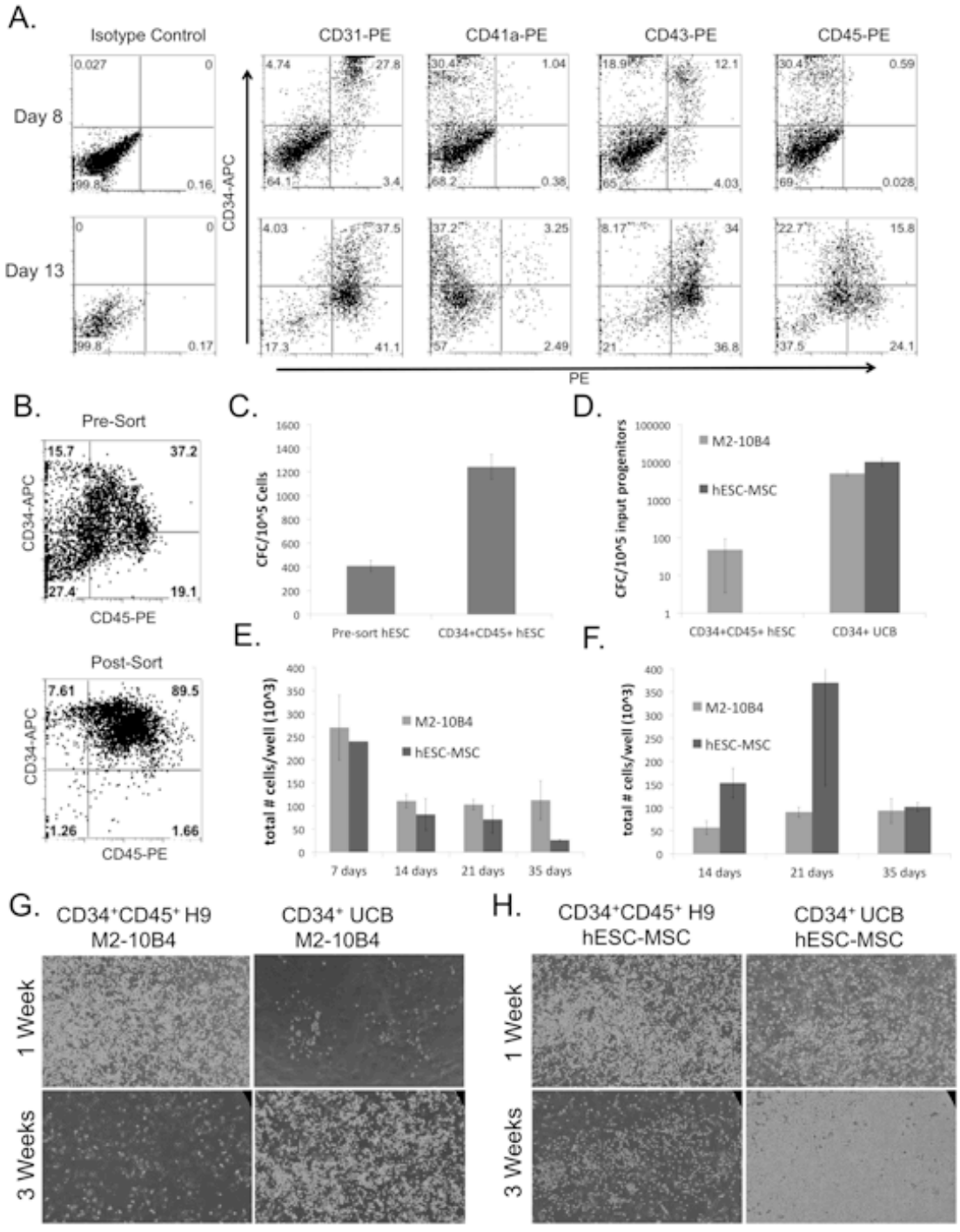
A.
Isotype Control
CD31-PE
CD41a-PE
CD43-PE
CD45-PE
Day 8
Day 13
CD34-APC
PE
B.
Pre-Sort
Post-Sort
CD34-APC
CD45-PE
C.
CFC/10^5 Cells
Pre-sort hESC
CD34+CD45+ hESC
D.
CFC/10^5 input progenitors
M2-10B4
hESC-MSC
CD34+CD45+ hESC
CD34+ UCB
E.
total # cells/well (10^3)
M2-10B4
hESC-MSC
7 days
14 days
21 days
35 days
F.
total # cells/well (10^3)
M2-10B4
hESC-MSC
14 days
21 days
35 days
G.
CD34+CD45+ H9
M2-10B4
CD34+ UCB
M2-10B4
1 Week
3 Weeks
H.
CD34+CD45+ H9
hESC-MSC
CD34+ UCB
hESC-MSC
1 Week
3 Weeks

Figure 3.3: Stromal-cultured LTC-ICs exhibit engraftment potential in NSG mice. Bulk cell populations were harvested from each LTC-IC condition after 5 weeks of culture. Cells were then divided among 2-4 non-lethally irradiated NSG mice and injected through the tail vain at a dose equivalent of 7.5 – 10 x 10^3 CD34+ UCB initially seeded per mouse. Each group had at least one male and at least one female and were divided evenly where possible. (A) Flow cytometric analysis of peripheral blood, spleen and bone marrow from a single mouse representing each experimental group. (B) Dot plot representing % human CD45 chimerism in each tissue for individual mice. Horizontal bars represent the group mean values.

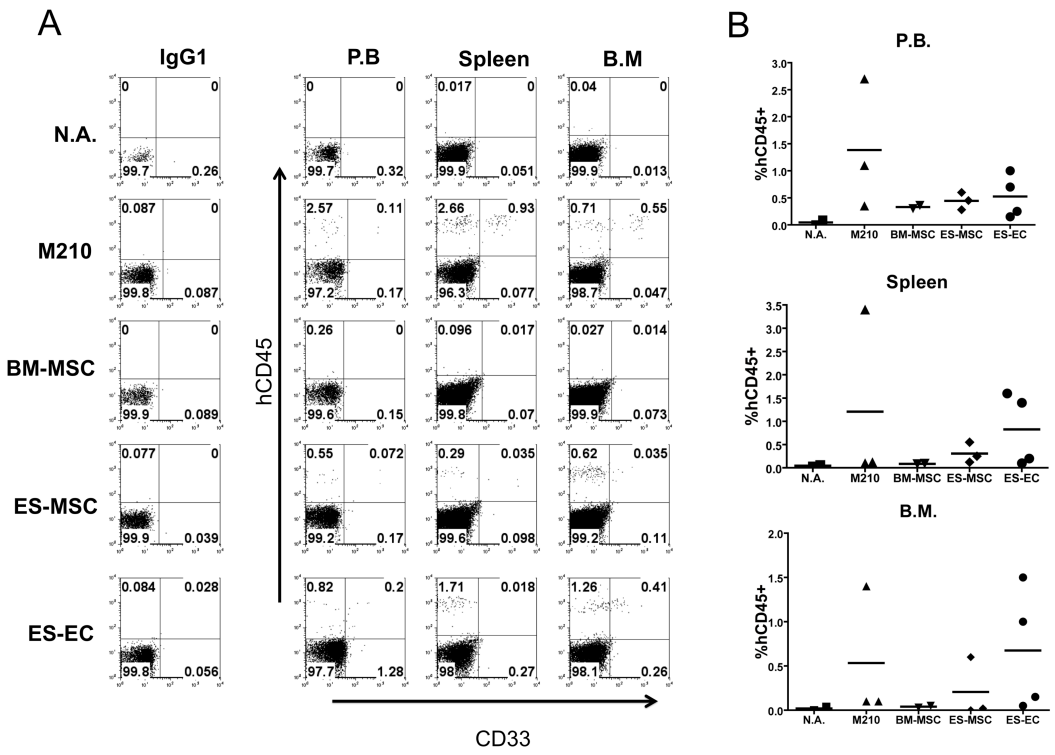
A
IgG1
P.B
Spleen
B.M
N.A.
M210
BM-MSC
ES-MSC
ES-EC
hCD45
CD33
B
P.B.
Spleen
B.M.
%hCD45+
N.A.
M210
BM-MSC
ES-MSC
ES-EC

Chapter 5:

Conclusions

The use of hPSCs for *in vitro* generation of HSCs to treat individuals with hematological disorders remains an extremely attractive possibility for regenerative medicine. In addition to the potential for theoretically unlimited production of cellular material for engraftment, iPSCs open the door for individuals harboring a disease-promoting mutation to have their own cells reprogrammed, genetically corrected, differentiated into functional HSCs or other blood lineages, then transplanted back into them. This patient-specific mode of therapeutics would ideally bypass the enormous complications associated with graft versus host disease (GVHD) that plague current standards of transplantation biology. However, before any of this is possible, we must first gain an adequate understanding of the physiology behind human *in vivo* HSC development and maintenance. To this end, using hPSCs as a model for human blood development provides us with a means to experiment with a variety of culture conditions, thus gradually refining our ability to recreate the *in vivo* HSC microenvironment.

The studies conducted as part of this thesis attempt to address these issues from both the perspectives of hPSC-derived hematopoietic progenitor physiology as well as an assessment of the supporting hematopoietic niche. Using a novel system to detect the transcriptional activity of genes known to be crucial for the first stages of mouse definitive hematopoietic development in differentiating hPSCs, we were able to determine that RUNX1c and PU.1 are activated in only particular sub-sets of human hematopoietic progenitors, and that these cells share a number of gene expression differences with SRC-containing populations such as $CD34^+$ UCB and FL. In addition, we demonstrated that hESC-derived stromal cells representing the hematopoietic

microenvironment were able to support the long-term survival of LTC-ICs from UCB equal to or better than primary BM niche populations. Furthermore, our results showing a lack of LTC-ICs in hPSC-derived hematopoietic progenitors are in support of previous findings which show these populations are also deficient for long-term, multilineage reconstitution.

Our initial hypothesis that RUNX1c expression would allow for the prospective isolation of engraftable hPSC-derived HSCs ultimately proved to be incorrect, as we found these cells were not even capable of long-term culture, which we contend is a pre-requisite for engraftment. However, this lofty expectation aside, our first-of-its-kind system for tracking human hematopoietic development yielded several positive results with implications regarding future research in this field. First, we were able to demonstrate that, as in mouse, RUNX1c expression identifies and is specific for hematopoietic populations as well as rare adherent cells which appear to be acting as an *in vitro* hemogenic endothelium. This again is consistent with *in vivo* mouse data showing RUNX1 expression in endothelial cells of the dorsal aorta directly prior to the emergence of definitive HSCs. Additionally, while our studies with the PU.1 reporter are incomplete, the preliminary results outlined here demonstrate that the promoter and URE are active in the same subsets of cells expressing RUNX1c, suggesting that these transcription factors are closely related as part of a distinct regulatory network in hPSC-derived hematopoietic cells.

Second, it is interesting and potentially very informative that the regulatory elements for these genes are only active in particular subsets of hPSC-derived

hematopoietic cells. We and others have speculated that part of the engraftment deficiency in hPSC-derived populations is due to their bias toward development of primitive progenitors. It then stands to reason that, if we are to develop conditions which skew this bias toward definitive development, given that it occurs, we need an accessible means to distinguish between these two types of progenitors as they emerge in culture. A few of our findings suggest that the RUNX1c and PU.1 reporters may serve this purpose. If we are to assume that *in vitro* hematopoiesis at least partially recapitulates that which occurs *in vivo*, we would then expect that the first hematopoietic cells to develop are part of the primitive system, and should be excluded from any model tracking definitive hematopoiesis. Indeed, the initial $CD34^+CD41a^+$ and $CD34^+CD43^+$ cells to emerge, both of which are enriched for primitive progenitors, lack expression of the reporter. It is not until several days later that the $CD31^+$, $CD43^+$ tdTom (RUNX1c) cells are detected. This could be interpreted as an *in vitro* recapitulation of the two hematopoietic waves with RUNX1c expression marking the definitive compartment, though more detailed experiments would be required to confidently reach such a conclusion. Our results using the SB inhibitor of primitive hematopoiesis are also in support of this hypothesis, as these conditions favored the development of $tdTom^+$ progenitors while decreasing proportion of initial $CD34^+CD41a^+$ and $CD34^+CD43^+$ emerging populations. Future studies should seek to evaluate in greater detail the origin and characteristics of these temporally distinct hPSC-derived subsets to determine if they indeed represent separate phases of hematopoietic development.

Finally, our genetic analysis showing distinct expression patterns differentiating all of the hPSC-derived populations from SRC-containing $CD34^+$ UCB and FL appears to support what is becoming an increasingly evident reality within the field: that current *in vitro* culture conditions are simply inadequate for the production of HSCs from hPSCs. While these populations indeed show phenotypic and functional qualities (CFU-enriched, $CD34^+$, etc) consistent with hematopoietic progenitors, their lack of long-term, multilineage engraftment is likely a consequence of these genetic differences. More specifically, the discrepancies involving genes associated with proliferation are particularly intriguing. Current studies are continually finding that populations of HSCs within the BM can be subdivided into those which are entering the cell cycle in order to replenish pools of MPPs, and those which remain quiescent, with the former being enriched for LTMR capability over the latter. Therefore, it appears that our hPSC-derived progenitors may be more similar to actively dividing HSCs, MPPs, or possibly an even more restricted subpopulation with respect to expression of genes that affect cell cycle and proliferation. This notion is further supported by our LTC-IC data, which demonstrate the hESC derived cells to proliferate for the first 1-2 weeks of culture while quickly dying out thereafter, losing the ability to produce CFUs. As such, modulation of gene expression using the key findings in our array analysis may help to circumvent this deficiency. For instance, conditional, enforced expression of Let-7 family members at early stages of *in vitro* differentiation may help to preserve any self-renewing, multipotent progenitors by negatively regulating cell-cycle entry genes such as the CCND family. Another potential target could be the HoxA family. A recent study has

shown the HoxA genes to promote self-renewal over differentiation in hematopoietic progenitor cells[226]. Increasing HoxA locus expression in hPSC-derived progenitors could bias their fate decisions toward self-renewal and increase their capacity for long-term engraftment. Finally, our finding that mir-181a is deficient in the hPSC-derived populations provides a potential cause for their apparent lack of multipotency in relation to B-cell development, and it too may be targeted in an attempt to further refine progenitor function. Whether forced conditional expression approaches will require numerous independent genetic modifications, or only a couple which result in a cascade of regulatory network alterations remains to be seen.

In light of this evidence, it seems increasingly evident that the prospect for *in vitro* production of hPSC-derived HSCs will require a 2-pronged approach: the development of culture conditions which more accurately simulate the hematopoietic niche and a detailed characterization of regulatory networks which influence not only HSC identity, but that of the precursors as well. At this point, the later method is probably seems a little less daunting, but will rely on access to large amounts of aborted fetal tissues as well as collaborative efforts to analyze these samples using recently developed technologies such as single-cell RNAseq. This way, the human-specific *in vivo* developmental progression from mesoderm to hemogenic endothelium to HSC can be articulated on a cell-by-cell basis, allowing us to identify the causative factors in our SRC-deficient hPSC-derived progenitors. Using reporter models such as those described here, we can then systematically design hPSC differentiation conditions aimed at alleviating these deficiencies. Indeed, though the *in vitro* production of HSCs seems to

be more complicated than researchers originally hoped, the combination of increasingly sophisticated technologies for analysis, mass-collaborative efforts and continued experimental creativity should eventually help us realize this goal.

1. Till JE, Mc CE. A direct measurement of the radiation sensitivity of normal mouse bone marrow cells. *Radiat Res*. 1961;14:213-222.
2. Siminovitch L, McCulloch EA, Till JE. The Distribution of Colony-Forming Cells among Spleen Colonies. *J Cell Physiol*. 1963;62:327-336.
3. Becker AJ, Mc CE, Till JE. Cytological demonstration of the clonal nature of spleen colonies derived from transplanted mouse marrow cells. *Nature*. 1963;197:452-454.
4. Wu AM, Till JE, Siminovitch L, McCulloch EA. A cytological study of the capacity for differentiation of normal hemopoietic colony-forming cells. *J Cell Physiol*. 1967;69(2):177-184.
5. Wu AM, Till JE, Siminovitch L, McCulloch EA. Cytological evidence for a relationship between normal hemotopoietic colony-forming cells and cells of the lymphoid system. *J Exp Med*. 1968;127(3):455-464.
6. Visser JW, Bauman JG, Mulder AH, Eliason JF, de Leeuw AM. Isolation of murine pluripotent hemopoietic stem cells. *J Exp Med*. 1984;159(6):1576-1590.
7. Szilvassy SJ, Humphries RK, Lansdorp PM, Eaves AC, Eaves CJ. Quantitative assay for totipotent reconstituting hematopoietic stem cells by a competitive repopulation strategy. *Proc Natl Acad Sci U S A*. 1990;87(22):8736-8740.
8. Muller-Sieburg CE, Whitlock CA, Weissman IL. Isolation of two early B lymphocyte progenitors from mouse marrow: a committed pre-pre-B cell and a clonogenic Thy-1-lo hematopoietic stem cell. *Cell*. 1986;44(4):653-662.
9. Morrison SJ, Weissman IL. The long-term repopulating subset of hematopoietic stem cells is deterministic and isolatable by phenotype. *Immunity*. 1994;1(8):661-673.
10. Spangrude GJ, Heimfeld S, Weissman IL. Purification and characterization of mouse hematopoietic stem cells. *Science*. 1988;241(4861):58-62.
11. Ikuta K, Weissman IL. Evidence that hematopoietic stem cells express mouse c-kit but do not depend on steel factor for their generation. *Proc Natl Acad Sci U S A*. 1992;89(4):1502-1506.
12. Kiel MJ, Yilmaz OH, Iwashita T, Yilmaz OH, Terhorst C, Morrison SJ. SLAM family receptors distinguish hematopoietic stem and progenitor cells and reveal endothelial niches for stem cells. *Cell*. 2005;121(7):1109-1121.
13. Good RA, Meuwissen HJ, Hong R, Gatti RA. Bone marrow transplantation: correction of immune deficit in lymphopenic immunologic deficiency and correction of an immunologically induced pancytopenia. *Trans Assoc Am Physicians*. 1969;82:278-285.
14. Cutler C, Antin JH. Peripheral blood stem cells for allogeneic transplantation: a review. *Stem Cells*. 2001;19(2):108-117.
15. Gluckman E, Broxmeyer HA, Auerbach AD, et al. Hematopoietic reconstitution in a patient with Fanconi's anemia by means of umbilical-cord blood from an HLA-identical sibling. *N Engl J Med*. 1989;321(17):1174-1178.
16. Wang JC, Doedens M, Dick JE. Primitive human hematopoietic cells are enriched in cord blood compared with adult bone marrow or mobilized peripheral blood as

measured by the quantitative in vivo SCID-repopulating cell assay. *Blood*. 1997;89(11):3919-3924.
17. Berenson RJ, Andrews RG, Bensinger WI, et al. Antigen CD34+ marrow cells engraft lethally irradiated baboons. *J Clin Invest*. 1988;81(3):951-955.
18. Berenson RJ, Bensinger WI, Hill R, et al. Stem cell selection--clinical experience. *Prog Clin Biol Res*. 1990;333:403-410; discussion 411-403.
19. Kamel-Reid S, Dick JE. Engraftment of immune-deficient mice with human hematopoietic stem cells. *Science*. 1988;242(4886):1706-1709.
20. Fulop GM, Phillips RA. The scid mutation in mice causes a general defect in DNA repair. *Nature*. 1990;347(6292):479-482.
21. Eaves C, Miller C, Cashman J, et al. Hematopoietic stem cells: inferences from in vivo assays. *Stem Cells*. 1997;15 Suppl 1:1-5.
22. Baum CM, Weissman IL, Tsukamoto AS, Buckle AM, Peault B. Isolation of a candidate human hematopoietic stem-cell population. *Proc Natl Acad Sci U S A*. 1992;89(7):2804-2808.
23. Bhatia M, Wang JC, Kapp U, Bonnet D, Dick JE. Purification of primitive human hematopoietic cells capable of repopulating immune-deficient mice. *Proc Natl Acad Sci U S A*. 1997;94(10):5320-5325.
24. Larochelle A, Savona M, Wiggins M, et al. Human and rhesus macaque hematopoietic stem cells cannot be purified based only on SLAM family markers. *Blood*. 2011;117(5):1550-1554.
25. Notta F, Doulatov S, Laurenti E, Poeppl A, Jurisica I, Dick JE. Isolation of single human hematopoietic stem cells capable of long-term multilineage engraftment. *Science*. 2011;333(6039):218-221.
26. Anjos-Afonso F, Currie E, Palmer HG, Foster KE, Taussig DC, Bonnet D. CD34(-) Cells at the Apex of the Human Hematopoietic Stem Cell Hierarchy Have Distinctive Cellular and Molecular Signatures. *Cell Stem Cell*. 2013;13(2):161-174.
27. Bai L, Shi G, Zhang X, Dong W, Zhang L. Transgenic expression of BRCA1 disturbs hematopoietic stem and progenitor cells quiescence and function. *Exp Cell Res*. 2013.
28. Larochelle A, Gillette JM, Desmond R, et al. Bone marrow homing and engraftment of human hematopoietic stem and progenitor cells is mediated by a polarized membrane domain. *Blood*. 2012;119(8):1848-1855.
29. Technau U, Scholz CB. Origin and evolution of endoderm and mesoderm. *Int J Dev Biol*. 2003;47(7-8):531-539.
30. F S. Studies on the origin of blood vessels and of red blood corpuscles as seen in the living blastoderm of chicks during the second day of incubation. *Contrib Embryol*. 1920;9(214).
31. Lawson KA, Meneses JJ, Pedersen RA. Clonal analysis of epiblast fate during germ layer formation in the mouse embryo. *Development*. 1991;113(3):891-911.
32. Palis J, Robertson S, Kennedy M, Wall C, Keller G. Development of erythroid and myeloid progenitors in the yolk sac and embryo proper of the mouse. *Development*. 1999;126(22):5073-5084.

33. Baron M. Induction of embryonic hematopoietic and endothelial stem/progenitor cells by hedgehog-mediated signals. *Differentiation*. 2001;68(4-5):175-185.
34. Artus J, Douvaras P, Piliszek A, Isern J, Baron MH, Hadjantonakis AK. BMP4 signaling directs primitive endoderm-derived XEN cells to an extraembryonic visceral endoderm identity. *Dev Biol*. 2012;361(2):245-262.
35. Nostro MC, Cheng X, Keller GM, Gadue P. Wnt, activin, and BMP signaling regulate distinct stages in the developmental pathway from embryonic stem cells to blood. *Cell Stem Cell*. 2008;2(1):60-71.
36. McGrath KE, Koniski AD, Malik J, Palis J. Circulation is established in a stepwise pattern in the mammalian embryo. *Blood*. 2003;101(5):1669-1676.
37. Fraser ST, Isern J, Baron MH. Maturation and enucleation of primitive erythroblasts during mouse embryogenesis is accompanied by changes in cell-surface antigen expression. *Blood*. 2007;109(1):343-352.
38. Medvinsky A, Dzierzak E. Definitive hematopoiesis is autonomously initiated by the AGM region. *Cell*. 1996;86(6):897-906.
39. de Bruijn MF, Speck NA, Peeters MC, Dzierzak E. Definitive hematopoietic stem cells first develop within the major arterial regions of the mouse embryo. *EMBO J*. 2000;19(11):2465-2474.
40. Taoudi S, Medvinsky A. Functional identification of the hematopoietic stem cell niche in the ventral domain of the embryonic dorsal aorta. *Proc Natl Acad Sci U S A*. 2007;104(22):9399-9403.
41. de Bruijn MF, Ma X, Robin C, Ottersbach K, Sanchez MJ, Dzierzak E. Hematopoietic stem cells localize to the endothelial cell layer in the midgestation mouse aorta. *Immunity*. 2002;16(5):673-683.
42. Richard C, Drevon C, Canto PY, et al. Endothelio-mesenchymal interaction controls runx1 expression and modulates the notch pathway to initiate aortic hematopoiesis. *Dev Cell*. 2013;24(6):600-611.
43. Boisset JC, Robin C. Imaging the founder of adult hematopoiesis in the mouse embryo aorta. *Cell Cycle*. 2010;9(13):2489-2490.
44. Boisset JC, van Cappellen W, Andrieu-Soler C, Galjart N, Dzierzak E, Robin C. In vivo imaging of haematopoietic cells emerging from the mouse aortic endothelium. *Nature*. 2010;464(7285):116-120.
45. Yoder MC, Hiatt K, Dutt P, Mukherjee P, Bodine DM, Orlic D. Characterization of definitive lymphohematopoietic stem cells in the day 9 murine yolk sac. *Immunity*. 1997;7(3):335-344.
46. Dzierzak E, Speck NA. Of lineage and legacy: the development of mammalian hematopoietic stem cells. *Nat Immunol*. 2008;9(2):129-136.
47. Gong JK. Endosteal marrow: a rich source of hematopoietic stem cells. *Science*. 1978;199(4336):1443-1445.
48. Nilsson SK, Johnston HM, Coverdale JA. Spatial localization of transplanted hemopoietic stem cells: inferences for the localization of stem cell niches. *Blood*. 2001;97(8):2293-2299.
49. Bielby R, Jones E, McGonagle D. The role of mesenchymal stem cells in maintenance and repair of bone. *Injury*. 2007;38 Suppl 1:S26-32.

50. Calvi LM, Adams GB, Weibrecht KW, et al. Osteoblastic cells regulate the haematopoietic stem cell niche. *Nature*. 2003;425(6960):841-846.
51. Wilson A, Murphy MJ, Oskarsson T, et al. c-Myc controls the balance between hematopoietic stem cell self-renewal and differentiation. *Genes Dev*. 2004;18(22):2747-2763.
52. Ding L, Saunders TL, Enikolopov G, Morrison SJ. Endothelial and perivascular cells maintain haematopoietic stem cells. *Nature*. 2012;481(7382):457-462.
53. Sugiyama T, Kohara H, Noda M, Nagasawa T. Maintenance of the hematopoietic stem cell pool by CXCL12-CXCR4 chemokine signaling in bone marrow stromal cell niches. *Immunity*. 2006;25(6):977-988.
54. Ding L, Morrison SJ. Haematopoietic stem cells and early lymphoid progenitors occupy distinct bone marrow niches. *Nature*. 2013;495(7440):231-235.
55. Arai F, Hirao A, Ohmura M, et al. Tie2/angiopoietin-1 signaling regulates hematopoietic stem cell quiescence in the bone marrow niche. *Cell*. 2004;118(2):149-161.
56. Solar GP, Kerr WG, Zeigler FC, et al. Role of c-mpl in early hematopoiesis. *Blood*. 1998;92(1):4-10.
57. Haug JS, He XC, Grindley JC, et al. N-cadherin expression level distinguishes reserved versus primed states of hematopoietic stem cells. *Cell Stem Cell*. 2008;2(4):367-379.
58. Sutherland HJ, Eaves CJ, Lansdorp PM, Thacker JD, Hogge DE. Differential regulation of primitive human hematopoietic cells in long-term cultures maintained on genetically engineered murine stromal cells. *Blood*. 1991;78(3):666-672.
59. Liu M, Miller CL, Eaves CJ. Human long-term culture initiating cell assay. *Methods Mol Biol*. 2013;946:241-256.
60. Duryagina R, Thieme S, Anastassiadis K, et al. Overexpression of Jagged-1 and Its Intracellular Domain in Human Mesenchymal Stromal Cells Differentially Affect the Interaction with Hematopoietic Stem and Progenitor Cells. *Stem Cells Dev*. 2013.
61. Wein F, Pietsch L, Saffrich R, et al. N-cadherin is expressed on human hematopoietic progenitor cells and mediates interaction with human mesenchymal stromal cells. *Stem Cell Res*. 2010;4(2):129-139.
62. Thomson JA. Embryonic Stem Cell Lines Derived from Human Blastocysts. *Science*. 1998;282(5391):1145-1147.
63. Keirstead HS, Nistor G, Bernal G, et al. Human embryonic stem cell-derived oligodendrocyte progenitor cell transplants remyelinate and restore locomotion after spinal cord injury. *J Neurosci*. 2005;25(19):4694-4705.
64. Schwartz SD, Hubschman JP, Heilwell G, et al. Embryonic stem cell trials for macular degeneration: a preliminary report. *Lancet*. 2012;379(9817):713-720.
65. Rezania A, Bruin JE, Riedel MJ, et al. Maturation of human embryonic stem cell-derived pancreatic progenitors into functional islets capable of treating pre-existing diabetes in mice. *Diabetes*. 2012;61(8):2016-2029.

66. Moon SH, Kang SW, Park SJ, et al. The use of aggregates of purified cardiomyocytes derived from human ESCs for functional engraftment after myocardial infarction. *Biomaterials*. 2013;34(16):4013-4026.
67. Roelandt P, Vanhove J, Verfaillie C. Directed differentiation of pluripotent stem cells to functional hepatocytes. *Methods Mol Biol*. 2013;997:141-147.
68. Kaufman DS, Hanson ET, Lewis RL, Auerbach R, Thomson JA. Hematopoietic colony-forming cells derived from human embryonic stem cells. *Proc Natl Acad Sci U S A*. 2001;98(19):10716-10721.
69. Ma F, Ebihara Y, Umeda K, et al. Generation of functional erythrocytes from human embryonic stem cell-derived definitive hematopoiesis. *Proc Natl Acad Sci U S A*. 2008;105(35):13087-13092.
70. Galic Z, Kitchen SG, Kacena A, et al. T lineage differentiation from human embryonic stem cells. *Proc Natl Acad Sci U S A*. 2006;103(31):11742-11747.
71. Woll PS, Martin CH, Miller JS, Kaufman DS. Human embryonic stem cell-derived NK cells acquire functional receptors and cytolytic activity. *J Immunol*. 2005;175(8):5095-5103.
72. Kaufman DS. Toward clinical therapies using hematopoietic cells derived from human pluripotent stem cells. *Blood*. 2009;114(17):3513-3523.
73. Cerdan C, McIntyre BA, Mechael R, et al. Activin A promotes hematopoietic fated mesoderm development through upregulation of brachyury in human embryonic stem cells. *Stem Cells Dev*. 2012;21(15):2866-2877.
74. Chadwick K, Wang L, Li L, et al. Cytokines and BMP-4 promote hematopoietic differentiation of human embryonic stem cells. *Blood*. 2003;102(3):906-915.
75. Wang L, Li L, Shojaei F, et al. Endothelial and hematopoietic cell fate of human embryonic stem cells originates from primitive endothelium with hemangioblastic properties. *Immunity*. 2004;21(1):31-41.
76. Woll PS, Morris JK, Painschab MS, et al. Wnt signaling promotes hematoendothelial cell development from human embryonic stem cells. *Blood*. 2008;111(1):122-131.
77. Kennedy M, D'Souza SL, Lynch-Kattman M, Schwantz S, Keller G. Development of the hemangioblast defines the onset of hematopoiesis in human ES cell differentiation cultures. *Blood*. 2007;109(7):2679-2687.
78. Park TS, Zimmerlin L, Zambidis ET. Efficient and simultaneous generation of hematopoietic and vascular progenitors from human induced pluripotent stem cells. *Cytometry A*. 2013;83(1):114-126.
79. Yamanaka S, Takahashi K. [Induction of pluripotent stem cells from mouse fibroblast cultures]. *Tanpakushitsu Kakusan Koso*. 2006;51(15):2346-2351.
80. Takahashi K, Tanabe K, Ohnuki M, et al. Induction of pluripotent stem cells from adult human fibroblasts by defined factors. *Cell*. 2007;131(5):861-872.
81. Miyoshi N, Ishii H, Nagai K, et al. Defined factors induce reprogramming of gastrointestinal cancer cells. *Proc Natl Acad Sci U S A*. 2010;107(1):40-45.
82. Liu H, Ye Z, Kim Y, Sharkis S, Jang YY. Generation of endoderm-derived human induced pluripotent stem cells from primary hepatocytes. *Hepatology*. 2010;51(5):1810-1819.

83. Hu K, Yu J, Suknuntha K, et al. Efficient generation of transgene-free induced pluripotent stem cells from normal and neoplastic bone marrow and cord blood mononuclear cells. *Blood*. 2011;117(14):e109-119.
84. Yu J, Vodyanik MA, Smuga-Otto K, et al. Induced pluripotent stem cell lines derived from human somatic cells. *Science*. 2007;318(5858):1917-1920.
85. Merling RK, Sweeney CL, Choi U, et al. Transgene-free iPSCs generated from small volume peripheral blood nonmobilized CD34+ cells. *Blood*. 2013;121(14):e98-107.
86. Park IH, Zhao R, West JA, et al. Reprogramming of human somatic cells to pluripotency with defined factors. *Nature*. 2008;451(7175):141-146.
87. Chun YS, Chaudhari P, Jang YY. Applications of patient-specific induced pluripotent stem cells; focused on disease modeling, drug screening and therapeutic potentials for liver disease. *Int J Biol Sci*. 2010;6(7):796-805.
88. Wu SM, Hochedlinger K. Harnessing the potential of induced pluripotent stem cells for regenerative medicine. *Nat Cell Biol*. 2011;13(5):497-505.
89. Ye Z, Zhan H, Mali P, et al. Human-induced pluripotent stem cells from blood cells of healthy donors and patients with acquired blood disorders. *Blood*. 2009;114(27):5473-5480.
90. Maehr R, Chen S, Snitow M, et al. Generation of pluripotent stem cells from patients with type 1 diabetes. *Proc Natl Acad Sci U S A*. 2009;106(37):15768-15773.
91. Onder TT, Daley GQ. New lessons learned from disease modeling with induced pluripotent stem cells. *Curr Opin Genet Dev*. 2012;22(5):500-508.
92. Brunstein CG, Wagner JE. Umbilical cord blood transplantation and banking. *Annu Rev Med*. 2006;57:403-417.
93. Miller CL, Audet J, Eaves CJ. Ex vivo expansion of human and murine hematopoietic stem cells. *Methods Mol Med*. 2002;63:189-208.
94. Goessling W, Allen RS, Guan X, et al. Prostaglandin E2 enhances human cord blood stem cell xenotransplants and shows long-term safety in preclinical nonhuman primate transplant models. *Cell Stem Cell*. 2011;8(4):445-458.
95. Parker MH, Loretz C, Tyler AE, et al. Activation of Notch signaling during ex vivo expansion maintains donor muscle cell engraftment. *Stem Cells*. 2012;30(10):2212-2220.
96. Boitano AE, Wang J, Romeo R, et al. Aryl hydrocarbon receptor antagonists promote the expansion of human hematopoietic stem cells. *Science*. 2010;329(5997):1345-1348.
97. Qiu C, Hanson E, Olivier E, et al. Differentiation of human embryonic stem cells into hematopoietic cells by coculture with human fetal liver cells recapitulates the globin switch that occurs early in development. *Exp Hematol*. 2005;33(12):1450-1458.
98. Ledran MH, Krassowska A, Armstrong L, et al. Efficient hematopoietic differentiation of human embryonic stem cells on stromal cells derived from hematopoietic niches. *Cell Stem Cell*. 2008;3(1):85-98.

99. Yahata T, Ando K, Sato T, et al. A highly sensitive strategy for SCID-repopulating cell assay by direct injection of primitive human hematopoietic cells into NOD/SCID mice bone marrow. *Blood*. 2003;101(8):2905-2913.
100. Wang J, Kimura T, Asada R, et al. SCID-repopulating cell activity of human cord blood-derived CD34- cells assured by intra-bone marrow injection. *Blood*. 2003;101(8):2924-2931.
101. Winkler IG, Sims NA, Pettit AR, et al. Bone marrow macrophages maintain hematopoietic stem cell (HSC) niches and their depletion mobilizes HSCs. *Blood*. 2010;116(23):4815-4828.
102. Kim J, Zanjani ED, Jeanblanc CM, Goodrich AD, Hematti P. Generation of CD34(+) cells from human embryonic stem cells using a clinically applicable methodology and engraftment in the fetal sheep model. *Exp Hematol*. 2013;41(8):749-758 e745.
103. Kennedy M, Awong G, Sturgeon CM, et al. T lymphocyte potential marks the emergence of definitive hematopoietic progenitors in human pluripotent stem cell differentiation cultures. *Cell Rep*. 2012;2(6):1722-1735.
104. Amabile G, Welner RS, Nombela-Arrieta C, et al. In vivo generation of transplantable human hematopoietic cells from induced pluripotent stem cells. *Blood*. 2013;121(8):1255-1264.
105. Suzuki N, Yamazaki S, Yamaguchi T, et al. Generation of engraftable hematopoietic stem cells from induced pluripotent stem cells by way of teratoma formation. *Mol Ther*. 2013;21(7):1424-1431.
106. Kyba M, Perlingeiro RC, Daley GQ. HoxB4 confers definitive lymphoid-myeloid engraftment potential on embryonic stem cell and yolk sac hematopoietic progenitors. *Cell*. 2002;109(1):29-37.
107. Chan KM, Bonde S, Klump H, Zavazava N. Hematopoiesis and immunity of HOXB4-transduced embryonic stem cell-derived hematopoietic progenitor cells. *Blood*. 2008;111(6):2953-2961.
108. Lee GS, Kim BS, Sheih JH, Moore M. Forced expression of HoxB4 enhances hematopoietic differentiation by human embryonic stem cells. *Mol Cells*. 2008;25(4):487-493.
109. Lu SJ, Feng Q, Ivanova Y, et al. Recombinant HoxB4 fusion proteins enhance hematopoietic differentiation of human embryonic stem cells. *Stem Cells Dev*. 2007;16(4):547-559.
110. Ran D, Shia WJ, Lo MC, et al. RUNX1a enhances hematopoietic lineage commitment from human embryonic stem cells and inducible pluripotent stem cells. *Blood*. 2013;121(15):2882-2890.
111. Kumano K, Chiba S, Kunisato A, et al. Notch1 but not Notch2 is essential for generating hematopoietic stem cells from endothelial cells. *Immunity*. 2003;18(5):699-711.
112. Robert-Moreno A, Espinosa L, de la Pompa JL, Bigas A. RBPjkappa-dependent Notch function regulates Gata2 and is essential for the formation of intra-embryonic hematopoietic cells. *Development*. 2005;132(5):1117-1126.

113. Lee JB, Werbowetski-Ogilvie TE, Lee JH, et al. Notch-HES1 signaling axis controls hemato-endothelial fate decisions of human embryonic and induced pluripotent stem cells. *Blood*. 2013;122(7):1162-1173.
114. Burns CE, Traver D, Mayhall E, Shepard JL, Zon LI. Hematopoietic stem cell fate is established by the Notch-Runx pathway. *Genes Dev*. 2005;19(19):2331-2342.
115. Nakagawa M, Ichikawa M, Kumano K, et al. AML1/Runx1 rescues Notch1-null mutation-induced deficiency of para-aortic splanchnopleural hematopoiesis. *Blood*. 2006;108(10):3329-3334.
116. Wang Q, Stacy T, Binder M, Marin-Padilla M, Sharpe AH, Speck NA. Disruption of the Cbfa2 gene causes necrosis and hemorrhaging in the central nervous system and blocks definitive hematopoiesis. *Proc Natl Acad Sci U S A*. 1996;93(8):3444-3449.
117. Lacaud G, Gore L, Kennedy M, et al. Runx1 is essential for hematopoietic commitment at the hemangioblast stage of development in vitro. *Blood*. 2002;100(2):458-466.
118. Okuda T, van Deursen J, Hiebert SW, Grosveld G, Downing JR. AML1, the target of multiple chromosomal translocations in human leukemia, is essential for normal fetal liver hematopoiesis. *Cell*. 1996;84(2):321-330.
119. Rhodes KE, Gekas C, Wang Y, et al. The emergence of hematopoietic stem cells is initiated in the placental vasculature in the absence of circulation. *Cell Stem Cell*. 2008;2(3):252-263.
120. North T, Gu TL, Stacy T, et al. Cbfa2 is required for the formation of intra-aortic hematopoietic clusters. *Development*. 1999;126(11):2563-2575.
121. Ottersbach K, Dzierzak E. The murine placenta contains hematopoietic stem cells within the vascular labyrinth region. *Dev Cell*. 2005;8(3):377-387.
122. Yokomizo T, Ogawa M, Osato M, et al. Requirement of Runx1/AML1/PEBP2alphaB for the generation of haematopoietic cells from endothelial cells. *Genes Cells*. 2001;6(1):13-23.
123. Chen MJ, Yokomizo T, Zeigler BM, Dzierzak E, Speck NA. Runx1 is required for the endothelial to haematopoietic cell transition but not thereafter. *Nature*. 2009;457(7231):887-891.
124. Kissa K, Herbomel P. Blood stem cells emerge from aortic endothelium by a novel type of cell transition. *Nature*. 2010;464(7285):112-115.
125. Hirai H, Ogawa M, Suzuki N, et al. Hemogenic and nonhemogenic endothelium can be distinguished by the activity of fetal liver kinase (Flk)-1 promoter/enhancer during mouse embryogenesis. *Blood*. 2003;101(3):886-893.
126. Jaffredo T, Gautier R, Eichmann A, Dieterlen-Lievre F. Intraaortic hemopoietic cells are derived from endothelial cells during ontogeny. *Development*. 1998;125(22):4575-4583.
127. Jaffredo T, Bollerot K, Sugiyama D, Gautier R, Drevon C. Tracing the hemangioblast during embryogenesis: developmental relationships between endothelial and hematopoietic cells. *Int J Dev Biol*. 2005;49(2-3):269-277.

128. Zarnegar MA, Chen J, Rothenberg EV. Cell-type-specific activation and repression of PU.1 by a complex of discrete, functionally specialized cis-regulatory elements. *Mol Cell Biol*. 2010;30(20):4922-4939.
129. Hoogenkamp M, Krysinska H, Ingram R, et al. The Pu.1 locus is differentially regulated at the level of chromatin structure and noncoding transcription by alternate mechanisms at distinct developmental stages of hematopoiesis. *Mol Cell Biol*. 2007;27(21):7425-7438.
130. Huang G, Zhang P, Hirai H, et al. PU.1 is a major downstream target of AML1 (RUNX1) in adult mouse hematopoiesis. *Nat Genet*. 2008;40(1):51-60.
131. Kim HG, de Guzman CG, Swindle CS, et al. The ETS family transcription factor PU.1 is necessary for the maintenance of fetal liver hematopoietic stem cells. *Blood*. 2004;104(13):3894-3900.
132. Scott EW, Fisher RC, Olson MC, Kehrli EW, Simon MC, Singh H. PU.1 functions in a cell-autonomous manner to control the differentiation of multipotential lymphoid-myeloid progenitors. *Immunity*. 1997;6(4):437-447.
133. Guo H, Ma O, Speck NA, Friedman AD. Runx1 deletion or dominant inhibition reduces Cebpa transcription via conserved promoter and distal enhancer sites to favor monopoiesis over granulopoiesis. *Blood*. 2012;119(19):4408-4418.
134. Ye M, Zhang H, Amabile G, et al. C/EBPa controls acquisition and maintenance of adult haematopoietic stem cell quiescence. *Nat Cell Biol*. 2013;15(4):385-394.
135. Filipowicz W, Bhattacharyya SN, Sonenberg N. Mechanisms of post-transcriptional regulation by microRNAs: are the answers in sight? *Nat Rev Genet*. 2008;9(2):102-114.
136. Guo S, Lu J, Schlanger R, et al. MicroRNA miR-125a controls hematopoietic stem cell number. *Proc Natl Acad Sci U S A*. 2010;107(32):14229-14234.
137. O'Connell RM, Chaudhuri AA, Rao DS, Gibson WS, Balazs AB, Baltimore D. MicroRNAs enriched in hematopoietic stem cells differentially regulate long-term hematopoietic output. *Proc Natl Acad Sci U S A*. 2010;107(32):14235-14240.
138. Li X, Li XQ, Zhang JH, et al. [Differential expression profiles of MicroRNA during the development of human cord blood CD34(+)CD38(-) cells to CD34(+)CD38(+) cells]. *Zhongguo Shi Yan Xue Ye Xue Za Zhi*. 2008;16(3):589-592.
139. Lu J, Guo S, Ebert BL, et al. MicroRNA-mediated control of cell fate in megakaryocyte-erythrocyte progenitors. *Dev Cell*. 2008;14(6):843-853.
140. Gururajan M, Haga CL, Das S, et al. MicroRNA 125b inhibition of B cell differentiation in germinal centers. *Int Immunol*. 2010;22(7):583-592.
141. Li QJ, Chau J, Ebert PJ, et al. miR-181a is an intrinsic modulator of T cell sensitivity and selection. *Cell*. 2007;129(1):147-161.
142. Peng W, Chen ZY, Wang L, Wang Z, Li J. MicroRNA-199a-3p is downregulated in gastric carcinomas and modulates cell proliferation. *Genet Mol Res*. 2013;12(3):3038-3047.
143. Huang Y, Hu Q, Deng Z, Hang Y, Wang J, Wang K. MicroRNAs in Body Fluids as Biomarkers for Non-small Cell Lung Cancer: A Systematic Review. *Technol Cancer Res Treat*. 2013.

144. Miao J, Wu S, Peng Z, Tania M, Zhang C. MicroRNAs in osteosarcoma: diagnostic and therapeutic aspects. *Tumour Biol*. 2013;34(4):2093-2098.
145. Kopp KL, Ralfkiaer U, Nielsen BS, et al. Expression of miR-155 and miR-126 in situ in cutaneous T-cell lymphoma. *APMIS*. 2013.
146. Komabayashi Y, Kishibe K, Nagato T, Ueda S, Takahara M, Harabuchi Y. Downregulation of miR-15a due to LMP1 promotes cell proliferation and predicts poor prognosis in nasal NK/T-cell lymphoma. *Am J Hematol*. 2013.
147. Bertero T, Gastaldi C, Bourget-Ponzio I, et al. miR-483-3p controls proliferation in wounded epithelial cells. *FASEB J*. 2011;25(9):3092-3105.
148. Bertero T, Bourget-Ponzio I, Puissant A, et al. Tumor suppressor function of miR-483-3p on squamous cell carcinomas due to its pro-apoptotic properties. *Cell Cycle*. 2013;12(14):2183-2193.
149. Lena AM, Shalom-Feuerstein R, Rivetti di Val Cervo P, et al. miR-203 represses 'stemness' by repressing DeltaNp63. *Cell Death Differ*. 2008;15(7):1187-1195.
150. Muller AM, Dzierzak EA. ES cells have only a limited lymphopoietic potential after adoptive transfer into mouse recipients. *Development*. 1993;118(4):1343-1351.
151. Muller AM, Medvinsky A, Strouboulis J, Grosveld F, Dzierzak E. Development of hematopoietic stem cell activity in the mouse embryo. *Immunity*. 1994;1(4):291-301.
152. Noort WA, Wilpshaar J, Hertogh CD, et al. Similar myeloid recovery despite superior overall engraftment in NOD/SCID mice after transplantation of human CD34(+) cells from umbilical cord blood as compared to adult sources. *Bone Marrow Transplant*. 2001;28(2):163-171.
153. Tian X, Woll PS, Morris JK, Linehan JL, Kaufman DS. Hematopoietic engraftment of human embryonic stem cell-derived cells is regulated by recipient innate immunity. *Stem Cells*. 2006;24(5):1370-1380.
154. Wang L, Menendez P, Shojaei F, et al. Generation of hematopoietic repopulating cells from human embryonic stem cells independent of ectopic HOXB4 expression. *J Exp Med*. 2005;201(10):1603-1614.
155. Cai Z, de Bruijn M, Ma X, et al. Haploinsufficiency of AML1 affects the temporal and spatial generation of hematopoietic stem cells in the mouse embryo. *Immunity*. 2000;13(4):423-431.
156. Dowdy CR, Xie R, Frederick D, et al. Definitive hematopoiesis requires Runx1 C-terminal-mediated subnuclear targeting and transactivation. *Hum Mol Genet*. 2010;19(6):1048-1057.
157. Fujita Y, Nishimura M, Taniwaki M, Abe T, Okuda T. Identification of an alternatively spliced form of the mouse AML1/RUNX1 gene transcript AML1c and its expression in early hematopoietic development. *Biochem Biophys Res Commun*. 2001;281(5):1248-1255.
158. Bee T, Swiers G, Muroi S, et al. Nonredundant roles for Runx1 alternative promoters reflect their activity at discrete stages of developmental hematopoiesis. *Blood*. 2010;115(15):3042-3050.

159. Tsuzuki S, Seto M. Expansion of functionally defined mouse hematopoietic stem and progenitor cells by a short isoform of RUNX1/AML1. *Blood*. 2012;119(3):727-735.
160. Challen GA, Goodell MA. Runx1 isoforms show differential expression patterns during hematopoietic development but have similar functional effects in adult hematopoietic stem cells. *Exp Hematol*. 2010;38(5):403-416.
161. Bee T, Liddiard K, Swiers G, et al. Alternative Runx1 promoter usage in mouse developmental hematopoiesis. *Blood Cells Mol Dis*. 2009;43(1):35-42.
162. Sroczynska P, Lancrin C, Kouskoff V, Lacaud G. The differential activities of Runx1 promoters define milestones during embryonic hematopoiesis. *Blood*. 2009;114(26):5279-5289.
163. Nottingham WT, Jarratt A, Burgess M, et al. Runx1-mediated hematopoietic stem-cell emergence is controlled by a Gata/Ets/SCL-regulated enhancer. *Blood*. 2007;110(13):4188-4197.
164. Ng CE, Yokomizo T, Yamashita N, et al. A Runx1 intronic enhancer marks hemogenic endothelial cells and hematopoietic stem cells. *Stem Cells*. 2010;28(10):1869-1881.
165. Newman M, Lardelli M. A hyperactive sleeping beauty transposase enhances transgenesis in zebrafish embryos. *BMC Res Notes*. 2010;3:282.
166. Ng ES, Davis R, Stanley EG, Elefanty AG. A protocol describing the use of a recombinant protein-based, animal product-free medium (APEL) for human embryonic stem cell differentiation as spin embryoid bodies. *Nat Protoc*. 2008;3(5):768-776.
167. Tian X, Kaufman DS. Hematopoietic development of human embryonic stem cells in culture. *Methods Mol Med*. 2005;105:425-436.
168. Bresnick EH, Lee HY, Fujiwara T, Johnson KD, Keles S. GATA switches as developmental drivers. *J Biol Chem*. 2010;285(41):31087-31093.
169. Wilber A, Linehan JL, Tian X, et al. Efficient and stable transgene expression in human embryonic stem cells using transposon-mediated gene transfer. *Stem Cells*. 2007;25(11):2919-2927.
170. Klimchenko O, Mori M, Distefano A, et al. A common bipotent progenitor generates the erythroid and megakaryocyte lineages in embryonic stem cell-derived primitive hematopoiesis. *Blood*. 2009;114(8):1506-1517.
171. Gori JL, Chandrasekaran D, Kowalski JP, et al. Efficient generation, purification, and expansion of CD34(+) hematopoietic progenitor cells from nonhuman primate-induced pluripotent stem cells. *Blood*. 2012;120(13):e35-44.
172. Majeti R, Park CY, Weissman IL. Identification of a hierarchy of multipotent hematopoietic progenitors in human cord blood. *Cell Stem Cell*. 2007;1(6):635-645.
173. Vodyanik MA, Thomson JA, Slukvin, II. Leukosialin (CD43) defines hematopoietic progenitors in human embryonic stem cell differentiation cultures. *Blood*. 2006;108(6):2095-2105.
174. Choi KD, Vodyanik MA, Slukvin, II. Generation of mature human myelomonocytic cells through expansion and differentiation of pluripotent stem

cell-derived lin-CD34+CD43+CD45+ progenitors. *J Clin Invest*. 2009;119(9):2818-2829.
175. Lam EY, Hall CJ, Crosier PS, Crosier KE, Flores MV. Live imaging of Runx1 expression in the dorsal aorta tracks the emergence of blood progenitors from endothelial cells. *Blood*. 2010;116(6):909-914.
176. Pearson S, Sroczynska P, Lacaud G, Kouskoff V. The stepwise specification of embryonic stem cells to hematopoietic fate is driven by sequential exposure to Bmp4, activin A, bFGF and VEGF. *Development*. 2008;135(8):1525-1535.
177. Knorr DA, Ni Z, Hermanson D, et al. Clinical-scale derivation of natural killer cells from human pluripotent stem cells for cancer therapy. *Stem Cells Transl Med*. 2013;2(4):274-283.
178. Gan OI, Murdoch B, Larochelle A, Dick JE. Differential maintenance of primitive human SCID-repopulating cells, clonogenic progenitors, and long-term culture-initiating cells after incubation on human bone marrow stromal cells. *Blood*. 1997;90(2):641-650.
179. Pflumio F, Izac B, Katz A, Shultz LD, Vainchenker W, Coulombel L. Phenotype and function of human hematopoietic cells engrafting immune-deficient CB17-severe combined immunodeficiency mice and nonobese diabetic-severe combined immunodeficiency mice after transplantation of human cord blood mononuclear cells. *Blood*. 1996;88(10):3731-3740.
180. Rollini P, Kaiser S, Faes-van't Hull E, Kapp U, Leyvraz S. Long-term expansion of transplantable human fetal liver hematopoietic stem cells. *Blood*. 2004;103(3):1166-1170.
181. Chen Y, Jacamo R, Konopleva M, Garzon R, Croce C, Andreeff M. CXCR4 downregulation of let-7a drives chemoresistance in acute myeloid leukemia. *J Clin Invest*. 2013;123(6):2395-2407.
182. Cai WY, Wei TZ, Luo QC, et al. The Wnt-beta-catenin pathway represses let-7 microRNA expression through transactivation of Lin28 to augment breast cancer stem cell expansion. *J Cell Sci*. 2013;126(Pt 13):2877-2889.
183. Vasilatou D, Papageorgiou SG, Kontsioti F, et al. Expression analysis of mir-17-5p, mir-20a and let-7a microRNAs and their target proteins in CD34+ bone marrow cells of patients with myelodysplastic syndromes. *Leuk Res*. 2013;37(3):251-258.
184. Liu Y, Yin B, Zhang C, Zhou L, Fan J. Hsa-let-7a functions as a tumor suppressor in renal cell carcinoma cell lines by targeting c-myc. *Biochem Biophys Res Commun*. 2012;417(1):371-375.
185. Shu J, Xia Z, Li L, et al. Dose-dependent differential mRNA target selection and regulation by let-7a-7f and miR-17-92 cluster microRNAs. *RNA Biol*. 2012;9(10):1275-1287.
186. Chen CZ, Li L, Lodish HF, Bartel DP. MicroRNAs modulate hematopoietic lineage differentiation. *Science*. 2004;303(5654):83-86.
187. Elefanty AG. Abstract from International Society for Stem Cell Research (ISSCR) 12th annual conference. 2012.

188. Pereira LA, Wong MS, Mossman AK, et al. Pdgfralpha and Flk1 are direct target genes of Mixl1 in differentiating embryonic stem cells. *Stem Cell Res*. 2012;8(2):165-179.
189. Hatzistavrou T, Micallef SJ, Ng ES, Vadolas J, Stanley EG, Elefanty AG. ErythRED, a hESC line enabling identification of erythroid cells. *Nat Methods*. 2009;6(9):659-662.
190. North TE, de Bruijn MF, Stacy T, et al. Runx1 expression marks long-term repopulating hematopoietic stem cells in the midgestation mouse embryo. *Immunity*. 2002;16(5):661-672.
191. Markova EN, Kantidze OL, Razin SV. Transcriptional regulation and spatial organisation of the human AML1/RUNX1 gene. *J Cell Biochem*. 2011;112(8):1997-2005.
192. Friedman AD. Transcriptional control of granulocyte and monocyte development. *Oncogene*. 2007;26(47):6816-6828.
193. Gangenahalli GU, Gupta P, Saluja D, et al. Stem cell fate specification: role of master regulatory switch transcription factor PU.1 in differential hematopoiesis. *Stem Cells Dev*. 2005;14(2):140-152.
194. Pio F, Kodandapani R, Ni CZ, et al. New insights on DNA recognition by ets proteins from the crystal structure of the PU.1 ETS domain-DNA complex. *J Biol Chem*. 1996;271(38):23329-23337.
195. Fisher RC, Lovelock JD, Scott EW. A critical role for PU.1 in homing and long-term engraftment by hematopoietic stem cells in the bone marrow. *Blood*. 1999;94(4):1283-1290.
196. Staber PB, Zhang P, Ye M, et al. Sustained PU.1 levels balance cell-cycle regulators to prevent exhaustion of adult hematopoietic stem cells. *Mol Cell*. 2013;49(5):934-946.
197. Burda P, Laslo P, Stopka T. The role of PU.1 and GATA-1 transcription factors during normal and leukemogenic hematopoiesis. *Leukemia*. 2010;24(7):1249-1257.
198. Li Y, Okuno Y, Zhang P, et al. Regulation of the PU.1 gene by distal elements. *Blood*. 2001;98(10):2958-2965.
199. Chen H, Zhang P, Radomska HS, Hetherington CJ, Zhang DE, Tenen DG. Octamer binding factors and their coactivator can activate the murine PU.1 (spi-1) promoter. *J Biol Chem*. 1996;271(26):15743-15752.
200. Chou ST, Khandros E, Bailey LC, et al. Graded repression of PU.1/Sfpi1 gene transcription by GATA factors regulates hematopoietic cell fate. *Blood*. 2009;114(5):983-994.
201. McIvor Z, Hein S, Fiegler H, et al. Transient expression of PU.1 commits multipotent progenitors to a myeloid fate whereas continued expression favors macrophage over granulocyte differentiation. *Exp Hematol*. 2003;31(1):39-47.
202. Fibbe WE, Noort WA, Schipper F, Willemze R. Ex vivo expansion and engraftment potential of cord blood-derived CD34+ cells in NOD/SCID mice. *Ann N Y Acad Sci*. 2001;938:9-17.

203. Petzer AL, Hogge DE, Landsdorp PM, Reid DS, Eaves CJ. Self-renewal of primitive human hematopoietic cells (long-term-culture-initiating cells) in vitro and their expansion in defined medium. *Proc Natl Acad Sci U S A*. 1996;93(4):1470-1474.
204. Punzel M, Moore KA, Lemischka IR, Verfaillie CM. The type of stromal feeder used in limiting dilution assays influences frequency and maintenance assessment of human long-term culture initiating cells. *Leukemia*. 1999;13(1):92-97.
205. Yildirim S, Boehmler AM, Kanz L, Mohle R. Expansion of cord blood CD34+ hematopoietic progenitor cells in coculture with autologous umbilical vein endothelial cells (HUVEC) is superior to cytokine-supplemented liquid culture. *Bone Marrow Transplant*. 2005;36(1):71-79.
206. Gottschling S, Saffrich R, Seckinger A, et al. Human mesenchymal stromal cells regulate initial self-renewing divisions of hematopoietic progenitor cells by a beta1-integrin-dependent mechanism. *Stem Cells*. 2007;25(3):798-806.
207. Scadden DT. The stem-cell niche as an entity of action. *Nature*. 2006;441(7097):1075-1079.
208. Chitteti BR, Cheng YH, Poteat B, et al. Impact of interactions of cellular components of the bone marrow microenvironment on hematopoietic stem and progenitor cell function. *Blood*. 2010;115(16):3239-3248.
209. Guezguez B, Campbell CJ, Boyd AL, et al. Regional Localization within the Bone Marrow Influences the Functional Capacity of Human HSCs. *Cell Stem Cell*. 2013;13(2):175-189.
210. Martin MA, Bhatia M. Analysis of the human fetal liver hematopoietic microenvironment. *Stem Cells Dev*. 2005;14(5):493-504.
211. Prewitz MC, Seib FP, von Bonin M, et al. Tightly anchored tissue-mimetic matrices as instructive stem cell microenvironments. *Nat Methods*. 2013;10(8):788-794.
212. Yang Y, Ma W, Wu D, et al. MiR-17 Partly Promotes Hematopoietic Cell Expansion through Augmenting HIF-1alpha in Osteoblasts. *PLoS One*. 2013;8(7):e70232.
213. Kopher RA, Penchev VR, Islam MS, Hill KL, Khosla S, Kaufman DS. Human embryonic stem cell-derived CD34+ cells function as MSC progenitor cells. *Bone*. 2010;47(4):718-728.
214. Hill KL, Obrtlikova P, Alvarez DF, et al. Human embryonic stem cell-derived vascular progenitor cells capable of endothelial and smooth muscle cell function. *Exp Hematol*. 2010;38(3):246-257 e241.
215. Barberi T, Willis LM, Socci ND, Studer L. Derivation of multipotent mesenchymal precursors from human embryonic stem cells. *PLoS Med*. 2005;2(6):e161.
216. Levenberg S, Golub JS, Amit M, Itskovitz-Eldor J, Langer R. Endothelial cells derived from human embryonic stem cells. *Proc Natl Acad Sci U S A*. 2002;99(7):4391-4396.
217. Lian Q, Lye E, Suan Yeo K, et al. Derivation of clinically compliant MSCs from CD105+, CD24- differentiated human ESCs. *Stem Cells*. 2007;25(2):425-436.

218. Ferreira LS, Gerecht S, Shieh HF, et al. Vascular progenitor cells isolated from human embryonic stem cells give rise to endothelial and smooth muscle like cells and form vascular networks in vivo. *Circ Res*. 2007;101(3):286-294.
219. Tian X, Hexum MK, Penchev VR, Taylor RJ, Shultz LD, Kaufman DS. Bioluminescent imaging demonstrates that transplanted human embryonic stem cell-derived CD34(+) cells preferentially develop into endothelial cells. *Stem Cells*. 2009;27(11):2675-2685.
220. Ng ES, Davis RP, Azzola L, Stanley EG, Elefanty AG. Forced aggregation of defined numbers of human embryonic stem cells into embryoid bodies fosters robust, reproducible hematopoietic differentiation. *Blood*. 2005;106(5):1601-1603.
221. Hexum MK, Tian X, Kaufman DS. In vivo evaluation of putative hematopoietic stem cells derived from human pluripotent stem cells. *Methods Mol Biol*. 2011;767:433-447.
222. Notta F, Doulatov S, Dick JE. Engraftment of human hematopoietic stem cells is more efficient in female NOD/SCID/IL-2Rgc-null recipients. *Blood*. 2010;115(18):3704-3707.
223. Kadereit S, Deeds LS, Haynesworth SE, et al. Expansion of LTC-ICs and maintenance of p21 and BCL-2 expression in cord blood CD34(+)/CD38(-) early progenitors cultured over human MSCs as a feeder layer. *Stem Cells*. 2002;20(6):573-582.
224. Giudice A, Trounson A. Genetic modification of human embryonic stem cells for derivation of target cells. *Cell Stem Cell*. 2008;2(5):422-433.
225. Wang L, Menendez P, Cerdan C, Bhatia M. Hematopoietic development from human embryonic stem cell lines. *Exp Hematol*. 2005;33(9):987-996.
226. Ross K, Sedello AK, Todd GP, et al. Polycomb group ring finger 1 cooperates with Runx1 in regulating differentiation and self-renewal of hematopoietic cells. *Blood*. 2012;119(18):4152-4161.

Appendix

Commonly used acronyms

AGM: Aorta-gonad-mesonephros. Region of the developing mouse embryo from which hematopoietic stem cells first emerge.

BM: Bone marrow. The primary site of adult HSC maintenance.

BM-MSC: Bone marrow-derived mesenchymal stromal cell. Cells derived from human bone marrow used for *in vitro* hematopoietic support.

CFU: Colony forming unit: A progenitor cell which gives rise to a hematopoietic colony.

Dub7: Umbilical cord blood-derived induced pluripotent stem cell line used for the RUNX1c reporter studies.

E: Embryonic day. Referring to the number of days post fertilization.

EB: Embryoid body. A spherical cluster of cells used hematopoietic differentiation protocols.

EC: Endothelial cell.

Ery^{P}: Primitive erythrocyte. The first blood cells to arise through the primitive hematopoietic program.

FL: Fetal liver. Tissue extracted from the liver of an aborted fetus.

GFP: green fluorescent protein. A fluorescent protein constitutively expressed in our transgenic reporter cell lines.

hESC: human embryonic stem cell. Pluripotent stem cells derived from the inner cell mass of a human blastocyst.

hESC-EC: endothelial cells derived from hESCs

hESC-MSC: mesenchymal stromal cells derived from hESCs

hPSC: human pluripotent stem cell. Collectively referring to hESCs and iPSCs.

HSC: hematopoietic stem cell. A progenitor cell capable of long-term self renewal and multilineage hematopoietic differentiation.

HSCT: Hematopoietic stem cell transplant.

IBMT: Intra-bone marrow transplantation. The practice of injecting material directly into the bone marrow.

iPSC: Induced pluripotent stem cell. An adult cell which has been reprogrammed to a pluripotent developmental state.

KTLS: $ckit^{+}Thy1.1^{lo}Lin^{-}Sca1^{+}$. Referring to the phenotype of an SRC enriched population of BM cells.

LTC-IC: Long-term culture initiating cell. A hematopoietic progenitor cell which can survive long-term (>5 weeks) in culture. Commonly thought of as an *in vitro* surrogate for an SRC.

LTMR: long-term, multilineage reconstitution. The ability of a cell population to reconstitute all blood lineage of a recipient upon transplantation.

mESC: mouse embryonic stem cell.

M2-10B4: A stromal cell line derived from mouse bone marrow used to induce hematopoiesis from hPSCs *in vitro.*

MPP: Multipotent progenitor. Typically referring to an HSC derivative capable of differentiating into myeloid and lymphoid lineages while lacking full HSC function.

MSC: Mesenchymal stromal cell.

PBI: Peripheral blood island. Pools of primitive erythrocytes within the vasculature of the embryonic yolk sac.

P1: The distal promoter which drives expression of the Runx1c isoform.

P2: The proximal promoter which drives expression of the Runx1b isoform.

SRC: SCID repopulating cell. A cell capable of LTMR in a SCID mouse.

UCB: Umbilical cord blood.